ไทโอเลตเตดควอเทอร์ไนซ์ไคโทซานที่มีสมบัติยึดติดเยื่อเมือกเพื่อเป็นระบบนำส่งยาต้านมะเร็ง

นายกชกร จันทพราหมณ์

วิทยานิพนธ์นี้เป็นส่วนหนึ่งของการศึกษาตามหลักสูตรปริญญาวิทยาศาสตรมหาบัณฑิต
สาขาวิชาปิโตรเคมีและวิทยาศาสตร์พอลิเมอร์
คณะวิทยาศาสตร์ จุฬาลงกรณ์มหาวิทยาลัย
ปีการศึกษา 2554
ลิขสิทธิ์ของจุฬาลงกรณ์มหาวิทยาลัย

MUCOADHESIVE THIOLATED QUATERNIZED CHITOSAN AS ANTICANCER
DRUG DELIVERY SYSTEM

Mr. Kotchakorn Juntapram

A Thesis Submitted in Partial Fulfillment of the Requirements
for the Degree of Master of Science Program in Petrochemistry and Polymer Science
Faculty of Science
Chulalongkorn University
Academic Year 2011

Thesis Title	MUCOADHESIVE THIOLATED QUATERNIZED CHITOSAN AS ANTICANCER DRUG DELIVERY SYSTEM
By	Mr. Kotchakorn Juntapram
Field of Study	Petrochemistry and Polymer Science
Thesis Advisor	Associate Professor Nongnuj Muangsin, Ph.D.
Thesis Co-Advisor	Assistant Professor Nalena Praphairaksit, D.V.M., Ph.D.

Accepted by the Faculty of Science, Chulalongkorn University in Partial Fulfillment of the Requirements for the Master's Degree

………………………………………Dean of the Faculty of Science

(Professor Supot Hannongbua, Dr.rer.nat.)

THESIS COMMITTEE

……………………………………………….. Chairman

(Assistant Professor Warinthorn Chavasiri, Ph.D.)

……………………………………………………. Thesis Advisor

(Associate Professor Nongnuj Muangsin, Ph.D.)

…………………………………………….. Thesis Co-advisor

(Assistant Professor Nalena Praphairaksit, D.V.M., Ph.D.)

…………………………………………….. Examiner

(Associate Professor Nuanphun Chantarasiri, Ph.D.)

…………………………………………….. External Examiner

(Associate Professor Pornsak Sriamornsak., Ph.D.)

กชกร จันทพราหมณ์: ไทโอเลตเตดควอเทอร์ไนซ์ไคโทซานที่มีสมบัติยึดติดเยื่อเมือกเพื่อ เป็นระบบนำส่งยาต้านมะเร็ง (MUCOADHESIVE THIOLATED QUATERNIZED CHITOSAN AS ANTICANCER DRUG DELIVERY SYSTEM) อ. ที่ปรึกษาวิทยานิพนธ์ หลัก: รศ. ดร. นงนุช เหมืองสิน, อาจารย์ที่ปรึกษาวิทยานิพนธ์ร่วม: ผศ. สพญ. ดร. นลินา ประไพรักษ์สิทธิ์, 114 หน้า.

งานวิจัยนี้มีแนวคิดที่จะดัดแปรไคโทซานเพื่อเพิ่มสมบัติยึดติดเยื่อเมือกในระบบนำส่งยา โดยการสังเคราะห์ไทโอเลตเตดไคโทซาน(CS-HT)   และไทโอเลตเตดควอเทอร์ไนซ์ไคโทซาน (QCS-HT) ซึ่งดัดแปรโดยโฮโมซิสเตอีน-ไทโอแลกโตน ศึกษาอัตราส่วนที่เหมาะสมในการยึดติด เยื่อเมือกของไคโทซานและควอเทอร์ไนซ์ไคโทซาน ต่อโฮโมซิสเตอีน-ไทโอแลกโตน พิสูจน์ เอกลักษณ์ของไคโทซานที่ทำการดัดแปรแล้วด้วยเทคนิค NMR, FTIR, XRD และ TGA ศึกษา สมบัติยึดติดเยื่อเมือกที่สภาวะ pH 1.2, 4.0 และ 6.4 รวมทั้งหาปริมาณของไทออลและไดซัลไฟด์ พบว่าอัตราส่วนที่เหมาะสมคือ 1:0.1 โดยน้ำหนัก และ QCS-HT ให้ความสามารถในการยึดติดเยื่อ เมือกมากกว่าไคโทซาน 6.33 เท่าที่ pH 1.2 จึงนำพอลิเมอร์ที่ได้มาใช้ควบคุมปลดปล่อยตัวยาต้าน มะเร็งชนิดแคมป์โธทีซิน (CPT) เตรียมร่วมกับอัลจิเนต (ALG) และคาร์ราจีแนน (CR) โดยใช้ เทคนิคอิเล็กโทรสเปรย์ นอกจากนี้ยังศึกษาลักษณะทางกายภาพ เช่น SEM, Particle size analyzer, FTIR และ TGA รวมทั้งประสิทธิภาพในการกักเก็บยาของอนุภาคที่เตรียมได้ ความสามารถในการ ยึดติดเยื่อเมือกของอนุภาค และอัตราการปลดปล่อยยา จากการศึกษาพบว่า CPT-mCS/ALG   มี ประสิทธิภาพในการควบคุมการกักเก็บยาประมาณ 70 เปอร์เซ็นต์ สามารถยึดติดเยื่อเมือกมากกว่า ไคโทซาน 5.6, 1.86 และ 1.55 เท่าในสภาวะ pH 1.2, 4.0 และ 6.4 ตามลำดับ นอกจากนั้นพอลิเมอร์ ดังกล่าวสามารถปลดปล่อยแคมป์โธทีซินนานถึง 12 ชั่วโมง

สาขาวิชา ปิโตรเคมีและวิทยาศาสตร์พอลิเมอร์ ลายมือชื่อนิสิต..
ปีการศึกษา 2554 .... ลายมือชื่อ อ. ที่ปรึกษาวิทยานิพนธ์หลัก.............
ลายมือชื่อ อ. ที่ปรึกษาวิทยานิพนธ์ร่วม.............

5272202923: MAJOR PETROCHEMISTRY AND POLYMER SCIENCE
KEYWORD: THIOLATED CHITOSAN/ MUCOADHESIVE/ DRUG DELIVERY SYSTEM

KOTCHAKORN JUNTAPRAM: MUCOADHESIVE THIOLATED QUATERNIZED CHITOSAN AS ANTICANCER DRUG DELIVERY SYSTEM, ADVISOR: ASSOC.PROF. NONGNUJ MUANGSIN, Ph.D., CO ADVISOR: NALENA PRAPHAIRAKSIT, D.V.M., Ph.D., 114 pp.

The objective of this research was to increase the mucoadhesive property of chitosan and then evaluate for its application in mucoadhesive drug delivery systems. Two mucoadhesive thiolated chitosan were synthesized by the covalent attachment of homocysteine thiolactone (HT) to chitosan (CS) and quaternized-CS (QCS) at various weight ratios of CS or QCS to HT. The modified chitosan (mCS) are characterized by NMR, FTIR, XRD, and TGA. The mucoadhesive and swelling properties of mCS were studied at pH 1.2, 4.0, and 6.4. The amount of thiol and disulfide groups immobilized on the CS influenced the polymer's mucoadhesion positively and negatively, respectively, with the optimal CS:HT (w/w) ratio being found to be 1:0.1. The QCS-HT displayed a 6.33-fold stronger mucoadhesive property compared to that of the unmodified CS at pH 1.2. Additionally, the mCS as anticancer drug delivery systems were investigated using camptothecin (CPT) as a model anticancer drug. The microspheres of pure mCS and its polyelectrolyte complexes with alginate (ALG) and carrageenan (CR) were fabricated using electrospray ionization technique. The microspheres were characterized by SEM, particle size analyzer, FTIR, TGA, encapsulation efficiency, mucoadhesive property and *in vitro* drug release behavior. The CPT loaded mCS/ALG microspheres exhibited over 70% drug entrapment efficiency. The CPT-mCS/ALG microspheres displayed a 5.60-, 1.86-, and 1.55-fold stronger mucoadhesive property compared to that of the unmodified CS at pH 1.2, 4.0, and 6.4, respectively. Moreover, the obtained microspheres not only reduced the burst effect but also prolonged release of CPT within 12 h.

Field of study: Petrochemistry   Student's Signature………….......…….

           and Polymer Science   Principal Advisor's Signature……..…..

Academic Year: 2011   Co-advisor's Signature…..…….....…….

ACKNOWLEDGEMENTS

CONTENTS

LIST OF TABLES

LIST OF FIGURES

LIST OF ABBREVIATIONS

%	percentage
μg	microgram
μL	microliter
μmol	micromole
APDs	avalanche photodiode array
aq	aqueous
cm	centimeter
cm^{-1}	unit of wave number
conc.	concentration
HT	homocysteine-thiolactone
CS	chitosan
QCS	quaternized chitosan
°C	degree Celsius (centrigrade)
CPT	camptothecin
TGA	thermogravimetric analysis
%DD	degree of deacetylation
EE	entrapment efficiency
FTIR	Fourier Transform Infrared Spectrophotometer
g	gram
h	hour
kDa	kilodalton
kV	kilovolt
M	concentration in molar
mCS	modifiedchitosan
ALG	alginate
mg	milligram
min	minute
mL	milliliter

mL/h	milliliter per hour
MW	molecular weight
nm	nanometer
PDI	polydispersity index
pH	power of hydrogen ion or the negative logarithm (base ten)
ppm	part per million
KBr	potassium bromide disk
r^2	correlation coefficient
rpm	round per minute
S.D.	standard deviation
SEM	Scanning Electron Microscope
t	time
T_m	melting temperature
UV	ultraviolet
v/v	volume/volume
w/w	weight/weight
XRD	X-ray diffraction
PAS	periodic acid schiff

CHAPTER I

INTRODUCTION

1.1 Introduction

Over the past few years, mucoadhesive polymers have gained substantially in interest as an alternative approach to improve the effectiveness of relevant drugs by maintaining their plasma concentration at therapeutic levels for a prolonged period of time, inhibiting the dilution of the drug in the body fluids, and allowing targeting and localization of the drug at a specific adsorption site [1-3].

The design and selection of polymers for drug delivery is partially based on the concept that mucoadhesive polymers should have hydrophilic functional groups, such as carboxyl (-COOH), hydroxyl (-OH) and amide (-NH$_2$) groups, or strong anionic or positive charges and chain flexibility. As such, these polymers would be able to interact more strongly with the mucus glycoproteins [4, 5].

Nowadays, a considerable number of studies focusing on the mucoadhesive properties of a wide range of polymeric materials have been performed using different method and techniques[6]. In general, adhesive polymer can be classified as synthetic and natural polymer. Natural bioadhesive macromolecules share similar structural properties with the synthetic polymers. They are generally linear polymers with high molecular weight, contain a substantial number of hydrophilic, negatively or positively charged functional groups, and form three dimensional expanded networks. In the class of synthetic polymer, poly(acrylic acid), cellulose ester derivatives, and polymethacrylate derivatives are the current choice. Chitosan and examples of various gums, such as guar and hakea (from *Hakea gibbosa*), are classified as natural bioadhesive polymer[2].

Chitosan (Figure 1.1b) is a cationic natural linear polysaccharide consisting of copolymers of D-glucosamine and *N*-acetyl-D-glucosamine units linked by β-(1-4)-glycosidic linkages. It is produced commercially by deacetylation of chitin (Figure

1.1a), which present in outer structure in marine crustaceans such as crabs and shrimp. The degree of deacetylation (%DD) has a significant effect on the solubility and rheogical properties of polymer. Chitosan is soluble in dilute acidic solution and gives positively charged with a charge density depending on pH and %DA value.

Chitosan is reportedly hydrophilic, nontoxic, biocompatible, and biodegradable. Other properties include adsorption, anti-microbial, and mucoadhesive properties. It is therefore considered to be suitable for application in pharmaceutical technology [7]. The primary amino group of CS allows for relatively easy chemical modification and salt formation with acids. The applications of chemically modified CS for improved characteristics include biomedical applications, such as drug delivery [8, 9], gene delivery carriers [10], wound healing accelerators [11] and tissue engineering scaffolds [12].
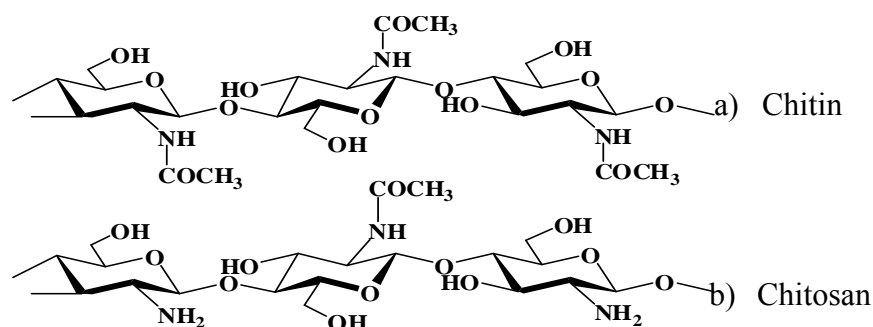
Figure 1.1 Structure of chitin, and chitosan

Among the carbohydrates generally used in the pharmaceutical field, the semi-synthetic cationic polymer chitosan has a well-known bioadhesive nature, by the establishment of electrostatic interactions with sialic groups of mucins in the mucus layer. It was also demonstrated that chitosan can enhance the absorption of hydrophilic molecules by promoting a structural reorganisation of the tigh juncion-associated proteins [13].

In order to improve its mucoadhesive property, various quaternized CS (QCS) compositions, which are partially quaternized derivatives of CS, have been synthesized [14]. In QCS the amount (density) of fixed and pH independent positive charges on the polymer chain is increased, causing expansion and allowing it to not

only interact with the negatively charged mucin glycoproteins, which endows it with mucoadhesive properties [15], but it also increases the solubility of CS in water at neutral and basic pH values [16].

The new generation of mucoadhesives can adhere directly to the cell surface, rather by means of specific receptors or covalent bonding instead of non-specific mechanisms, which are characteristic of the previous polymers. Through a covalent attachment between a cysteine residue of mucin and a polymer of chitosan, a new generation of mucoadhesive polymers have been created. The modified polymer, which contain a thiol bond, exhibit mucin-improved bioadhesive properties. Recently, it could be shown that polymers with thiol groups provide much higer adhesive properties than polymers generally considered to be mucoadhesive [17, 18]. The enhancement of mucoadhesion can be explained by the formation of covalent bonds between the polymers and the mucus layer which are stronger than non-covalent bonds. The thiolated polymers, or the so-called thiomers (Figure 1.2a) , are supposed to interact with cysteine-rich subdomains of mucus glycoproteins via disulfide exchange reaction[19] (Figure 1.2b).
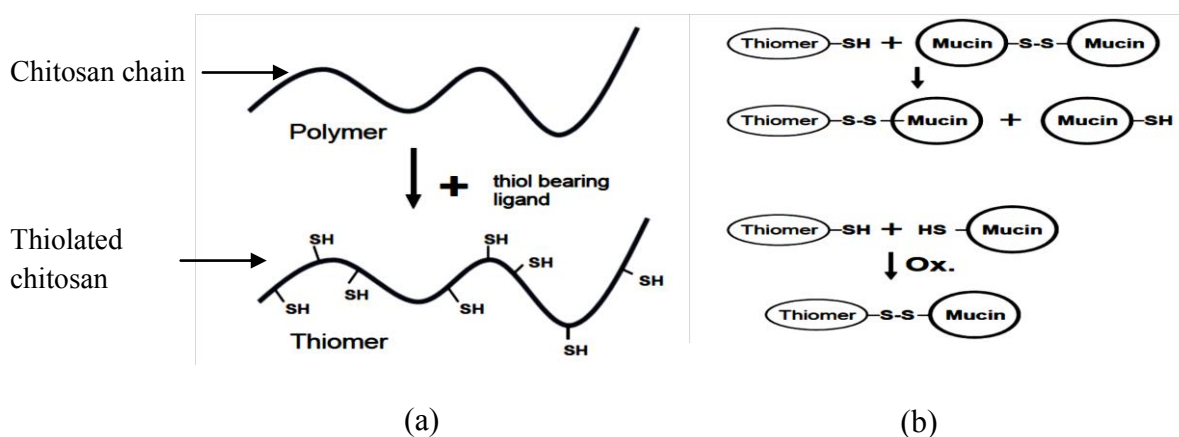
Figure 1.2 Structures of (a) thiolated chitosan and (b) mechanism of disulfide bond formation between thiomers and mucus glycoproteins (mucins)

In order to further enhance the mucoadhesive properties of chitosan, different chitosan derivatives have been developed based on various therories explaining the

mechanism of mucoadhesion. By applying the known concept of the immobilization of thiol groups to the primary amino groups of chitosan, the above-mentioned properties of the polymer were strongly improved [20]. Some research have found that mucoadhesive polymers provide a much higher adhesive properties after thiol group attachment [21]. The explanation for this observed enhancement of the mucoadhesion is that the formation of the covalent bonds between the thiol groups of the polymer and the cysteine-rich subdomains of the mucus layer are stronger than the non-covalent bonds. These thiolated CSs, such as CS-thioglycolic acid conjugates [18, 22, 23], CS-cysteine conjugates [24] and CS-iminothiolane [25], are supposed to interact with the cysteine-rich subdomains of the mucus glycoproteins via disulfide exchange reactions [19].

The aim of this work was to prepare a mucoadhesive polymer that would be potentially suitable for application in a mucoadhesive drug delivery system. Therefore we aim to improve mucoadhesive property by grafting homocysteine thiolactone (HT) onto chitosan and quaternizedchitosan chain.
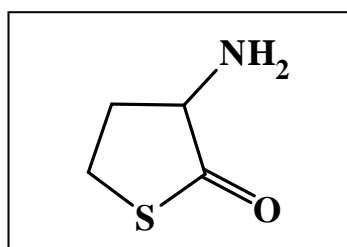
Figure 1.3 Structures of homocysteine thiolactone

Homocysteine thiolactone (HT) (Figure 1.3) was discovered by serendipity in 1934 as a by-product of the digestion of methionine with hydriodic acid, a produre used then for the determination of protein methionine. HT is a product of homocysteine metabolism by mothionyl-tRNA systhetase in all cell types[26].

The modified of chitosan by HT was to improve mucoadhesive properties of unmodified chitosan. The product obtained chitosan-homocysteine thiolactone (CS-HT) and quater nizedchitosan-homocysteine thiolactone (QCS-HT) (Figure 1.4) has

large amount of hydrophilic side chain, high molecular weight, chain flexiblility. Moreover, HT have specialized functional groups which is thiol goups that form disulfide covalent bond with cysteine rich-subsomain of mucus glycoprotein to enhance mocoadhesive properties in the preparation of pharmaceutical products.
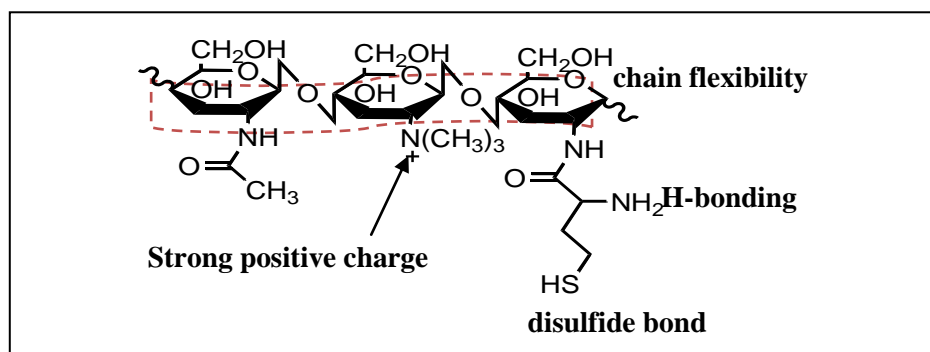
Figure 1.4 Influence of polymer to mucoadhesive properties

Camptothecin (CPT) (figure 1.5), a natural plant akaloid extracted from *Camptotheca acuminate*, has been shown to be a potent, anticancer agent acting through the inhibition of topoisomerase I during the S-phase of the cell cycle. CPT and CPT analogs are increasingly in clinical use and show great utility in the treatment of various cancer including primary and metastatic colon carcinoma, small cell lung carcinoma, ovarian, breast, pancreatic, and stomach cancer [8]. However, CPT having promising antitumor efficicacy has not been successfully used in cancer therapy because of water insolubility and lactone ring in instability [27]. Because of these inadequacies, many types of drug delivery system have been developed in order to reduce severe systemic toxicities, enhance antitumor effects by improving their phamacokinetics [28].
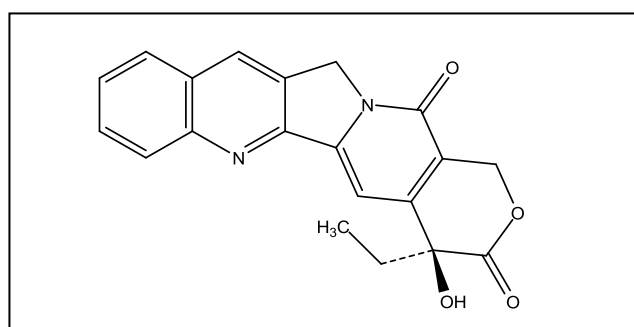
Figure 1.5 Chemical structure of camptothecin

Biodegradable and biocompatible polymeric particles are good candidates to delivery CPT drugs. These systems have been used as potential drug delivery devices because of their ability to protect CPT from degradation. Previous studies showed that the CPT was controlled release upon the incorporation of the drug into a lipid bilayer structure like liposomes [29], microsphere [30], upon conjugation to synthetic polymer [31], nanohybrids [32], and polymer micelles [33, 34]. In this study, the major components for preparing the microspheres were a positively-charged counterpart, chitosan and chitosan derivative and a negatively-charged polymer, alginate (ALG).
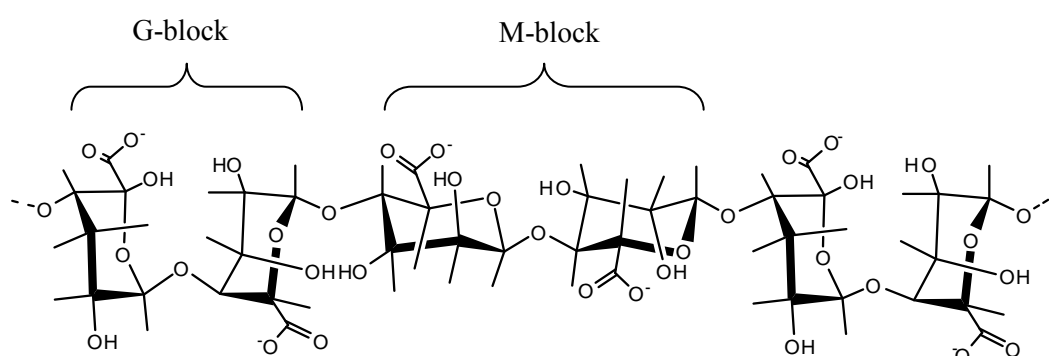
Figure 1.6 Copolymer of α-L-guluronic acid and β-D-mannuronic acid
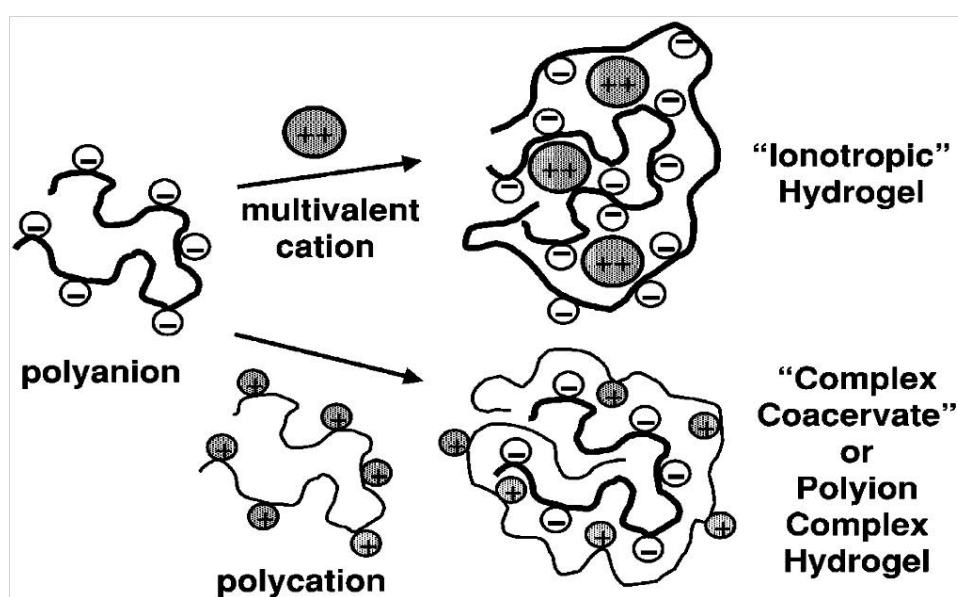
Figure 1.7 A schematic representation of chitosan formed with polyelectrolyte polymer [35].

Alginate (Figure 1.6) is a naturally occurring anionic polymer that is extracted from marine brown algae and consists of linear chains of α-L-guluronic acid (G) and β-D-mannuronic acid (M) residues joined by 1,4-glycosidic linkages. Alginate is widely used in the controlled release of drugs and other chemicals. In some applications, the active ingredient is placed in a calcium alginate bead and slowly released when the bead is exposed in the appropriate environment.

Oppositely charged polyelectrolytes bound together by electrostatic interaction are defined as polyelectrolyte complexes (Figure 1.7). has been widely used to obtain devices for the controlled release of drug [36].

Furthermore, drug-polymer complexes can be included in the definition of polyelectrolyte complexes. Embedding of drugs in polymer-polymer actrices as well as polymer-drug associations is of major interest [37].

The alginate/chitosan polyelectrolyte complex that is biocompatibility, non-toxicity and ability to encapsulate many of low molecular drug [36]. Therefore the alginate/chitosan system is suitable for drug delivery system.

Various method for preparation of alginate/chitosan micro/nanoparticles have been reported such as ionotropic gelation [38] and solvent emulsification/internal gelation [39], but the droplet easily agglomerate and coaglulate, moreover they gave a wide size distribution. One of the novel techniques for preparation nanoparticles is known as electrohydrodynamic atomization or electrospray, that a method of liquid of atomization by means of electrical forces. The polymer flowing out of the nozzle in the form of droplet when applied high voltage potential forces (Figure 1.8).
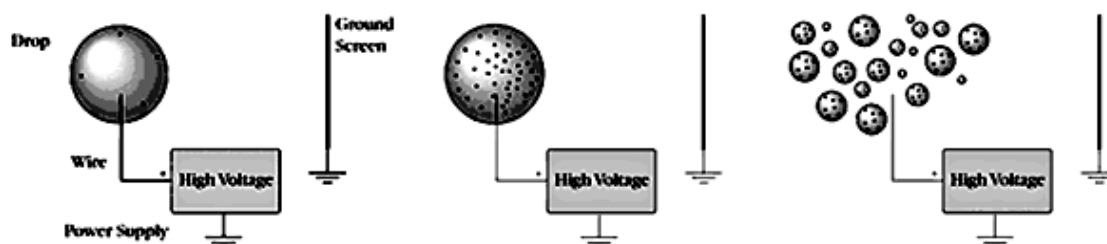
Figure 1.8 The droplet is generated by electrical force[40]

Electrospray systems have several advantages over mechanical atomizers such as the droplet size can be range from hundrate micrometers down to several tens of nanometer, the size distribution of the droplets can be nearly monodisperse, droplet generation and droplet size can be controlled by adjust the flow rate and voltage applied [12]. Moreover the droplet produced by electrospraying are highly charged, that prevents their coaglulation and agglomeration [40]. Electrospray technique has many applications such as fabrication of inorganic nanoparticles, thin films, and fibers, production of pharmaceutical particles, deposition of nanoparticles and generation of micro/nanoencapsulation [41].

The purpose of the present work was to prepare controlled release microsphere of CPT, using CS/ALG and mCS/ALG as the retarding material, by application of electrospray ionization.

Therefore, the aim of this work was to develop the mucoadhesive polymer for application in a mucoadhesive delivery system, especially at the low pH environment. Therefore, thiolatedchitosan was developed from CS by covalent attatchment homocysteine thiolactone (HT) onto CS and QCS using imidazole as a reactive intermediate to improve mucoadhesive property compared with unmodified chitosan as shown in Scheme1. The prepared thiolatedchitosan was characterized by FTIR, NMR, XRD, and TGA. Degree of thiol subsitution was found out using Ellman's method. Moreover, the *in vitro* mucoadhesion properties was evaluated by periodic-acid schiff (PAS) method, these properties have been assessed by evaluation of the interaction between chitosan and mucin in various aqueous solution. Furthermore, the swelling properties of modified chitosan were investigated in 0.1N SGF pH1.2, 0.1 N pH4.0, and 0.1N SIF pH 6.4.
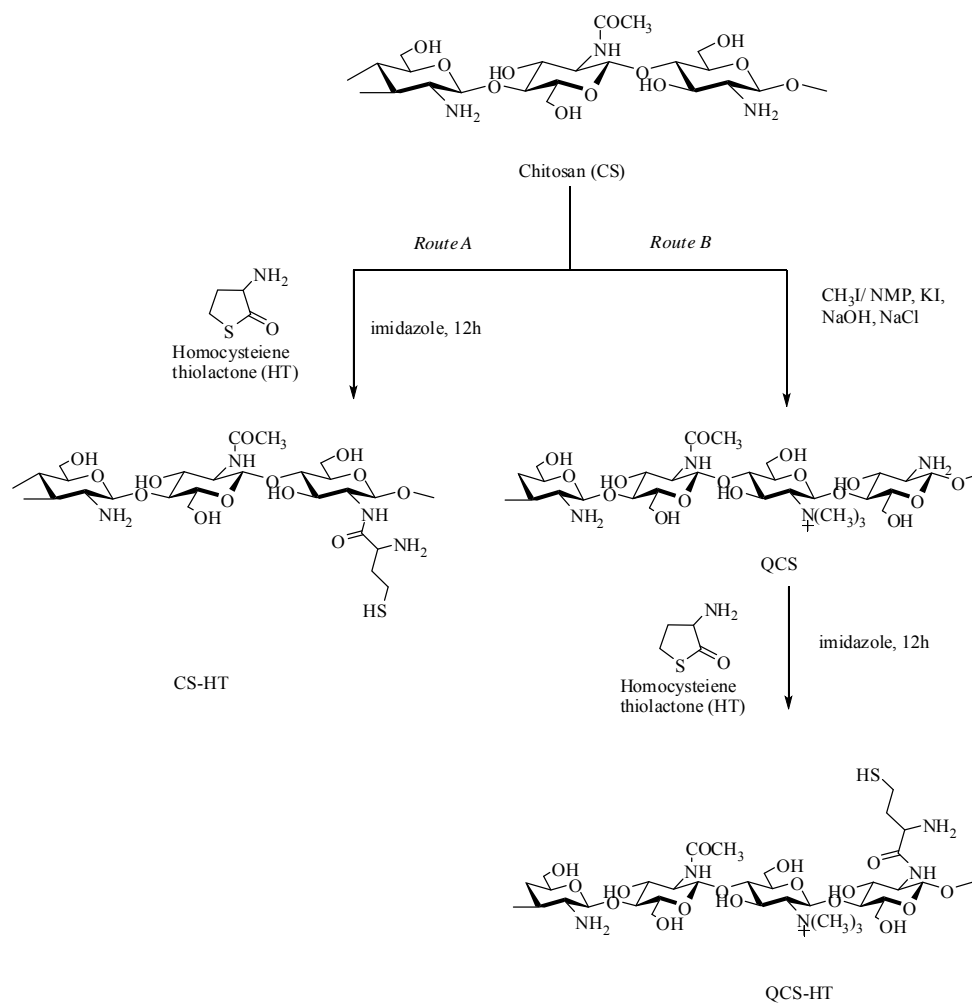
Figure 1.9: Synthesis scheme of CS-HT (*route A*) and QCS-HT (*route B*)

Additionally, the release profiles of model drug (camptothecin) from microspheres (Figure 1.9), which is prepared by electrospray ionization technique were studies. Characterization of the obtained microspheres in terms of morphology, size and size distribution, zeta potential, chemical analysis and thermal behavior. Study the *In vitro* release behavior of the spheres in various pH buffers (pH1.2, 4.0, and 6.4). All methods were followed to figure 1.11.
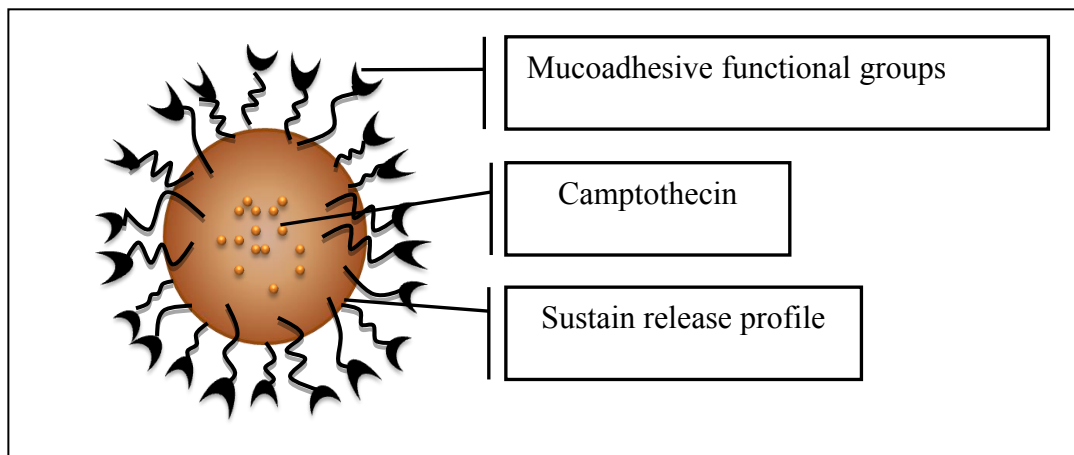
Figure 1.10 Schematic of drug loaded mucoadhesive microspheres

1.2 The objectives of this research

1) To improve mucoadhesive property of chitosan

2) To investigate the possiblity of using modified chitosan as a drug delivery carrier

1.3 The scope of research

The scope of this research was devided into 2 main steps:

i) Literature review of related research works

ii) Modifying chitosan

    a. Preparation of thiolated chitosan

    b. Characterization of the physical and chemical properties of chitosan and modified chitosan usign FTIR, ^{1}H-NMR, ^{13}C-NMR, TGA, XRD, degree of quaternization, and determination degree of thiol and disulfide substitution

    c. *In vitro* investigation of mucoadhesive property and swelling behavior in various pH conditions

iii) Fabrication and evaluation of the mCS as a drug delivery carrier

    a. Preparation of the microspheres with and without drug

    b. Characterization of the obtained microspheres in terms of morphology, size and size distribution, zeta potential, chemical analysis and thermal behavior.

    c. Determination of the drug encapsulation efficiency

    d. Study the *In vitro* release behavior of the spheres by using UV-Vis method

iv) Report, Discussion and Writing up thesis.
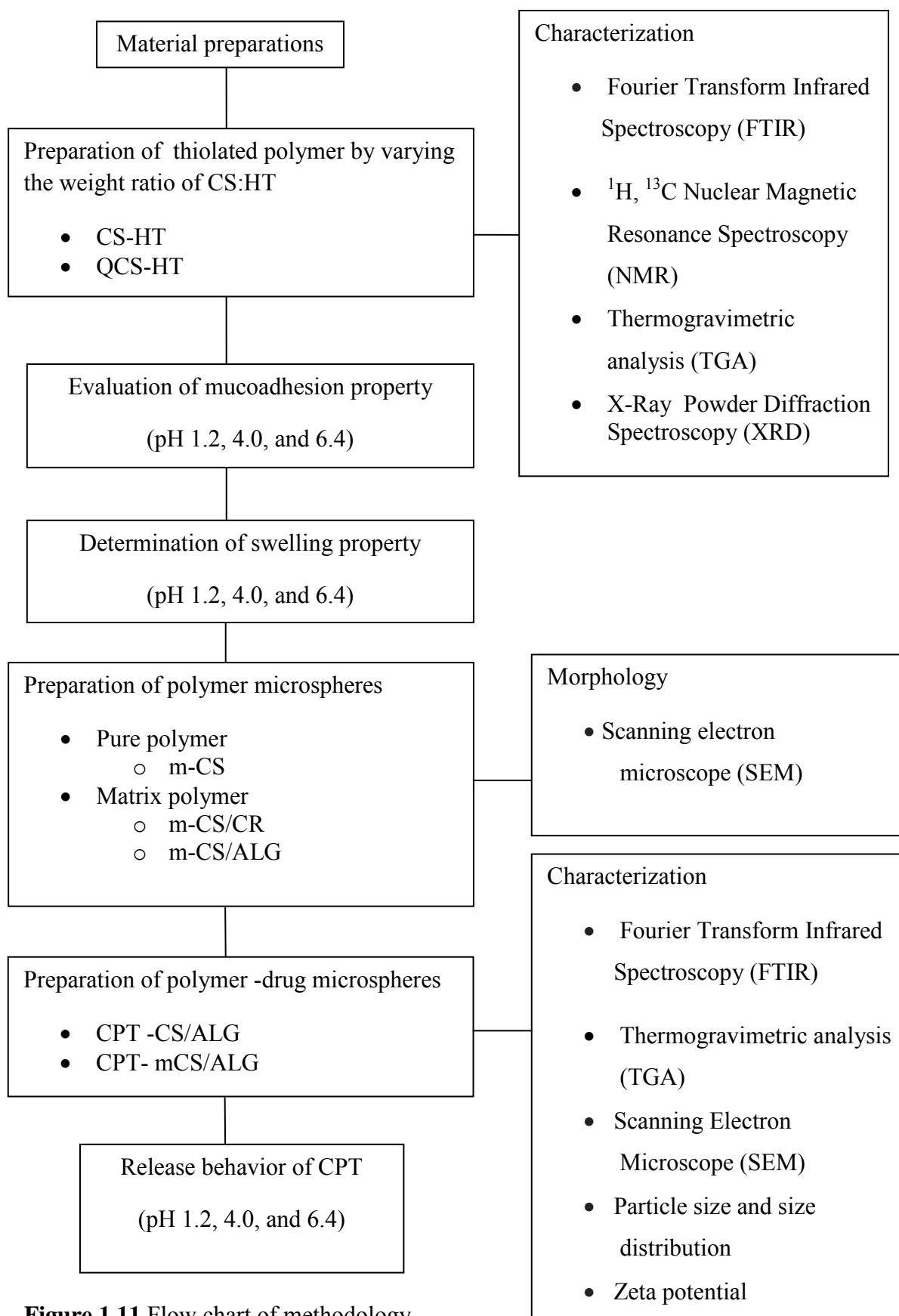
Figure 1.11 Flow chart of methodology

CHAPTER II

BACKGROUND AND LITERATURE REVIEWS

2.1 Mucoadhesion/ bioadhesion

In 1986, Longer and Robinson defined the term "bioadhesion" as the "attachment" of a synthetic or natural macromolecule to mucus and/or an epithelial surface" [1]. The general definition of adherence of a polymeric material to biological surfaces (bioadhesives) or to the mucosal tissue (mucoadhesives) still holds. Therefore, mucoadhesive polymer has been interesting as a promising strategy to prolong the residence time and improve the specific localization of drug delivery systems on various membrances [2].

2.1.1 The mucoadhesive interaction

Mucus is a complex viscous adherent secretion which is synthesized by specialized goblet cells. Mucus is composed mainly of water (>95%) and mucins, which are glycoproteins of exceptionally high molecular weight. Furthermore, pendant sialic acid and sulphate groups located on the glycoprotein molecules result in mucin behaving as an anionic polyelectrolyte at neutral pH [3, 4]. Other non-mucin components of mucus include secretory lysozyme, lactoferrin, lipids, polysaccharides, and various other ionic species [3].

For adhesion to occur, molecule must bond across the interface. These bonds can arise in the following way [5].

1. Ionic bonds

A bond formed by the interaction between two oppositely charged ions (*e.g.* in a salt crystal).

2. Covalent bonds

A bond formed by the sharing of pairs of electrons between atoms. These are also strong bonds (*e.g.* thiomer).

3. Hydrogen bonds

A bond is the interaction of a hydrogen atoms with an electronegative

atoms such as oxygen, fluorine or nitrogen. The hydrogen bond is stronger than Van–der– Waals bonds and weaker than ionic or covalent bonds.

4. Van – der – Waals bonds

The Van – der – Waals bonds are weak compared the chemical bonds. The bond formed of interaction from dipole – dipole and dipole – induced dipole attractions in polar molecule, and dispersion forces with non – polar substances.

5. Hydrophobic bonds

The bond that occur when non – polar groups are present in an aqueous solution. Water molecule adjacent to non – polar groups form hydrogen bonded structure, which lowers the system entropy. There is therefore an increase in the tendency of non – polar groups to associate with each other to minimize this effect.

2.1.2 Mucoadhesion theories of polymer attachment

Mucoadhesion is a complex process and numerous theories have been presented to explain the mechanisms involved[3, 6].

1. The wettability theory

The ability of bioadhesive polymer to spread spontaneously onto surface and develop intimate contact with the mucus membranes. The wettability theory is mainly applicable to liquid or low viscosity mucoadhesive systems and is essentially a mesasure of the spreadability of the delivery system across the biological subtrate.

2. The electronic theory

This theory describes adhesion occuring by menas of electron transfer between the mucus and the mucoadhesive system arising through differences in their electronic sturctures. The electron transfer between the mucus and the mucoadhesive rusults in the formation of double layer of electrical charges at the mucus and mucoadhesive interfiace.

3. The fracture theory

The fracture theory relates the force for polymer detachment from the mucus to the strength of their adhesive bond. The work fracture has been found to be greater

when the polymer network strands are long or if the degree of cross-linking within such as system is reduced.

4. The adsorption theory

In this instance, adhesion is defined as being the result of various surface interactions (primary and secondary bonding) between the adhesive polymer and mucus substrate. Primary bonds due to chemisorption rusult in adhesion due to ionic, covalent and metalic bonding, which is generally undesirable due to their permanency. The secondary bonds arise mainly due to van der Waas forces, hydrophobic interactions and hydrogen bonding.

5. The diffusion-interlocking theory

This theory proposes the time-dependent diffusion of mucoadhesive polymer chains into the glycoprotein chain network of the mucus layer. This is a two-way diffusion process with penetration rate being dependent upon the diffusion coefficients of both interaction polymers.

2.1.3 Mucoadhesion dosage forms

In considering the mechanism of mucoadhesion, the mucoadhesive bond formation are possible (Figure 2.1). These include:
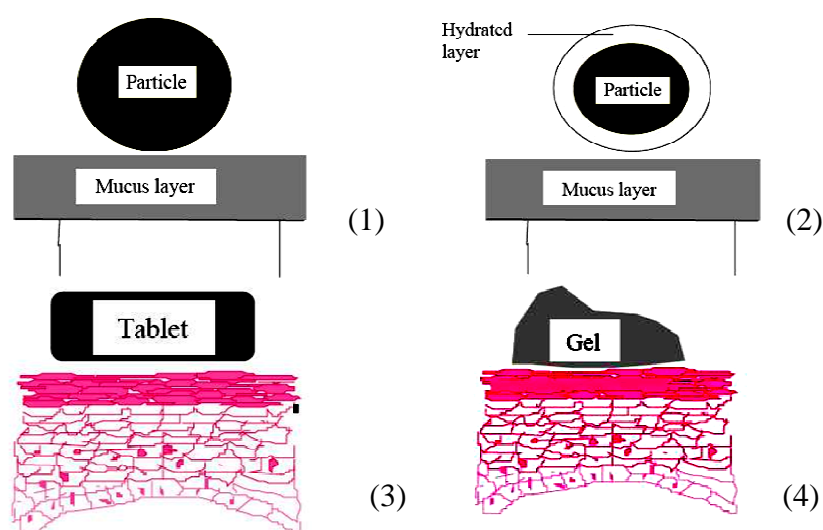
Figure 2.1 Some scenarios where mucoadhesion occur[7]

(1) Dry or partially hydrated dosage forms contacting surfaces with substantial mucus layers (typically particulates administered into the nasal cavity).

(2) Fully hydrated dosage forms contacting surfaces with substantial mucus layers (typically particulates of many 'First Generation' mucoadhesives that have hydrated in the luminal contents on delivery to the lower gastrointestinal tract).

(3) Dry or partially hydrated dosage forms contacting surfaces with thin/discontinuous mucus layers (typically tablets or patches in the oral cavity or vagina).

(4) Fully hydrated dosage forms contacting surfaces with thin/discontinuous mucus layers (typically aqueous semisolids or liquids administered into the oesophagus or eye).

In the study of adhesion generally, the adhesive process have been two steps identified, the interaction between mucoadhesive materials and a mucous membrane are shown in Figure 2.2 [5]

Step 1 Contact stage: An intimate contact (wetting) occurs between the mucoadhesive and mucous membrane

Step 2 Consolidation stage: Various physicochemical interaction occur to consolidate and strengthen the adhesive joint, leading to prolonged adhesion.
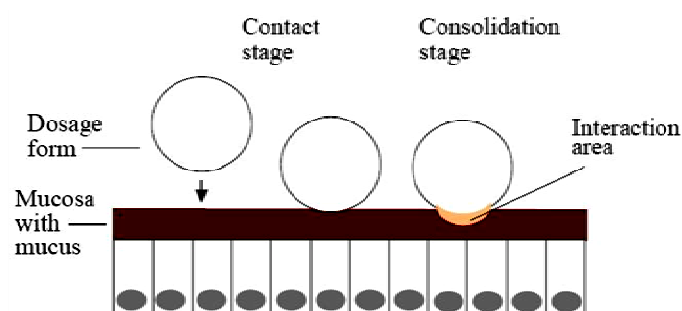
Figure 2.2 The two stages in mucoadhesive[5]

2.1.4 Polymer in pharmaceutical field

Polymers are becoming increasingly important in field of pharmaceutical industry as both drug encapsulants and vehicles of drug delivery in order to either protect an active agent during its passage through the body until its release, or control its release. Carrier technology obtained the drug delivery system by coupling the drug to the carrier polymers in various dosage forms such as beads, microspheres, nanoparticles, liposomes. Those formulations could delay the release of drug and also generate a response in a specific area or organ of the body requiring treatment. Moreover, a target drug, encapsulated in a polymer can be released sustainedly to improve drug therapeutic efficacy and decrease the dosing time and side effect [11].

Naturally occurring polymers are attractive as drug delivery system since they possess the biocompatibility, biodegradability and non-toxicity required for used in human [41].

2.1.5 Mucoadhesive polymers

Mucoadhesive polymers have been also used for coating medical devices. As an example a new generation of intestine inspection device has been recently developed in which mucoadhesive polymer coating make intestinal locomotion possible.

Numerous polymers adhere to mucosal tissues. These include synthetic polymers, for instance, poly(acrylic acid) (PAA) [44], hydroxypropyl methylcellulose, poly(methylacrylate) derivatives and thiolated polymers [45], as well as naturally occurring polymers such as hyaluronic acid [46] and CS [47]. Among these various possible bioadhesive polymeric hydrogels, PAA has been considered as a good mucoadhesive. However, due to a high transition temperature and higher interfacial free energy, PAA does not wet the mucosal surface to the optimal level, causing loose interdiffusion of the polymer. Therefore, PAA is copolymerized with polyethylene glycol (PEG) or poly(vinyl pyrrolidone) (PVP) to improve these properties. It is important to realise that balanced adhesive and cohesive properties for a polymer is

essential for its application in a transmucosal drug delivery systems, especially for the removable devices.

Table 2.1 The relative bioadhesive property of various polymers [8]

Polymer	Bioadhesive property
Poly(acrylic acid) (neutralized)	+++
Carbomer (neutralized)	+++
Hyaluronan	+++
Chitosan	++
Na carboxymethylcellulose	++
Poly(galacturonic acid)	++
Na alginate	++
Pectin	++

NOTE: +++ : Excellent

++ : Good

2.2 Controlled release system
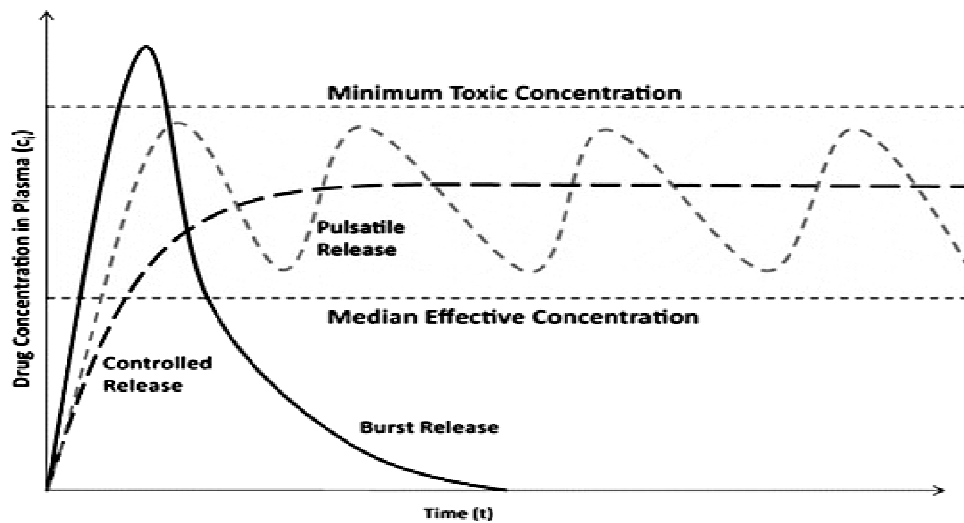
Figure 2.3 A schematic drawing illustrating the controlled (zero-order) drug release.

The means by which a drug is introduced into the body is almost as important as the drug itself. Drug concentration at the site of action must be maintained at a level that provides maximum therapeutic benefit and minimum toxicity (Figure 2.3). The pharmaceutical developer must also consider how to transport the drug to the appropriate part of the body and, once there, make it available for use [9]

Controlled drug delivery (Figure 2.4) occurs when a polymer is combined with the drug or other active agents in such a way that the active agent is released from the material in a predesigned manner.
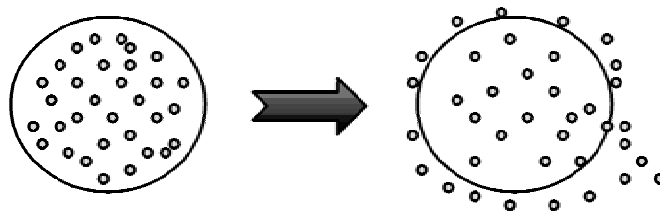
Figure 2.4 Presentation of controlled release system

The drug can be released from the system by 3 mechanisms[10].

1) **Diffusion Controlled Release** (Figure 2.5a)

Diffusion occurs when drug molecules pass from the polymer matrix to the external environment. As the release continues, its rate normally decreases with this type of system, since drug has progressively longer distance to travel and therefore requires a longer diffusion time to release.

2) **Swelling Controlled Release** (Figure 2.5b)

The swelling of the carrier increases the aqueous solvent content within the polymer matrix, enabling the drug to diffuse through the swollen network into the external environment. Most of materials used are based on hydrogel. The swelling can be triggered by a change in the environment surrounding such as pH, temperature, ionic strength, etc.

3) **Erosion Controlled Release** (Figure 2.5c)

The drug can be released from the matrix due to erosion of polymers, which can be classified into 2 types.

Bulk erosion: The polymer degrades in a fairly uniform manner throughout the polymer matrix.

Surface erosion: The degradation occurs only at the surface of the polymer device.
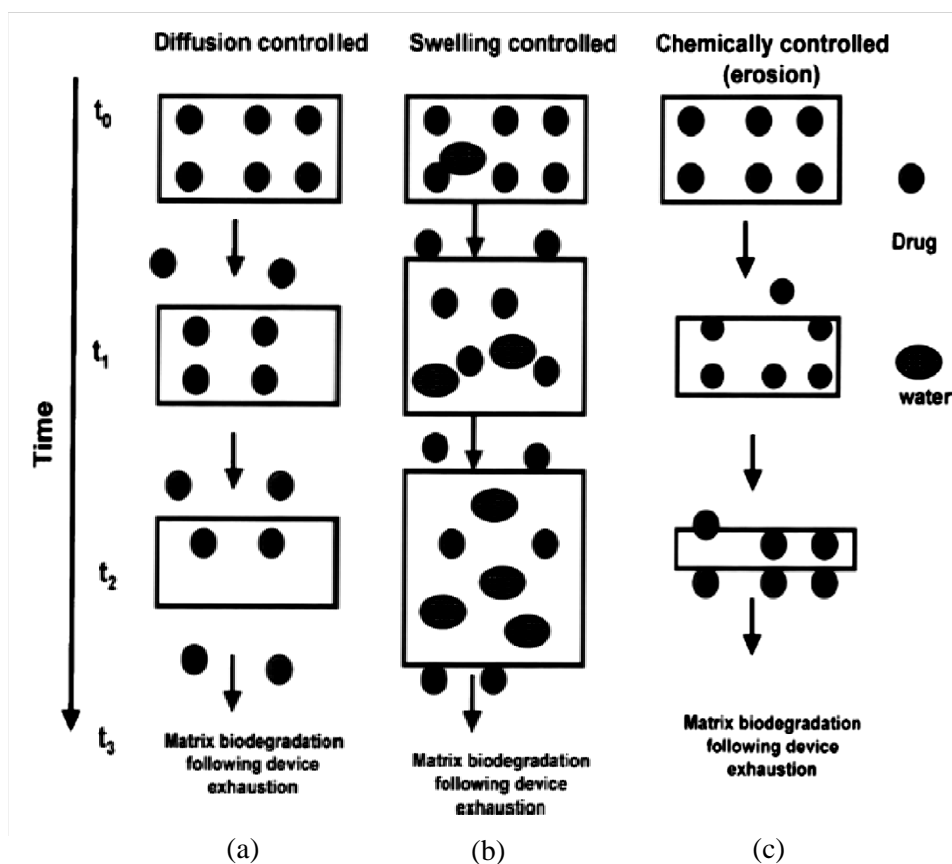
Figure 2.5 A schematic drawing illustrating the three mechanisms for controlled drug release from a polymeric matrix [10]

2.3 Cancer

Cancer is a generic term use for diseases caused by unregulated proliferation of cells and are able to invade other tissue (Figure 2.1). Cancer affects people at all ages with the risk for most types increasing with age. According to World Health Organization (WHO), it is causing 7.6 million deaths every year or 13% of deaths worldwide in 2007. Deaths from cancer worldwide are projected to continue rising, with an estimated 12 million deaths in 2030. In addition, it is the second major cause of death following cardiovascular diseases [32]. The total number of cases of cancer is predicted to increase in between 2000 and 2020 by 73% in the developing countries and by 27% in the developed countries [33]. In Thailand, the rate of people dying

from cancer is still increasing every year and it is the first leading cause of death [34]. There are various methods of treatment for cancer such as: surgery, radiation therapy, immunotherapy and biologic therapy, chemotherapy and etc.

Chemotherapy is a kind of cancer treatment that uses of drugs to eliminate cancer cells. It is most effective against cancers that divide rapidly and have a good blood supply. Chemotherapy is most commonly given by pill or intravenously, but can be given in other ways. However, the administered of drug will be depend on the most effective way to treat your cancer and on the chemical properties of the drug. Many of the currently effective anti cancer drugs are used in the clinical activity such as: etoposide, taxol, doxorubicin and etc
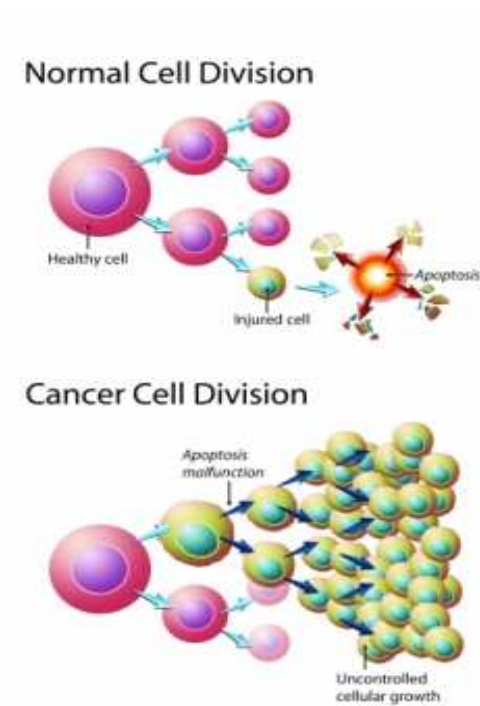
Figure 2.6 Cell division of normal and cancer cell [11]

2.4 Camptothecin

Camptothecin (CPT) is a cytotoxic quinoline alkaloid which inhibits the DNA enzyme topoisomeras I (topoI). It was discovered in 1966 by M.E. Wall and M.C. Wani in systematic screening of natural products for anticancer drugs. It was isolated from the bark and stem of *Camtotheca acuminata* (Campthotheca, Happy tree), a tree antive to China. CPT showed remarkable anticancer activity in preliminary clinical trials but also low solubility and (high) adverse drug reaction. Because of these disadvantages synthtic and medicinal chemists have developed numerous syntheses of Campthothecin and various derivatives to increase the benefits of the chemical.

2.4.1 Structure

CPT has a planar pentacyclic ring structure, that includes a pyrrolo [3,4-β]-quinoline moiety (ring A,B and C), conjugated pyridone moiety (ring D) and one chiral center at position 20 within the alpha-hydroxy lactone ring with (S) configuration (the E-ring). Its planar structure is thought to be one of the most important factors in topoisomers inhibiton.
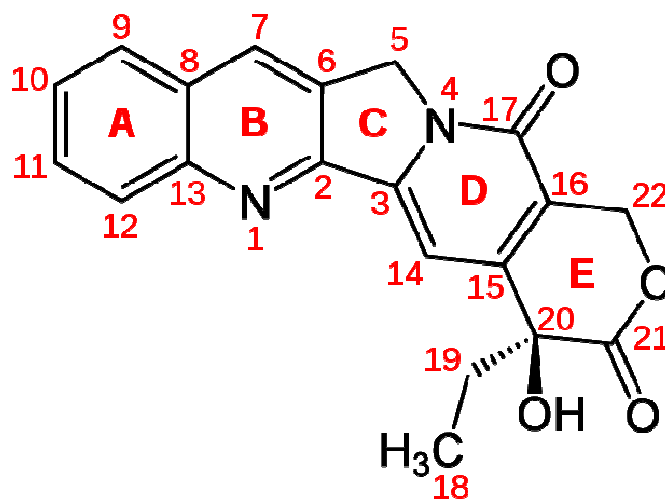
Figure 2.7 Chemical structure of CPT

2.4.2 Binding

CPT binds to the topo I and DNA complex (the covalent complex) resulting in a ternary complex, and thereby stabilizing it. This prevents DNA re-ligation and

therdfore causes DNA damage which results in apoptosis. CPT binds both to the enzyme and DNA with hydrogen bonds. The most important part of the structure is the E-ring which interacts from three differents postions with the enzyme.The hydroxyl group in position 20 forms hydrogen bond to the side chain on aspartic acid in the enzyme.

2.4.2 Physical and chemical properties

The lactone ring in CPT is highly susceptible to hydrolysis. The open ring form is inactive and it must therfore by closed to inhibit topo I. The closed form is fovored in acidic condition, as it is in many cancer cells microenvironment. CPT is transported in to the cell by passive diffusion. Cellular uptake is favored by lipophilicity, which enhances intracellular acumulation.

2.4.3 Topoisomerase

Topoisomerases are enzyme that regulate the overwinding or underwinding of DNA. The winding problem of DNA arised due to the intertwined nature of its double helical structure.Fore examle, during DNA replication, DNAbecomes overwound ahead of a replication fork. If lelf unabated, this tension would eventually grind replication to a halt.

In order to help overcome these types of topological problem caused by the double helix, topoisomierase bind to either single-stranded or double-stranded DNA and cut the phosphate backbone of the DNA. This intermediate break allows the DNA to be untagnled or unwound, and, at the end of these processes, the DNA backbone is resealed again. Since the overall chemical composition and connectivity of the DNA does not change, the tangled and untangled DNAs are chemical isomers, differing only in their globle topology, thus their name. Topoisomerases are isomerase enzymes that act on the topology of DNA.

2.5 Electrospray deposition technique/ Electrospray ionization technique

Electrospray (electrohydrodynamic spraying) is a method of generating a very fine droplet through electrical force (Figure 2.8). In this process, liquid flowing out from a capillary nozzle maintained at high potential, is subjected to an electric field, which causes elongation of the meniscus to a form of jet or spindle. The jet deforms and disrupts into droplets due mainly to electrical force. In the electrospraying, no additional mechanical energy, other than that from the electric field alone, is needed for liquid atomization [12] (Figure 2.9).
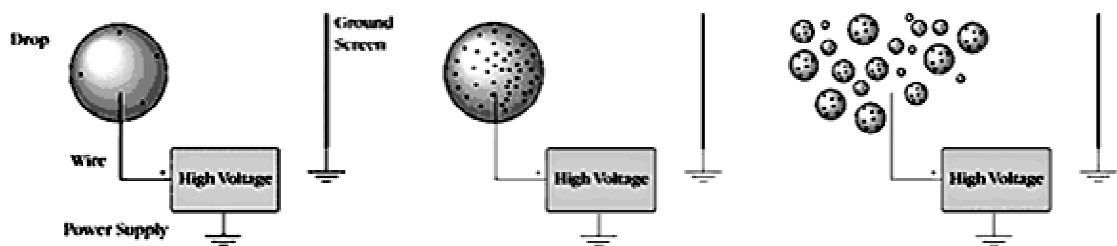
Figure 2.8 The droplet is generated by electrical force [13]

The applications of electrospraying reviewed by Kruis et al. [14], such as the particles size smaller than 10 mm applied for ceramic coatings, paints, or emulsion production, as powder in the cosmetic or pharmaceutical industries, or as toner in electro-reprographic systems. Nowadays, electrospray is involved in nanotechnology and nanoelectronics for thin-film deposition [15].

The electrospraying has some advantages over conventional mechanical spraying systems with droplet charged by induction such as

1. Droplet size is smaller than that available from conventional mechanical atomisers, and can be smaller than 1 mm.

2. The size distribution of the droplets is usually narrow, with small standard deviation that allows production of particles of nearly uniform size.

3. Charged droplets are self-dispersing in space (due to their mutual repulsion), resulting also in the absence of droplet coagulation.

4. The motion of charged droplets can be easily controlled (including deflection or focusing) by electric fields.

5. The deposition efficiency of a charged spray on an object is order of magnitudes higher than for un-charged droplets.
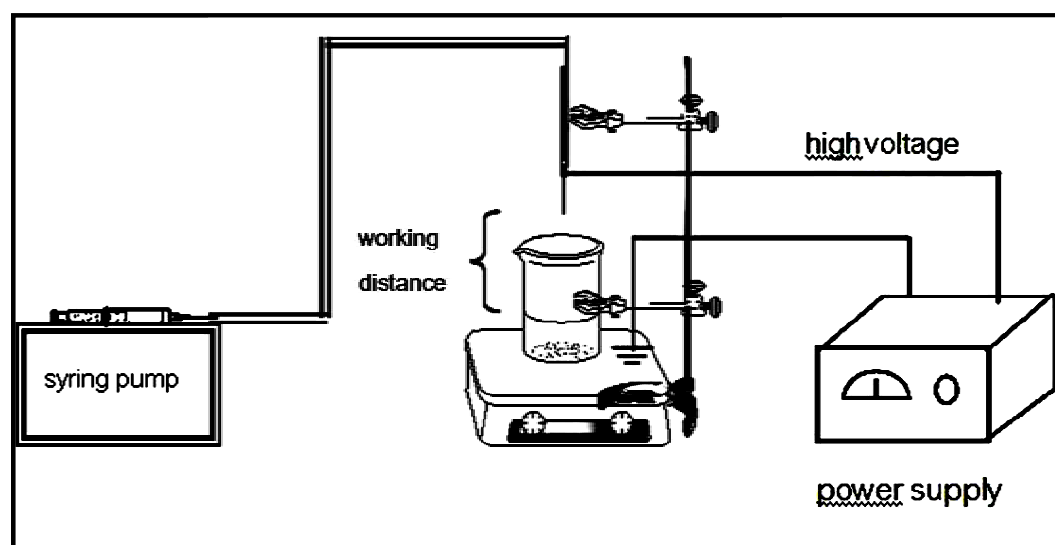
Figure 2.9 Schematic diagram of the instrumentation for electrospray technique

CHAPTER III

EXPERIMENTAL

3.1 Materials

The following materials were obtained from commercial suppliers.

3.1.1 Model drug

(S)-(+)-Camptothecin (CAS number : 7689-03-4, ~95%HPLC, powder obtained by Sigma Aldrich, USA)

3.1.2 Polymers

-Chitosan, food grade, $\overline{M}_w$ 100 kDa., Deacetylation 95 %, Lot No. 497613, (Bonafides, Thailand)

-Sodium Alginate, High $\overline{M}_w$, Lot No. 9005-38-3, (Carlo Erba reagent)

-κ-Carrageenan High $\overline{M}_w$, Lot No. 9015-24-3, (Carlo Erba reagent)

3.1.3 Chemicals

- Ethanol 95 %, commercial grade (Merck, Germany)

- Hydrochloric acid fuming 37%, AR grade (Merck, Germany)

- Lactic acid, AR grade (Union chemicals, Thailand)

- Mucin from porcine stomach (type 2), AR grade (Sigma-Aldrich, USA)

- Potassium dihydrogen phosphate, AR grade (Merck, Germany)

- Potassium bromide, AR grade (Merck, Germany)

- Potassium iodide, AR grade (Merck, Germany)

- Sodium chloride, AR grade (Merck, Germany)

- Sodium hydrogen phosphate, AR grade (Merck, Germany)

- Sodium hydroxide, AR grade (Merck, Germany)

- Sodium tripolyphosphate, AR grade (Sigma-Aldrich, USA)

- Iodomethane, AR grade (Merck, Germany)

- N-methylpyrrolidone, AR grade (Merck, Germany)

- Acetone, commercial grade (Merck, Germany)

- Calcium chloride AR grade, (Carlo Erba Reactifs SA)

- Dialysis membrane with $\overline{M}_w$ cut off at 12,000 – 14,000 Da (Spectrum Laboratories Inc.)

- Cellulose dialysis membrane with $\overline{M}_w$ cut off at 3,500 Da (Spectrum Laboratories Inc.)

3.2 Instruments

Instrument	Manufacture	Model
Diaphragm vacuum pump	Becthai	ME 2
Freeze dryer	Labconco	Freeze 6
FTIR spectrometer	Nicolet	6700
High voltage	Ormond beach	GAMMA
Horizotal shaking water-bath	Lab-line instrument	3575-1
Micropipette	Mettler Toledo	Volumate
NMR spectrometer	Bruker	400 Hz
Scanning Electron Microscope	Philips	XL30CP
Particle sizer	Malvern Instruments	Zetasizer nanoseries
Syringe pump	Pennyful	kdScience
TGA	PerkinElmer	Pyris Diamond
UV-VIS spectrometer	PerkinElmer	Lambda 800
Ultrasonic bath	Ney Ultrasonik	28 H

3.3 Methods

3.3.1 Synthesis of Thiolatedchitosan

3.3.1.1 Synthesis of CS-HT

CS samples were thiolated using HT by covalent attachment, as schematically summarized in Fig. 3.2 *routeA*, using different (w/w) ratios of CS: HT to evaluate the effect of varying this ratio on the properties of the obtained CS-HT. Briefly, 100 mL of 1% (w/v) of CS in 1% (v/v) lactic acid was added to an aqueous solution of imidazole (0.68 g in 2.5 mL water), followed by the drop wise addition of HT (0.05, 0.1, 0.5 and 1.0 g in 100 mL DI water) and stirred at room temperature in a nitrogen atmosphere for 12 h. The reaction mixture was adjusted pH 7, precipitated with excess acetone and harvested by centrifugation (12000 rpm for 2 min). The pellet was resolvated in water and dialyzed (Mw 12-14 kDa) against changes of 1 L of water for 2 days prior to being lyophilized at -30 °C and 0.01 mbar. The dry product was stored at 4°C before use.

3.3.1.2 Synthesis of QCS-HT

The QCS derivatives were prepared from the corresponding CS by methylation as previously reported [58]. Briefly, 100 mL of a 1% (w/v) CS in 1% (v/v) lactic acid solution, 5 mL of 15% (w/v) sodium hydroxide and 30 mL of a 1:1 (v/v) ratio of iodomethane: *N*-methylpyrrolidone were mixed and reacted at 60°C for 45 min with stirring. The resulting QCS was precipitated using 80% (v/v) ethanol and collected by centrifugation (12000 rpm for 2 min). The polymer precipitate was dissolved in aqueous 5% (w/v) NaCl, to exchange I⁻ with Cl⁻, and subsequently precipitated with 80% (v/v) ethanol and (after resolvation in water) 80% (v/v) acetone with collection by centrifugation (12000 rpm for 2 min). The pellet was then air dried.

QCS-HT was synthesized following the route schematically summarized in Fig 3.2B. Firstly, 100 mL of a 1% (w/v) of QCS in 1% (v/v) lactic acid solution was added to an aqueous solution of imidazole (0.68 g in 2.5 mL water), followed by the drop wise addition of HT (0.1% (w/v) aqueous) to the desired final concentration and stirred at room temperature under a nitrogen atmosphere for 12 h. The reaction

mixture was adjusted pH to 7 and then precipitated, dialyzed, lyophilized and stored as described in section 3.3.1.1.
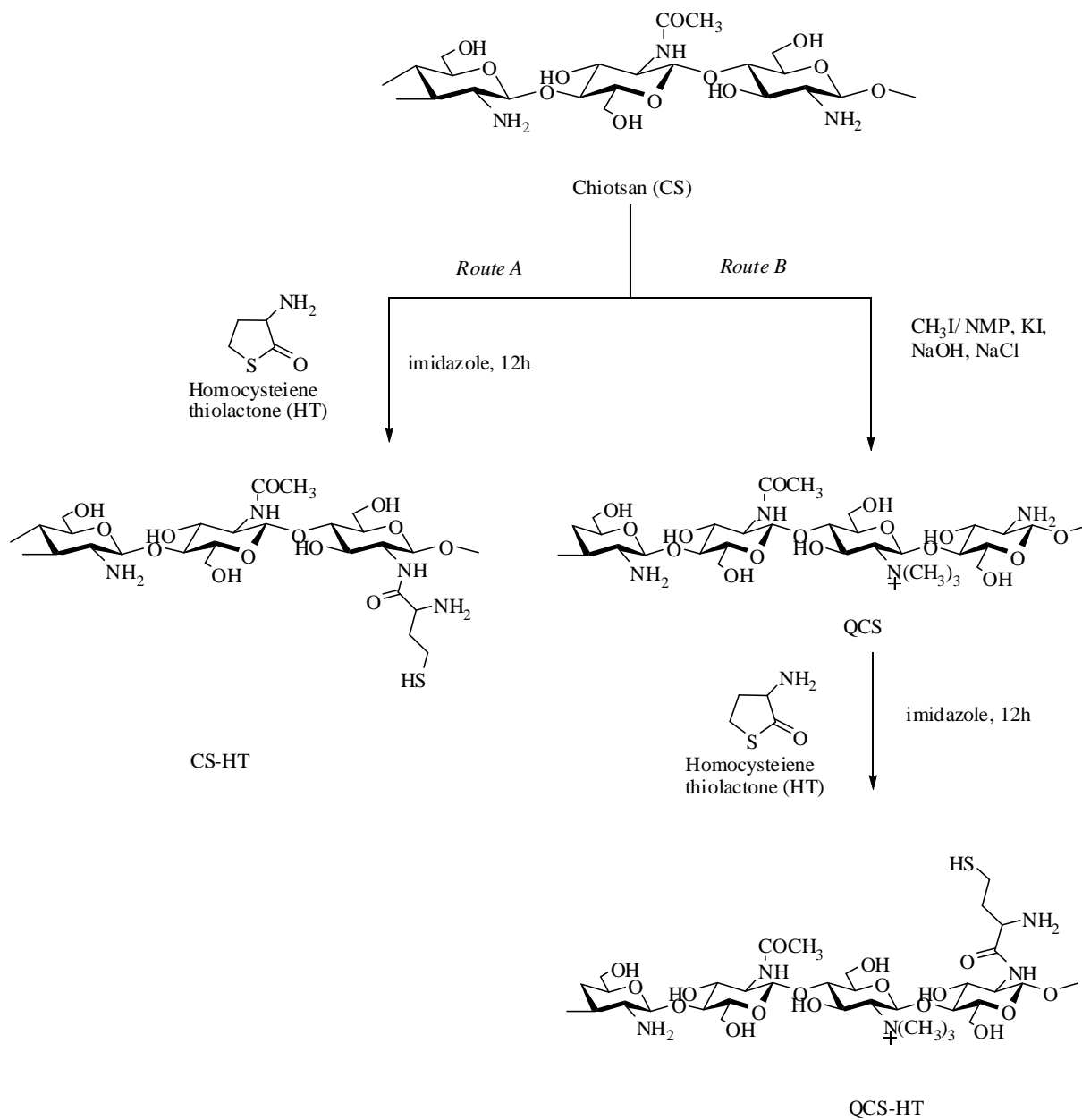
Figure 3.1 Reaction scheme of the covalent attachment of HT onto CS backbone

The thiolated chitosan were prepared by the above mentioned method with varying weight ratios of chitosan to HT. The ratio of chitosan to HT was 1:0.05, 1:0.1, 1:0.5 and 1:1, respectively. The appropriate ratio was selected from the preparation with the highest thiol groups imply that this polymer will give more stronger mucoadhesive than the others feeding ratio. Therefore, this ratio was chosen to be optimal ratio to synthesize QCS-HT derivative for study of mucoadhesive properties.

3.3.2 Chemical characterization

3.3.2.1 Fourier Transformed Infrared Spectroscopy (FTIR)

In order to confirm the formation of the thiolate polymer from HT, i.e. to study the chemical interaction between each of these constituents, samples were analyzed by FT-IR. The CS, HT and two types of thiolated CS derivatives (CS-HT and QCS-HT) were dried and ground into a powder form. The spectra were obtained on KBr pellets in the region from 4000 cm^{-1} to 400 cm^{-1} using a FTIR spectrometer (Nicolet 6700)

3.3.2.2 ^{1}H- and ^{13}C- Nuclear Magnetic Resonance spectroscopy (NMR)

For the characterization of CS and the three CS derivatives (CS-HT, QCS and QCS-HT), about 5-8 mg of each compound were dissolved in 2% (v/v) trifluoroacetic acid (CF$_3$COOH) in deuterium oxide (D$_2$O). ^{1}H-NMR and ^{13}C-NMR spectra were recorded using Bruker NMR spectrometer operated at 400 MHz. The degree of quaternization (DQ) is one of the important characteristics of CS and its derivatives. NMR spectroscopy is considered to yield the most reliable results and so the DQ was calculated using the data obtained from the ^{1}H-NMR spectra according to Eq. as previously described [59, 60].

$$\%DQ = \left[\frac{[(CH_3)_3]}{[H3-H6]} \times \frac{4}{9} \right] \times 100$$

Where, $[(CH_3)_3]$ is the integral of the chemical shift of the trimethyl amino group at 2.96 ppm and [H3-H6] is the integral of the ^{1}H peak between 3.6 and 4.2 ppm.

Determination of the thiol group and disulfide group content

The degree of modification was determined by quantifying the amount of thiol groups on thiolated chitosan was determined spectrophotometrically with Ellman's reagent [22]. First, 0.50 mg conjugated were hydrated in 250 µl of deionized water. Then 250 µL 0.5 M phosphate buffer (pH 8.0) and 500 µL Ellman's reagent (3 mg of 5,5'-dithio-bis(2-nitrobenzoic acid) in 10 mL of 0.5 M phosphate buffer, pH 8) were added. The sample were incubated for 3 h at room temperature. The supernatant was separated from the precipitated polymer by centrifugation (3200 rpm, 5 min). Thereafter 200 µL of the supernatant were transferred to a microtitration plate and the absorbance was measured at a wavelength of 450 nm. with an microtitration plate reader. The amount of thiol moieties was calculated from an according standard curve obtained by chitosan solution with increasing amounts of cysteine HCl standards.

The amount of disulfide bonds within the obtained polymer was evaluated to the following test. Briefly, 0.5 mg of the thiolated polymer was hydrated in 1 mL of 50 mM phosphate buffer pH 8.0 for 30 min. 600 µL of 3% sodium-borohydride solution was added to the polymer solution, and the mixture was incubated for 2 h in an oscillating waterbath. 500 µL of 1M HCl were added in order to destroy the remaining sodium-borohydride. After the addition of acetone (100 µL) the mixture was agitated for 5 min. Thereafter, 1 mL of 1M phosphate buffer pH 8.5 and 200 µL of 0.5% (w/v) DTNB dissolved in 0.5M phosphate buffer pH 8.0 were added. After incubation for 15 min at room temperature aliquots of 200 µL were transferred to a 96-well microtitration plate and the free sulfhydryl groups were determined as decribed above. The amount of disulfide bonds was calculated by subtracting the quantity of free thiol groups as determined by the method described above from the totality of thiol moieties present on the polymer.

3.3.2.3 X-ray powder diffraction (XRD) pattern

The X-Ray powder diffraction (XRD) pattern was performed using a Rigaku X-ray diffractometer Dmax 2200 Ultima at room temperature with a speed scan of 5°/min using CuK-alpha radiation (l = 1.54 Å, 40 kV, 30 mA).

3.3.2.4 Thermogravimetric analysis (TGA)

The thermal stability of each of the samples was evaluated using TGA analysis. These experiments were performed on a PerKinElmer Pyris Diamond TG/DTA machine under a nitrogen flow at a rate of 30 mL/min. Approximately 5 mg of samples were placed in the alumina pan, sealed and heated at 10°C/min from 25 to 500°C.

3.3.3 *In vitro* bioadhesion of mucin to CS and the CS derivative polymers

(a) Mucus glycoprotein assay

The Periodic acid schiff's (PAS) method is widely used for both the quantitative and qualitative analysis of mucins, glycoproteins, glycogen and other polysaccharides in tissues and cells [61]. The PAS colorimetric assay for the detection of glycoproteins was used as previously reported (Mantle and Allen, 1978) for the determination of the free mucin concentration, so as to evaluate the amount of mucin adsorbed onto the CS and its three derivatives. Schiff reagent contained 100 mL of 1% (w/v) basic fuchsin (pararosaniline) in an aqueous solution and 20 mL of 1 M HCl. To this was added sodium metabisuphite (1.67% (w/v) final) just before use, and the resultant solution was incubated at 37°C until it became colorless or pale yellow. Periodic acid reagent was freshly prepared by adding 10 µL of 50% (v/v) periodic acid solution to 7 mL of 7% (v/v) acetic acid solution.

Standard calibration curves were prepared from the four mucin standard solutions (0.125, 0.25, 0.375 and 0.5 mg/mL). After adding 0.1 mL of periodic acid reagent, the solutions were incubated at 37°C for 2 h before 0.1 mL of Schiff reagent was added and incubated at room temperature for 30 min. Next 0.1 mL aliquots of the solution were transferred in triplicate into a 96-well microtiter plate and the

absorbance at 555 nm was recorded. The mucin contents were then calculated by reference to the standard calibration curve.

(b) Adsorption of mucin on CS and the three derivatives (QCS, CS-HT and QCS-HT)

A 0.5% (w/v) mucin solution in each of three broadly isoosmotic solutions that differ in pH, namely SGF (pH 1.2), 0.1 M sodium acetate buffer (pH 4.0) and SIF (pH 6.4) media, were prepared. CS and its three derivatives were dispersed (at 20 mg/1.5 mL final) in the above mucin solutions, vortexed, and shaken at 37°C for 2 h. Then the dispersions were centrifuged at 12000 rpm for 2 min to pellet the CS-mucin or (Q)CS-HT-mucin complex and the supernatant was harvested and used for the measurement of the free mucin content. The mucin concentration was calculated by reference to the calibration curve, and the amount of mucin adsorbed to the microspheres was calculated as the difference between the total amount of mucin added and the free mucin content in the supernatant.

3.3.4 Swelling study of CS and its three derivatives (QCS, CS-HT and QCS-HT)

Films of CS and the three CS derivatives were prepared as follows. A 2 g portion of the CS or derivative (QCS, CS-HT and QCS-HT) was dissolved in 50 mL of 1% (v/v) aqueous lactic acid to yield a 1% (w/v) CS or CS derivative solution, poured into an 8×10 cm tray and air dried. The CS or CS derivative films were then cut into 5.0 mm diameter circles and each one was immersed in one of SGF, SIF or 0.1 N sodium acetate buffers (pH 4.0). The swelling properties were determined by measuring the change in the diameters of each film at various time intervals (0 - 8 h). Equilibrium was assumed to be attained when no further swelling (increase in disc diameter) was measured over time (i.e. at the asymptote of the swelling level *vs.* incubation time plot). The swelling percentage (S_w) for each sample determined at time *t* was calculated from as previously reported [62].

$$S_w = \frac{D_t - D_0}{D_0} \times 100$$

Where, D_t is the film diameter at time t and D_0 is the initial film diameter.

3.4 Pharmaceutcal applications

In order to study a phamaceutical application potential of modified thiolated chitosan (mCS) as a drug delivery system, the sodium alginate (ALG) was used to form polyelectrolyte complex with CS and mCS. The microspheres were prepared by electrospray technique using camptothecin (CPT) as a anticancer drug is the representation model drug for studying the drug delivery system. The properties of drug loaded microspheres, e.g. morphology, particle size, zeta potential, encapsulation effieciency, and drug release profiles were investigated.

3.4.1 Preparation of drugs-loaded polymer microspheres

In order to study phamaceutical application potential of modified chitosan as a drug delivery system, the microspheres using CPT as a model drug. Thiolatedquaternized chitosan (1.0-0.1 w/w) was used to preparaed microspheres due to mucoadhesion at all pH showed the highest than all formulations.

Modified thiolated chitosan/alginate microspheres were prepared by electrospray technique follows to figure 3.2. Camptothecin (CPT) dissolved with DMSO and transferred to alginate solution 1% w/w. A 10 mL of 0.25 mg/mL alginate solution with and without CPT is ejected from a reservoir using a syringe pump into a syringe-nozzle system. A high electric field applied to the polymer solution in the syringe. Droplets fall into a coagulant bath containing 50 mL of 1 mg/mL $CaCl_2$ solution and 2.5 mL of 1 mg/mL of CS or mCSsolution, stirred at 400 rpm for 30 min. The microspheres were separated by centrifugation at 12,000 for 5 min and washed by DI for 3 times.
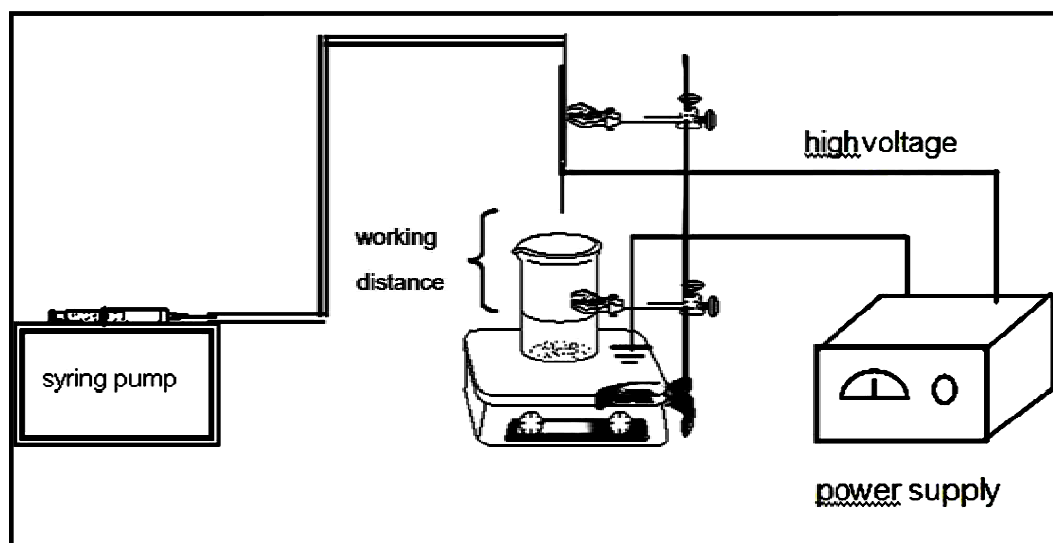
Figure 3.2 Preparation of CPT loaded CS/ALG and mCS/ALG microspheres

Table 3.2   The conditions for the microspheres preparation

Applied voltage (kV)	12
Flow rate (mL/h)	1.2
Needle gauge (G)	26
Working distance (cm)	8

3.4.2 Characterization of the microspheres

3.4.2.1 Scanning Electron Microscope (SEM)

The morphology and surface appearance of the spheres (before and after the drug loading) were examined by SEM. The sample was mounted onto an aluminum stub using double-sided carbon adhesive tape and coated with gold-palladium. Coating was achieved at 18 mA for at least 4 min. Scanning was performed under high vacuum and ambient temperature with beam voltage of 10-20 kV.

3.4.2.2 Particle size measurement

The particle size and size distribution of microspheres were evaluated with a particle size analyzer after suspension of the microspheres in an aqueous 5% (w/v) sodium tripolyphosphate solution. The particle size calculation was based on dynamic light scattering (DLS) method, as a software protocol. The scattered light was collected at an angle of 90° through fiber optics and converted to an electrical signal by an avalanche photodiode array (APDs). All samples were sonicated and run in triplicate with the number of runs set to five and run duration set to 10 seconds.

3.4.2.3 Zeta potential

Zeta potential of the microspheres were determined using particle sizer. The analysis was performed at a scattering angle of 90°. All samples were sonicated and run in triplicate with the number of runs set to 5 and run duration set to 10 seconds.

3.4.2.4 Fourier Transform Infrared (FTIR) Spectroscopy

The FTIR spectra of the microspheres were examined by using the potassium bromide disk (KBr) method with a Fourier transform infrared (FTIR) spectrometry in the range of 4000-400 cm^{-1}.

3.4.3 Study of the drug behavior of the microspheres

3.4.3.1 Calibration curve of CPT in dimethylsulfoxide (DMSO)

The standard stock CPT solution was prepared in 1% (v/v) DMSO. CPT 5 mg was accurately weighed and dissolved with 1% (v/v) DMSO into 50 mL volumetric flask and adjusted to volume (100 ppm).

The stock CPT solution was diluted to 10, 20, 30, 40, and 50 ppm with 1% (v/v) DMSO in volumetric flask.

The absorbance of standard solution was determined by UV-Vis spectrophotometer at 370 nm. The 1% (v/v) DMSO was used as a reference solution. The absorbance and calibration curve of CPT in 1% (v/v) DMSO was shown in appendix 1C

3.4.3.2 Calibration curve of CPT in various buffers (pH 1.2, 4.0, and 6.4)

The standard stock CPT solution was prepared in 1% (v/v) DMSO in pH 1.2, 4.0, and 6.4. CPT 5 mg was accurately weighed and dissolved with 1% (v/v) DMSO into 50 mL volumetric flask and adjusted by various buffers to volume (100 ppm).

The stock CPT solution was diluted to 10, 20, 30, 40, and 50 ppm with three different buffers in volumetric flask.

The absorbance of standard solution was determined by UV-Vis spectrophotometer at 370 nm. The 1% (v/v) DMSO was used as a reference solution. The absorbance and calibration curve of CPT in 1% (v/v) DMSO was shown in appendix 2C-4C.

3.4.3.3 Determination of drug loading efficiency (EE)

The dried CPT immobilized onto CS/ALG and mCS/ALG microspheres (2mg) were immersed in 10 mL of DMSO. The mixture was stirred at room temperature for 30 min. The supernatant of solution was collected and determined by UV-Vis spectrophotometer at 370 nm. All experimants were performed in triplicate.

The percentage of encapsulation efficiency of CPT was calculated from the following equation:

$$Drug\ encapsulation\ efficiency = \frac{actual\ amount\ of\ drug\ loaded\ in\ micrpspheres}{theory\ amount\ of\ drug\ loaded\ in\ micrspheres} \times 100$$

3.4.3.4 *In vitro* drug release

The CPT release from CS/ALG and mCS/ALG micrpspheres were studied in three difference buffers by dialysis bag diffusion technique. The accuarate weighted quantities of 10 mg of the spheres were enclosed in a dialysis bag with a molecular weight cut off of 3500 Da and immersed into 50 mL of SGF pH 1.2, pH 4.0, and SIF pH 6.4 in a flask. The flask was placed in a shaken water bath at speed of 100 rounds per minutes and incubated $37 \pm 1°C$. The incubated solution was collected at designated interval of time points and equat volume of fresh medium was compensated. The released CPT amount was determined in 12 h by UV spectroscopy, detection at 370 nm.

The amount of CPT released was calculated by interpolation from a calibration curves containing increasing concentrations of CPT. The percentages of cumulative CPT release were calculated from this equation.

$$\%Cumulative\ release\ = \frac{Amount\ of\ CPT\ from\ release}{Amount\ of\ CPT\ before\ release} \times 100$$

CHAPTER IV
RESULT AND DISCUSSION

4.1 Synthesis of CS-HT and QCS-HT

The reaction of CS or QCS and HT to form CS-HT or QCS-HT, respectively, was carried out via ring-opened reaction. The sulfhydryl compound homocysteine thiolactone (HT) was first fomed a reactive intermediate $HS-CH_2-CH_2-CH(NH_2)-C(O)-Im$ (where Im=1-imidazoyl group) [1] ,after that HT was covalently reacted at amino group of CS (Figure 4.1) and QCS (Figure 4.2) via formation of amide bonds.
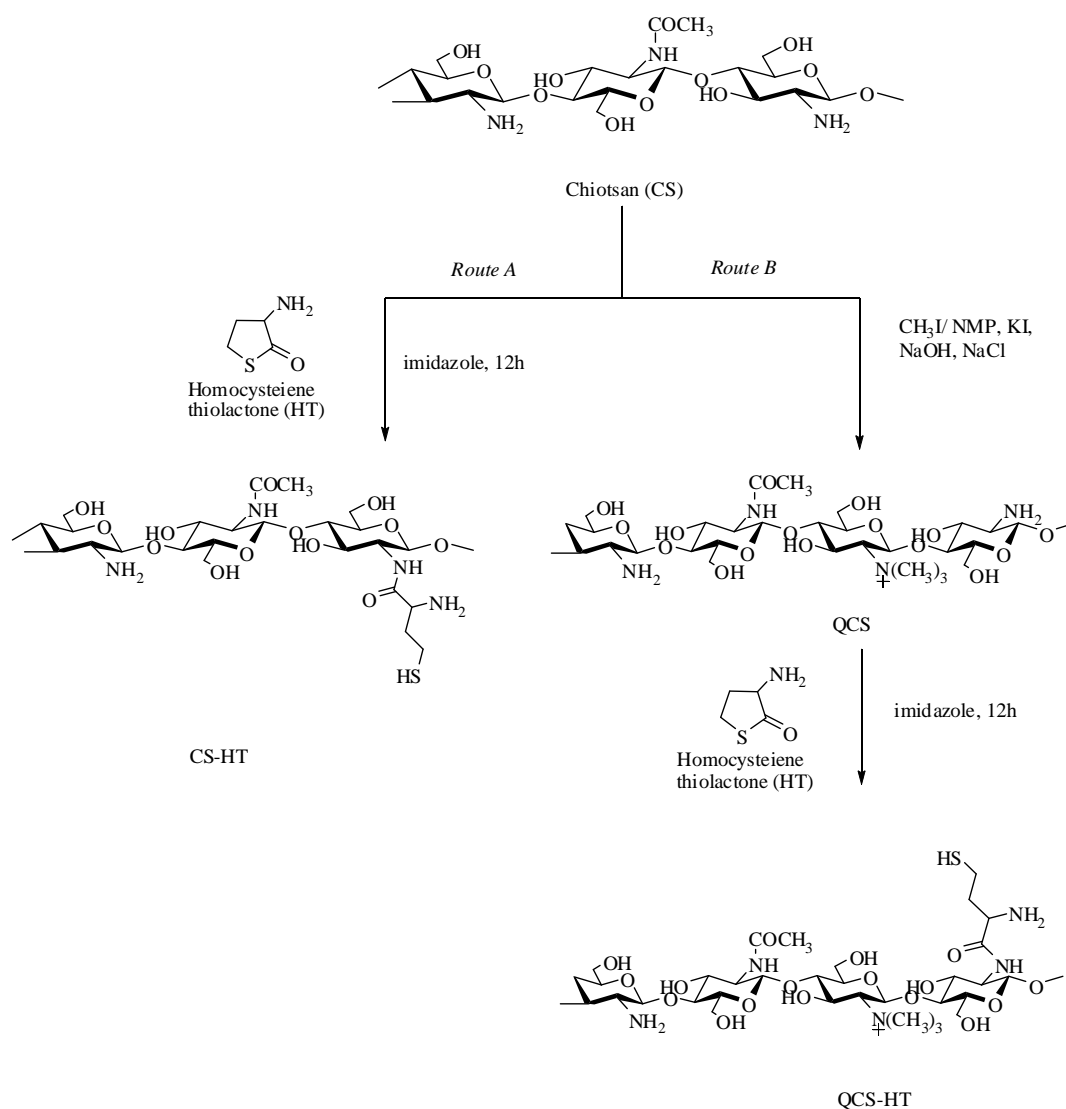
Figure 4.1 Reaction scheme of CS-HT (*route A*) and QCS-HT (*route B*)

The result obtained from these reactions appeared as pale light brown powder and amorphous. The products were characterized by FTIR, ^{1}H-NMR, ^{13}C-NMR, XRD, and TGA.

4.2 Characterization and physical properties of chitosan and modification of chitosan

4.2.1 Fourier Transform Infrared Spectroscopy (FTIR)

The FTIR spectra of CS and the three CS derivatives (QCS, CS-HT and QCS-HT) are shown in Figure 4.2. The FTIR spectrum of CS showed the characteristic absorption bands of CS at 1634 cm^{-1} (C=O amide) and 1077 cm^{-1} (C-O stretching), while the HT spectrum showed the C=O ketone group absorption band at 1705 cm^{-1}. After grafting of the HT onto the C2-amine groups of CS, the characteristic signal at 1652 cm^{-1}, attributed to the stretching vibration of the C=O acetamide of CS-HT (amide I band), appeared. In addition, the absorption peak at 1588 cm^{-1} (amide II band) and 1319 cm^{-1} (amide III band) were stronger than those seen in CS, which can be attributed to the additional amide group of HT. The peaks at 1256 cm^{-1} and 622 cm^{-1} correspond to the disulfide and thiol groups, respectively [2].

After quaternization of CS, the resultant QCS spectrum showed peaks at 1642 and 1582 cm^{-1} that are assigned to the C=O (amide) and N-H (amine) vibrations, respectively, and peaks at 1415 and 1389 cm^{-1} that result from the coupling of the C-N axial stretching and N-H angular deformation. The broad overlapping bands in the 1153 to 848 cm^{-1} range are likely to be due to the polysaccharide skeleton, including the stretching of the glycosidic bonds, C-O and C-O-C. Moreover, the intensity of the CH$_2$OH peak at the 1140-1080 cm^{-1} range changed because of the substitution of –CH$_3$ at the 6-hydroxyl group of CS [3]. For the QCS: HT sample (1:0.1 (w/w) ratio), the band at 1675 cm^{-1} is attributed to the stretching vibration of the C=O acetamide group of QCS-HT. Compared with CS, the absorption band at 1230 cm^{-1} corresponds to an increased level of alkyl group C-C bonds. These results are all consistent with the successful preparation of CS-HT and QCS-HT conjugates.
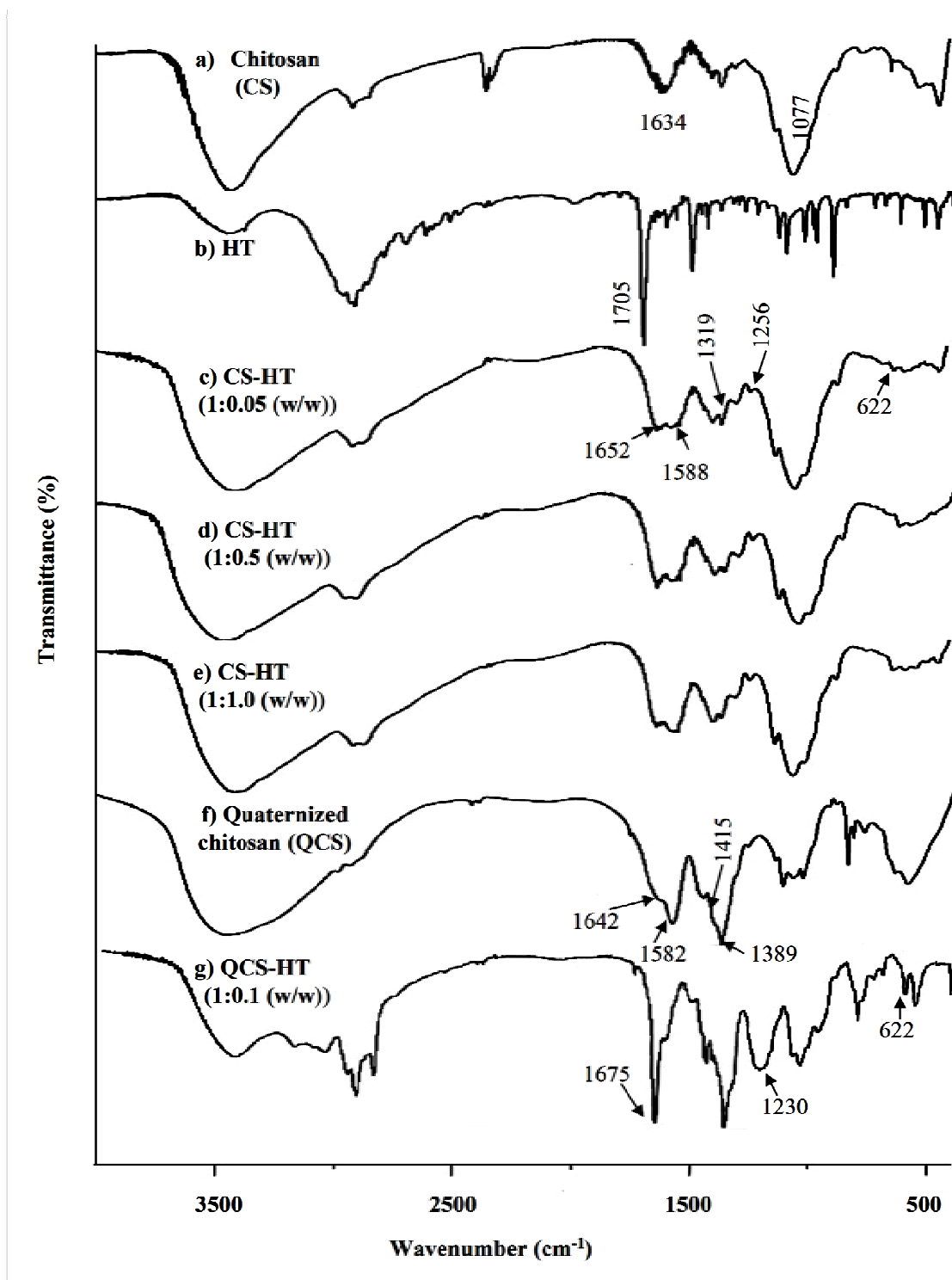
Figure 4.2 Representative FTIR spectra of (a) CS, (b) HT, (c-e) CS-HT polymers from a CS: HT (w/w) ratio of (c) 1:0.05, (d) 1:0.5 and (e) 1:1.0, plus (f) QCS and (g) QCS-HT (1:0.1 (w/w) QCS: HT

4.2.2 Nuclear Magnetic Resonance (NMR) Spectroscopy
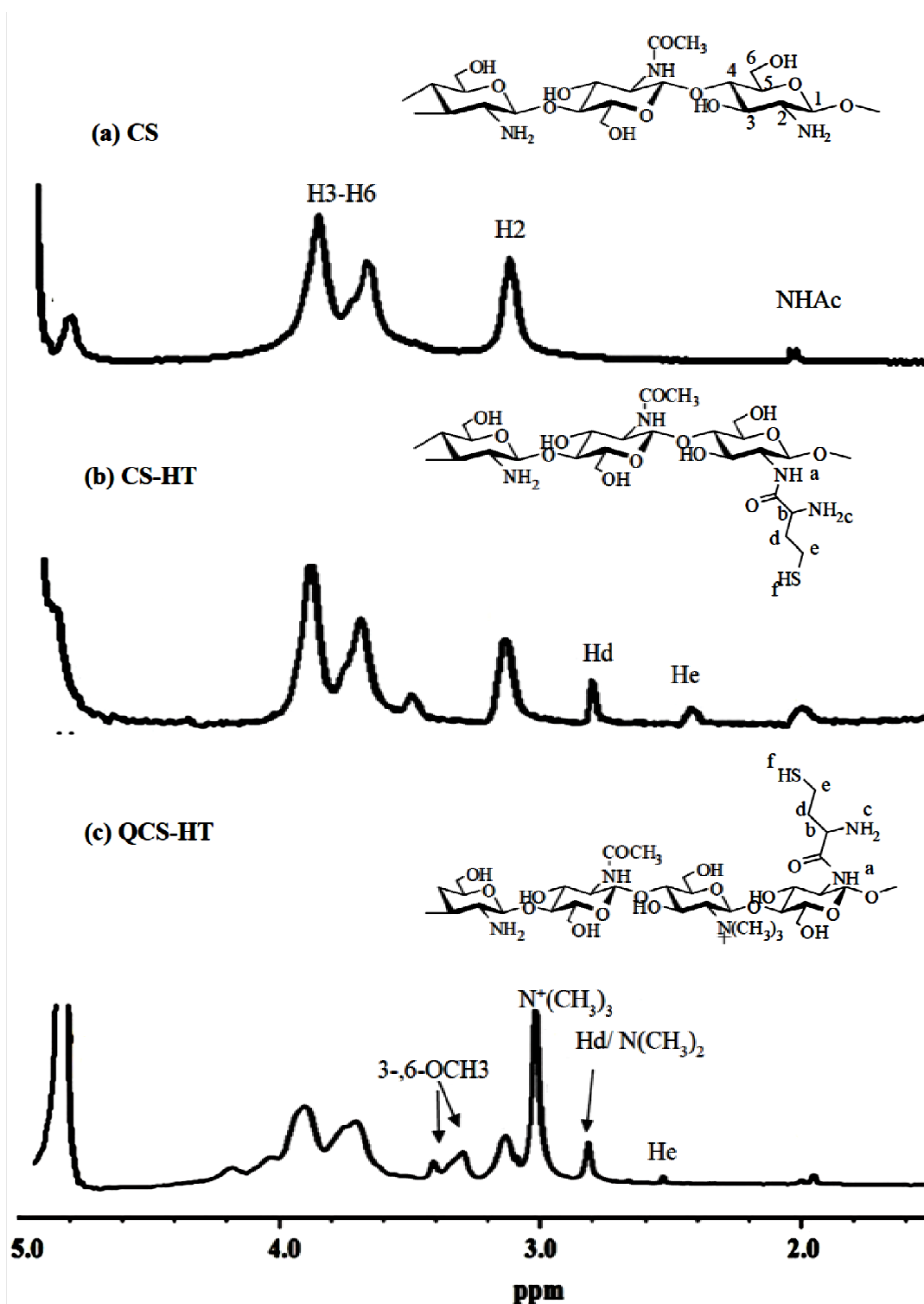
Figure 4.3 Representative [^1]H-NMR spectra of (a) CS, (b) CS-HT (1:0.1 (w/w) CS: HT) and (c) QCS-HT (1:0.1 (w/w) QCS: HT).
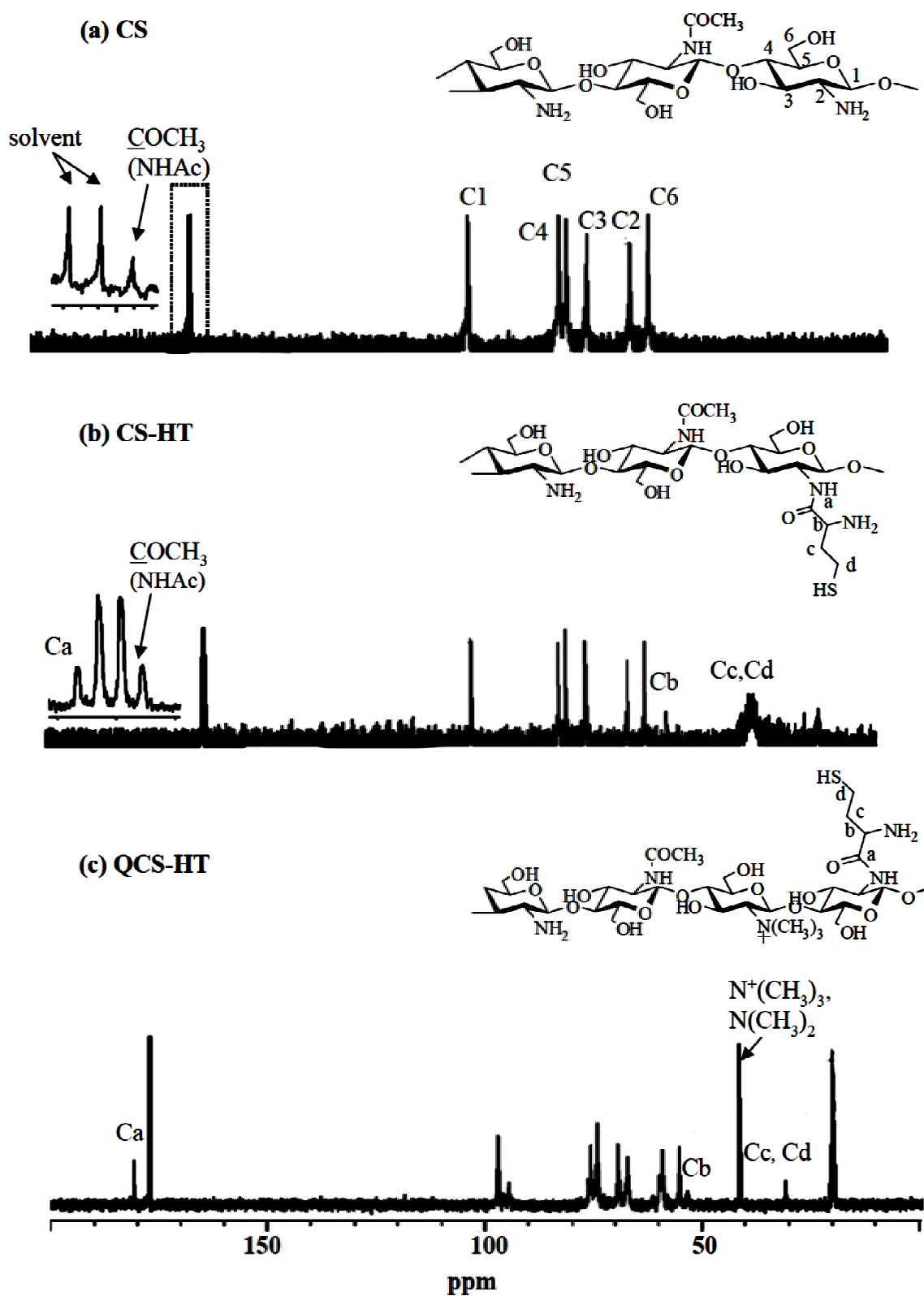
Figure 4.4 Representative ^{13}C-NMR spectra of (a) CS, (b) CS-HT (1:0.1 (w/w) CS: HT) and (c) QCS-HT (1:0.1 (w/w) CS: HT).

4.2.2.1 ^{1}H NMR spectrum of thiolatedchitosan

Representative ^{1}H-NMR of CS, CS-HT and QCS-HT are shown in Fig 3. The peaks for CS-HT at chemical shifts 3.4-4.0, 3.1 and 2.0 ppm were ascribed to the H3-H6, H2 (GluN) and acetyl (GluNAc) protons in the CS skeleton, respectively. The appearances of new proton positions from the ring opened side chain of HT were observed as at 2.8 and 2.5 ppm and are assigned to the Hd and He, respectively. The spectra of QCS-HT showed a chemical shift at 3.6-4.2, 3.2-3.4, 3.1, 3.0 and 2.0 ppm, which were attributed to H3-H6, 3-,6-OCH_3, H2, ^{+}N $(CH_3)_3$ and acetyl (GluNAc) protons in the QCS backbone, respectively. The chemical shifts at 2.8 and 2.5 belonged to Hd overlapped with $(CH_3)_2$ and He, respectively. The %DQ was 5.9%.

4.2.2.2 ^{13}C NMR spectrum of thiolatedchitosan

Representative ^{13}C-NMR spectrum of CS, CS-HT and QCS-HT are shown in Fig. 4., where the chemical shifts at δ 97.6, 59.9, 69.9, 76.4, 74.8 and 55.7 ppm are assigned to the C1, C2, C3, C4, C5 and C6, respectively. The signal at 161.6 is attributed to the carbonyl group of CS [4]. The spectrum of CS-HT is broadly similar to that of CS, except for the new high intensity peaks at around 24.5-35.7 ppm that are assigned to the methylene group of the grafted cysteine side chain (Cd, Ce). In addition, the peak at δ 50.0 ppm is assigned to the Cb alkyl carbon, and the characteristic peak at δ 161-163 ppm is assigned to the two types of carbonyl group, the C=O carbonyl group of the acetyl GluNAc of CS and the CS-HT side chain at 161 and 162.6 ppm, respectively. In the QCS-HT spectra of QCS-HT, peaks related to C1, C2, C3, C4, C5 and C6 of the saccharide ring and the peak of dimethyl (overlapped with the trimethyl group) at chemical shifts of 97.8, 59.8, 70.2, 76.7, 75.1, 55.8 and 41.9 ppm respectively, were all observed. The appearance of the peak at δ 182.0 ppm, assigned to the C=O carbonyl of the amide group, verified the covalent attachment of QCS and HT via an amide bond. The[13]C-NMR spectrum confirmed that CS-HT and QCS-HT was successfully prepared.

4.2.3 Quantification of the thiol levels in CS-HT and QCS-HT

The amount of free thiol groups and disulfide bonds immobilized in the CS-HT and QCS-HT derived polymers are summarized in Table 1. The CS-HT polymer derived from a 1:0.1 (w/w) ratio of CS: HT exhibited the highest amount of free thiol groups (64 µmol/g), which implies that this polymer will be the strongest mucoadhesive compared to the three other CS-HT polymers derived from the other CS: HT ratios. In addition, at the highest tested HT proportion (a 1:1 (w/w) ratio of CS: HT) the highest level of total disulphide groups (~220 µmol/g) was observed, some 3.59- to 5.48- fold higher than the other CS-HT polymers derived from the lower HT proportions. The results imply that the optimum proportion of HT should not exceed that of 1:0.1 (w/w) CS: HT, since an excess HT only yields a higher level of disulfide bonds.

Therefore, QCS-HT was synthesized at the 1:0.1 (w/w) ratio of QCS: HT, and was then evaluated compared to CS-HT to ascertain the potential effect of the permanent pH-independent positive charges on the mucoadhesive property of the polymer.

Table 4.1 Comparison of the different CS: HT mass ratio derived polymers and the levels of their free thiol and disulfide groups

Batch	CS-HT ratio	Total thiol groups (µmol/g) ($\pm$SD, n=3)	Total disulfide groups (µmol/g) ($\pm$SD, n=3)
CS	-	-	-
CS-HT	1.0:0.05	35.13 $\pm$ 0.05	61.32 $\pm$ 0.12
CS-HT	1.0:0.10	64.15 $\pm$ 0.04*	40.15 $\pm$ 0.03
CS-HT	1.0:0.50	49.99 $\pm$ 0.05	45.69 $\pm$ 0.08
CS-HT	1.0:1.00	50.56 $\pm$ 0.05	220.05 $\pm$ 0.14*
QCS-HT	1.0:0.10	32.48 $\pm$ 0.03	38.74 $\pm$ 0.72

* The mean difference is significant (P<0.01) compared to CS-HT 1.0:0.05 using LSD method.

4.2.4 X-ray diffraction (XRD) analysis
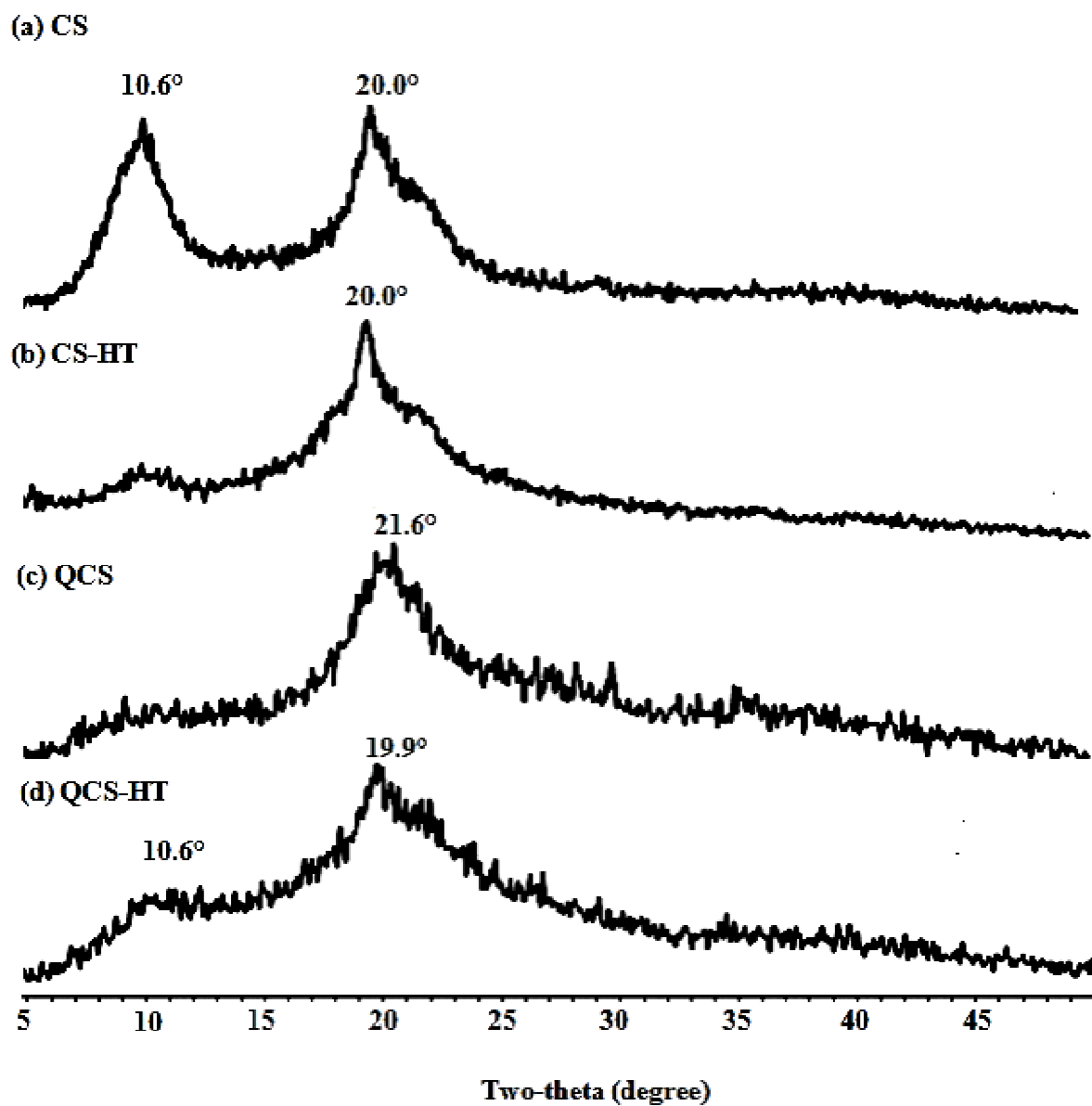
Figure 4.5 Representative XRD spectra of (a) CS, (b) CS-HT (1:0.1 (w/w) CS: HT) (c) QCS and (d) QCS-HT (1:0.1 (w/w) CS: HT).

Representative X-ray diffractograms for the CS, CS-HT, QCS and QCS-HT polymers are shown in Figure 4.5, where some differences in the peak height, width and position between the four compounds were observed. CS powder exhibited two typical peaks at 10.6° and 20.0°, which corresponded to crystal forms I and II, respectively [5].

However, after HT substitution, the peak at 10.6° was significantly weaker (almost absent) in the CS-HT spectrum, suggesting that the original crystallinity of CS was destroyed. The CS-HT (and QCS-HT) was more amorphous in nature, which may well improve their biodegradability and mucoadhesive properties [6].

The XRD pattern exhibited a characteristic peak at 21.6° for QCS that corresponds to the crystal form II. Compared with CS, the intensities of these peaks were decreased. However, the degree of crystallinity of QCS-HT is higher than QCS since the QCS-HT depicted two XRD peaks at 10.2° and 19.9°. It is possible that an increase in the HT moiety level resulted in a change in the crystallinity of the QCS backbone. If so, this could be attributed to the decreasing level of primary amino groups, and so a lower cationic charge density would be found on the CS backbone in QCS-HT than in CS [6]. Thus, the three CS derivatives (CS-HT, QCS and QCS-HT) were more amorphous than CS. The results also support that HT was successfully introduced into the CS and QCS backbone.

4.2.5 Thermogravimetric analysis (TGA)

The thermal properties of the polymers were investigated by TGA. The TG curves and the corresponding DTG curves of CS, CS-HT, QCS and QCS-HT are displayed in Fig. 4.6.

The TG curve of the unmodified CS showed two stages of weight loss, the first being water loss (13.5% of the total weight) at 26°C to 160°C, whilst the second stage was from ~208°C to 288°C, accounting for a loss of 34.6% of the total weight and was ascribed to the degradation of CS backbone.

In contrast, the CS-HT sample (1:0.1 (w/w) ratio of CS: HT) showed three stages of weight loss. The first stage, due to water evaporation was found at below 100°C and accounted for 5.3% total weight loss. This was followed by a sharp weight loss in the 196 to 262°C range, accounting for 34.1% of the total weight and ascribed to the thermal degradation of the HT grafted side chain. The final stage, ranging from

260°C to 440°C was attributed to the decomposition of CS and accounted for 29.6% of the total weight.

For QCS the thermal decomposition showed two stages, the first from < 100 – 160 °C being due to the evaporation of water (34.3% total weight), followed by the more obvious weight loss (35.9% total weight) at 160°C to 225°C that is due to the degradation of the QCS matrix and cleavage of the substituent groups [7]. The weight loss of QCS-HT was lower than that of QCS. The first stage in the thermal decomposition of QCS-HT, at 26°C to 160°C was due to dehydration (5.9% total weigh loss). The second stage at 187°C to 250°C (23.3% total weight) is attributed to the thermal degradation of the HT, whilst the final stage at 250-440°C   (42.8% total weight) was attributed to the decomposition of the QCS matrix.

Overall, the TGA analysis demonstrate the loss of the thermal stability for CS-HT and QCS-HT compared to the original CS. Introduction of the HT side chain into the polysaccharide structure should disrupt the crystalline structure of CS, especially through the loss of the hydrogen bonding [8].
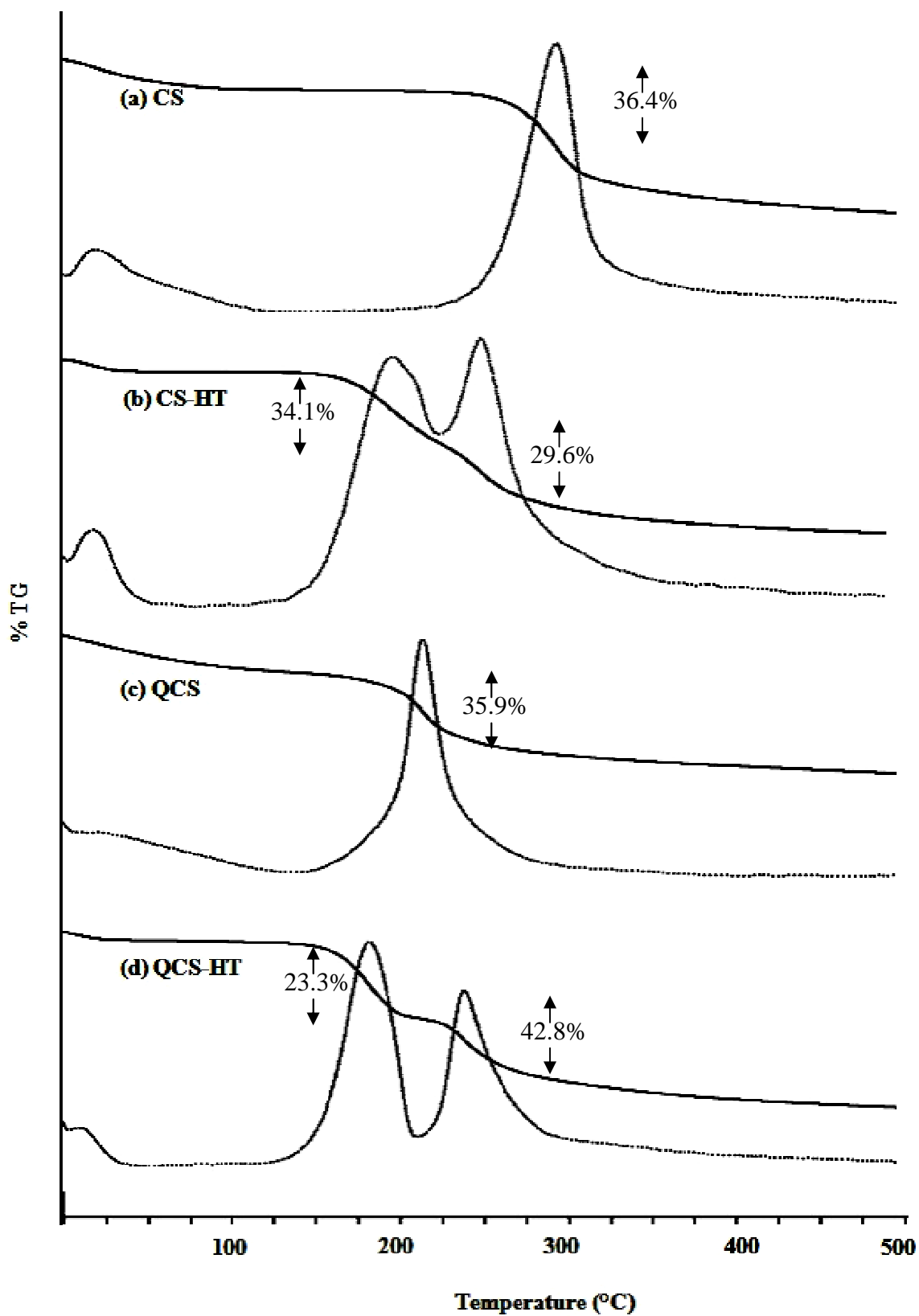
Figure 4.6 Representative TGA thermograms (TG and DTG curves) of (a) CS, (b) CS-HT (1:0.1 (w/w) CS: HT), (c) QCS and (d) QCS-HT (1:0.1 (w/w) QCS: HT).

4.3 Mucoadhesive properties

4.3.1 Assessment of the mucoadhesive behavior of CS and the three derivatives (QCS, CS-HT and QCS-HT) by mucus glycoprotein assay

The mechanism of mucoadhesion has been theoretically reported to be based on the six general components of electrostatic, wetting, adsorption, diffusion, mechanical and fracture theories [9]. Many methods have been employed to evaluate these interactions *in vitro* and *in vivo*.

In this study, we selected a commercial powder preparation of porcine mucin type II, which is typically used in mucoadhesion assays due to its lower batch-to-batch variability and higher between assay reproducibility [10, 11]. As a strong interaction exists between mucin and CS or its derivatives, mucin should be spontaneously adsorbed onto the surface of the CS or its three derivatives (QCS, CS-HT and QCS-HT).

Therefore, the mucoadhesive property of the CS and its three derivatives was assessed by suspension of mucin in their aqueous solutions at room temperature. The spectrophotometric detection method used here allowed very dilute solutions of mucin (125-500 µg/mL) to be measured and showed a linear relationship between the amount of mucin and the absorbance at 555 nm, with the linear regression equations obtained by the least square method being $y = 0.5629x - 0.0452$, $y = 1.41x + 0.0832$ and $y = 1.9268x + 0.0415$ for the assay in pH 1.2 (SGF), pH 4.0 and pH 6.4 (SIF), respectively (Appendix B). As the mucin concentration increased, so the amount of mucin adsorbed also increased.

Table 4.2 Comparison of the different CS:HT mass ratio to mucoadhesive property

Batch	CS-HT ratio	Total thiol groups (µmol/g) (±SD, $n=3$)	Total disulfide groups (µmol/g) (±SD, $n=3$)	Adsorbed of mucin at pH 1.2 (mg) (±SD, $n=3$)	Adsorbed of mucin at pH 4.0 (mg) (±SD, $n=3$)	Adsorbed of mucin at pH 6.4 (mg) (±SD, $n=3$)
CS	-	-	-	0.06 ± 0.01	0.31 ± 0.05	0.42 ± 0.03
CS-HT	1.0:0.05	35.13 ± 0.05	61.32 ± 0.12	0.22 ± 0.01^{a}	0.55 ± 0.02^{a}	0.65 ± 0.01^{a}
CS-HT	1.0:0.10	$64.15 \pm 0.04*$	40.15 ± 0.03	$0.22 \pm 0.02^{a,b}$	0.60 ± 0.03^{a}	$0.72 \pm 0.01^{a,d}$
CS-HT	1.0:0.50	49.99 ± 0.05	45.69 ± 0.08	0.25 ± 0.03^{a}	0.54 ± 0.03^{a}	0.67 ± 0.02^{a}
CS-HT	1.0:1.00	50.56 ± 0.05	$220.05 \pm 0.14*$	0.26 ± 0.01^{a}	0.51 ± 0.02^{a}	0.62 ± 0.04^{a}
QCS-HT	1.0:0.10	32.48 ± 0.03	38.74 ± 0.72	$0.38 \pm 0.01^{a,c,e}$	$0.79 \pm 0.03^{a,c,e}$	$0.75 \pm 0.01^{a,c,f}$

* The mean difference is significant ($P<0.01$) compared to CS-HT 1.0:0.05 using LSD method.
[a] The mean difference is significant ($P<0.01$) compared to CS using LSD method.
[b] The mean difference is insignificant ($P>0.01$) compared to CS-HT 1.0:0.05 using LSD method.
[c] The mean difference is significant ($P<0.01$) compared to CS-HT 1.0:0.05 using LSD method.
[d] The mean difference is significant ($P<0.01$) compared to CS-HT 1.0:0.05 using LSD method.
[e] The mean difference is significant ($P<0.01$) compared to CS-HT 1.0:0.1 using LSD method.
[f] The mean difference is insignificant ($P>0.05$) compared to CS-HT 1.0:0.1 using LSD method.
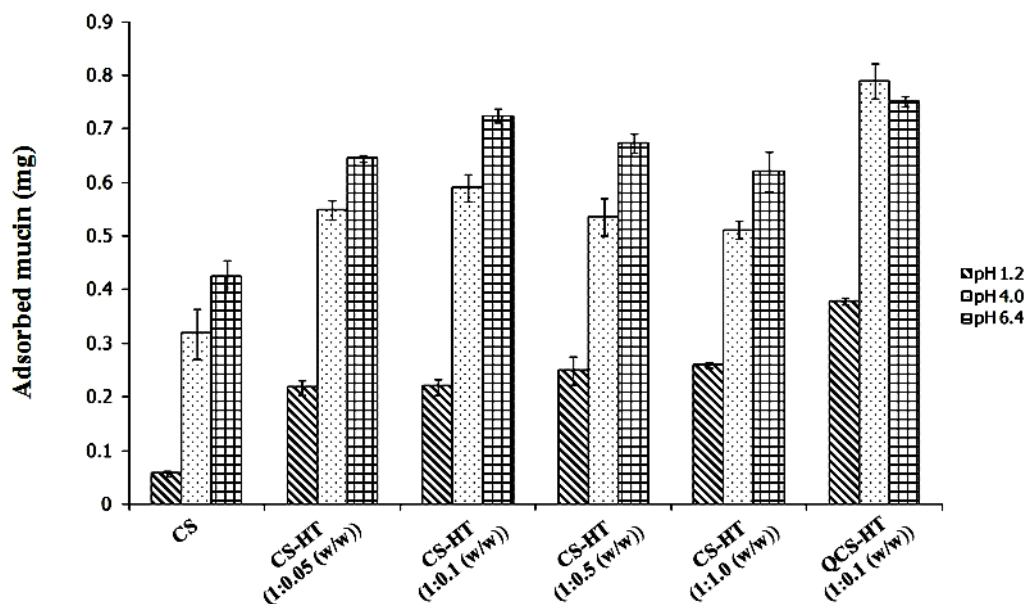
Figure 4.7 Adsorption of mucin on CS, CS-HT polymers of different CS: HT (w/w) ratios and QCS-HT at pH 1.2, 4.0 and 6.4. Data are shown as the mean $\pm$ 1 SD and are derived from three independent repeats. Means with a different lower case letter are significantly different ($P < 0.01$; Duncan's multiple means test).

4.3.2 Adsorption of mucin on polymer

The amount of mucin that was adsorbed onto the polymer (CS or its three derivatives) decreased at lower pH values, being maximal at pH 6.4 (SIF) and minimal at pH 1.2 (SGF) (Fig.4.7), because the degree of the ionization of sialic acid or the different forms of the glycoprotein will be influenced by the pH value of the environment. Sialic acid is a saccharide acid, and mucin is a glycoprotein. The values of pK_a and pI for sialic acid and mucin are 2.6 [12] and ~3-5, respectively. Hence, the ionization of the sialic acid and the glycoprotein will be more sensitive to pH, in the acidic environment. As the pH value decreases, the amount of ionized sialic acid also decreases [13], and so reduces the potential for interaction with CS or its three derivatives.

CS and QCS, along with their thiolated derivatives (CS-HT and QCS-HT, respectively), were evaluated for their mucin adsorption ability as a measure of their mucoadhesiveness. The thiolated derivative polymers dramatically and significantly increased the mucin adsorption level above that seen with CS or QCS in all three pH

mediums evaluated (Fig. 7). The results revealed that the representative CS-HT (derived from a 1:0.1 (w/w) ratio of CS: HT) absorbed mucin about 3.9-, 1.9- and 1.7- fold more than CS at pH 1.2, 4.0 and 6.4, respectively, whilst the corresponding QCS-HT sample showed some ~6.7-, 2.5- and 1.8-fold higher mucoadhesion than QCS at pH 1.2, 4.0 and 6.4, respectively. Comparing the two corresponding (i.e. 1:0.1 (w/w) ratio (QCS: HT) thiolated CS polymers, a higher mucoadhesion level was seen for QCS-HT than CS-HT at all three pH values, but this difference was more marked in the more acidic media, being ~1.72-, 1.37- and 1.04- fold higher at pH 1.2, 4.0 and 6.4, respectively.

At the low pH range (pH 1.2 and 4.0), when the proportion of HT in the CS: HT (w/w) ratio increased from 1:0.05 to 1:0.1, a statistically significant increase in the level of thiol groups was observed (Table 2), but the slight numerical changes in the mucoadhesion level were not statistically significant (Fig. 7). This might be due to the reactivity of the thiol groups on the polymer. In the lower the pH, the the thiol group in the thiolated are less reactive, hence oxidation of thiol groups occurs before contact with the mucus gel layer. [14]. Hence, the mucoadhesive ability of CS was increased by the addition of the thiol groups because of the electrostatic and hydrophobic effects. With respect to the electrostatic effect, this is due to the remaining NH_3^+ moieties of both the CS backbone and the HT side chain being able to interact with either the COO^- or SO_3^- groups on the mucin carbohydrate side chain in an acidic media. For the hydrophobic effect, the $-CH_2$ moieties of HT interact in part with the $-CH_3$ groups on the mucin side chains which, lead to a high mucoadhesive adsorption. Therefore, the effect of both electrostatic and hydrophobic effects impact on the mucoadhesion of CS and its three derivatives in the lower pH range.

In contrast, however, at pH 6.4 a statistically stronger mucoadhesiveness was observed with the CS-HT sample derived from the lower HT proportion (1:0.1 (w/w) CS: HT), with an ~1.1-fold higher level of adsorbed mucin being observed that that from the CS-HT polymer derived from a 1:0.05 (w/w) ratio. However, since these experiments were performed at a pH above 6, which will result in an increased concentration of the reactive form of thiolate anions, $-S^-$, this may have lead to a greater extent of oxidation

and nucleophilic attack [15]. Regardless, the potential influence of the level of thiol groups on the mucoadhesive properties of the polymer could clearly be observed, and so not only electrostatic and hydrophobic effects are at play but also the level of covalently linked thiol groups in the polymer is an important determinant of the polymer's mucoadhesiveness. The higher the density of thiol groups covalently attached to the copolymer, the higher the amount of mucin was bound onto the polymer (Table 1 and Fig. 7). This can be explained by the formation of covalent disulfide bonds between the thiol-bearing side chains of the thiolated polymer and cysteine-rich subdomains of the mucus glycoprotein. [16].

With respect to the level of disulfide bonds, the CS-HT sample derived from a 1:1. CS: HT (w/w) ratio showed a significant increase in the level of disulfide groups (Table 1), but no statistically significant increase in the mucoadhesion ability (Fig. 7). Thus, it is possible that the level of total disulfide bonds is not a principal factor influencing the mucoadhesive properties of the thiolated CS polymers.For QCS-HT a significant reduction in the total thiol group level was seen (Table 2) because the quaternization of CS leads to a steric inhibition effect from the fixed positively charged quaternary ammonium group charges making it difficult for the HT groups to interact with the CS amine group. However, a statistically ($P > 0.01$) higher mucoadhesion level for the QCS-HT was observed compared to that for CS and CS-HT at pH 1.2 and 4.0 being ~1.7- and 1.3- fold higher than that seen in the CS-HT (derived from a 1:0.1 (w/w) CS: HT ratio) at pH 1.2 and 4.0, respectively. This was expected since the $^+N(CH_3)_3$ group found in QCS-HT would be able to interact with the COO^- or the SO_3^- groups on the mucin glycoprotein side chain given that most mucin glycoproteins have a high sialic acid and sulfate content, and so a strongly negative surface charge [17].

On the other hand, QCS-HT showed only a slightly (1.04-fold) numerically larger (and not statistically significant) mucoadhesion level at pH 6.4 compared to the corresponding (1:0.1 (w/w) ratio CS: HT) CS-HT polymer, which is likely to be due to the fact that the influence of the positive charge was not enough to increase the mucoadhesion when compared with the effect of the thiol group at a higher pH (pH 6.4).

4.4 Swelling study

The swelling properties are of paramount importance in any prospective evaluation of biomaterials, and they can be affected by many factors, such as the cross-linking density and the hydratability of the materials, and the ionic strength and pH value of the media [18].

In this research the swelling ratio was measured in three broadly isoosmotic buffer solutions that differ in their pH, being SGF (pH 1.2), 0.1 M acetate buffer (pH 4.0) and SIF (pH 6.4) and the swelling ratio was calculated using detailed in section 3.3.4.

The results, as the variation in the swelling ratio with time, for the four CS-HT polymers that varied in CS: HT ratios, showed essentially the same pattern (data not shown) and so that for the CS-HT polymer derived from a 1:0.1 (w/w) ratio of CS: HT is shown as an example, along with the data for the CS and QCS-HT polymers in Figure 4.8. All three polymers swelled rapidly (within 30 min) in all three different pH media, with the CS-HT and QCS-HT presenting a higher swelling ratio than that of CS. This may be attributed to the fact that the hydrophility of the thiolated CS was greater than that for CS [19].

In addition to the influence of HT grafting upon the polymer swelling, a clear pH dependence was also noted. As the pH value increased the degree of observed swelling decreased, especially from pH 4 to pH 6.4. This could be explained from the pH-dependent charge balance of CS-HT, QCS-HT and CS, and so the degree of interaction between these three polymers is modified in accord with their charge balance. The QCS-HT sample is here selected as an example to explain the potential mechanism due to the statistically significant changes in the swelling behavior with pH compared to that for the control CS.
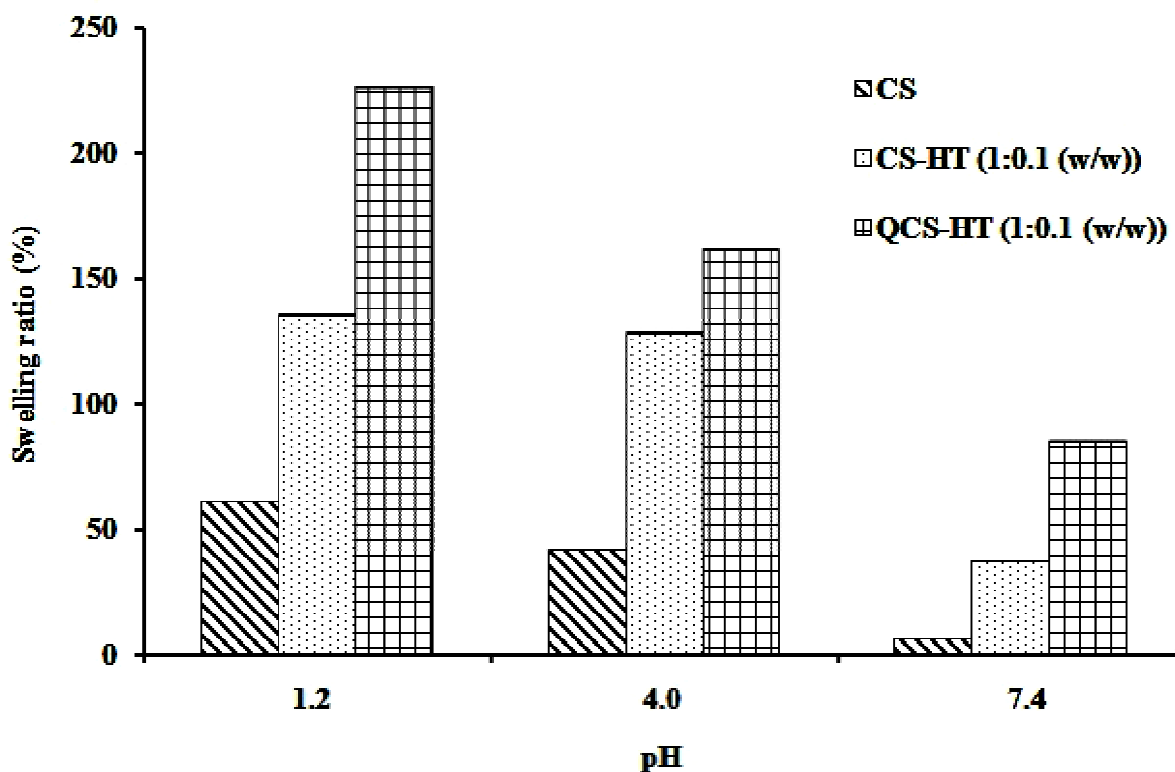
Figure 4.8 Swelling behavior of the CS and the thiolated CS derivatives (CS-HT and QCS-HT, both from a 1:0.1 (w/w) ratio (Q)CS: HT) as a function of the media pH. Data are shown at equilibrium (60 min swelling time) as the mean $\pm$ 1 SD and are derived from three independent repeats. Means with a different lower case letter are significantly different (p < 0.01; Mann-Whitney U test with Holm correction).

In strongly acidic medium (pH 1.2), the high swelling behavior can be explained by the amine group of the QCS being protonated which then favors chain expansion [20], through the electrostatic repulsions between the like-charged polymer segments(Figure 4.9) [21]. Furthermore, there is an overall increase in the swelling ratio after grafting HT side chains onto CS. This is in good agreement with the literature, where it has been reported previously that adding more hydrophilic groups to CS increases its water absorption [22]. In order to investigate the effect of the thiol group on the degree of swelling at the lower pH of the thiolated polymer, the thiol groups may be oxidized [14] leading to less reactive of the thiol groups. Hence, the influence of the thiol groups was attributed to the effect of the interruption of the dominant amine groups.

At a high pH (pH 6.4), the swelling ratio is strongly reduced due to the almost complete deprotonization of the CS amine group [21] leading to a re-association of

the inter-chain hydrogen bonds and consequently to weaker interactions between the polymer chains and the aqueous media. It is known that a low concentration of charged ionic groups in the polymer decreases swelling behavior. On the other hand, at pH levels above 6 the thiolate groups become charged anions, $-S^-$, which represents the reactive oxidation form [15], and thereby leads to electrostatic repulsion between the polymer segments. However, the polymers have only a relatively low density of thiol groups compared to that for the amine groups, and so the affects of the amino group are dominant.
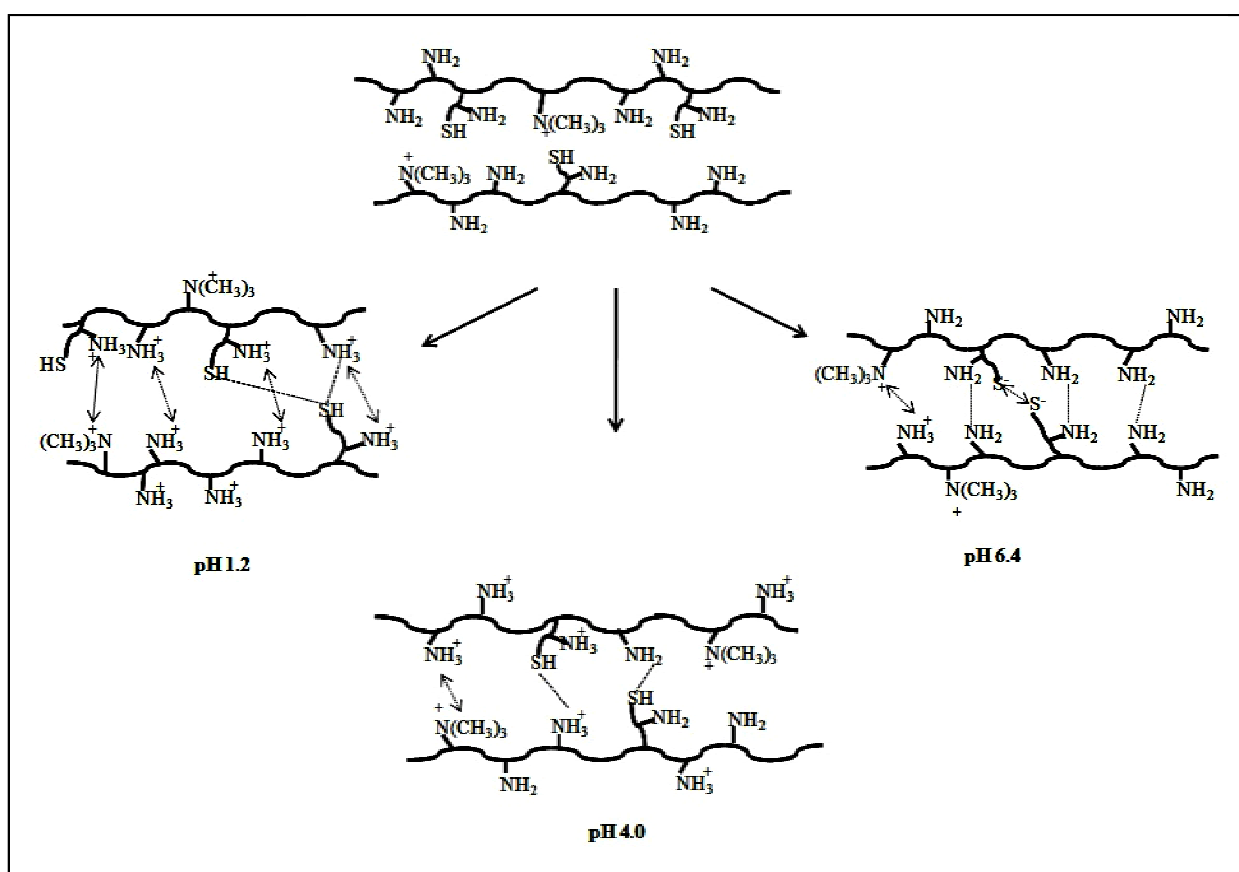
Figure 4.9 Representative swelling mechanism of the QCS-HT in pH 1.2, 4.0, and 6.4

4.2.1 Morphology

4.2.1.1 mCS

The results from the studies of electrospray parameters on the polymer fabrication showed that the CPT-CS/ALG and CPT-mCS/ALG microspheres were successfully prepared using electrospray parameters as follows: working distance of 8 cm, needle gauge of 26 G, flow rate of 1.2 mL/h, stirring rate of 400 rpm and electrospraying voltage of 12 kV

Here in after, QCS-HT refered as mCS. The SEM micrographs of mCS microspheres were shown in Figure 4.10. As can be seen, the majority of the spheres were spherical with smooth surfaces and without visible pores. This may be attributed to the fact that modified chitosan successfully fabribated to spherical shapes.
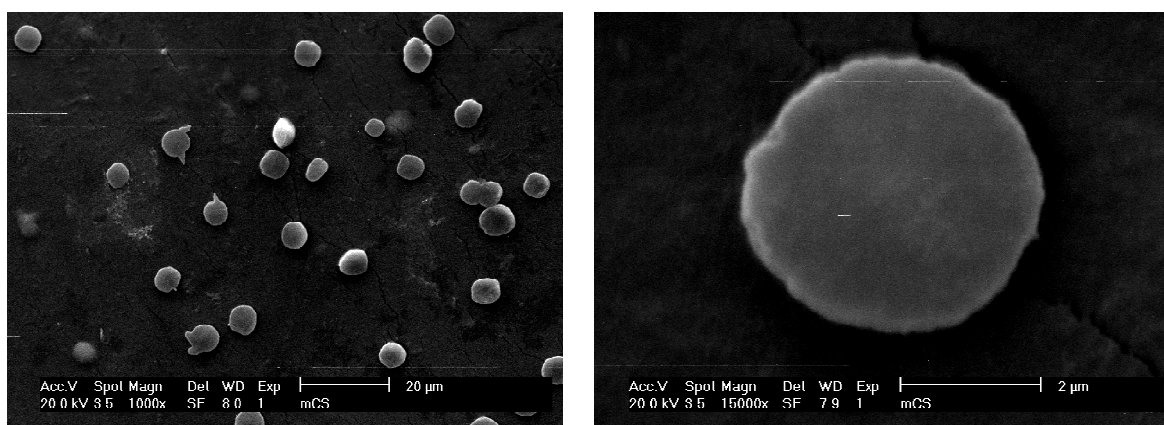
Figure 4.10 Scanning electron micrographs of mCS (QCS-HT)

In this research, carrageenan(CR) and alginate(ALG) were chosen form polymer composite with modified chitosan.

4.2.1.2 mCS/Carrageenan (CR)

Carrageenans are naturally ocurring linear polysaccharides extracted from red seaweed. They have hight molecular weight and are composed of repeating galactose residues. They have long been used commercially in the food industry, and now increasingly in pharmaceutical formulation studies [2].
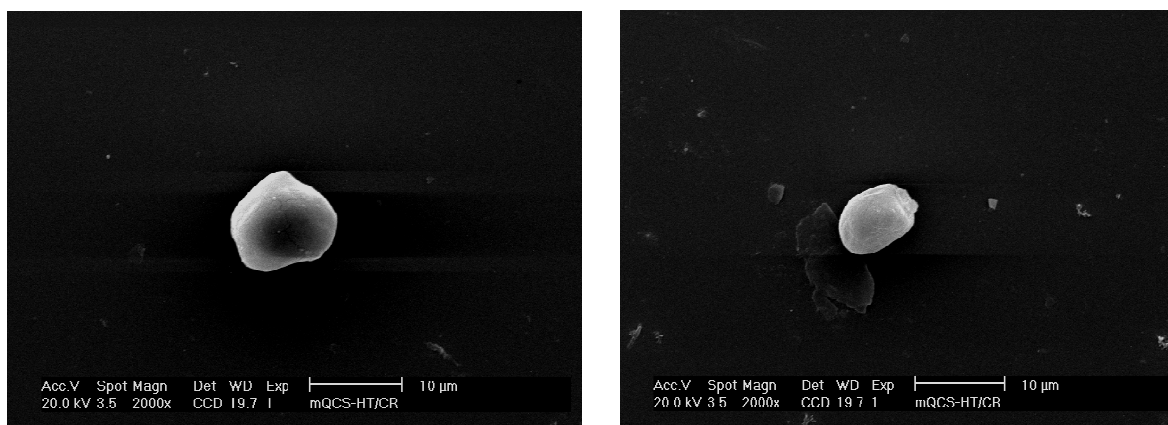
Figure 4.11 Scanning electron micrographs of mCS/CR

From the SEM micrographs (Figure 4.11) it can be concluded that electrospray facilitates the production of mCS/CR particles. But the mCS/CR does not uniform and spherical in shape because the CR has high viscosity. This phenomenon was explained by Paine et al. [3]. For the liquid of higher viscosity, more energy is required to drive the liquid from the meniscus, therefore, the droplets are generated with lower frequency than for liquids of low viscosity.

4.2.1.2 mCS/Alginate(ALG)

Alginate are naturally occuring substances found in brown seaweed and algae, have received much attention for use in pharmaceutical dosage forms, particularly as a vehicle for controlled drug delivery [4].

(1a)

(1b)

(2a)

(2b)
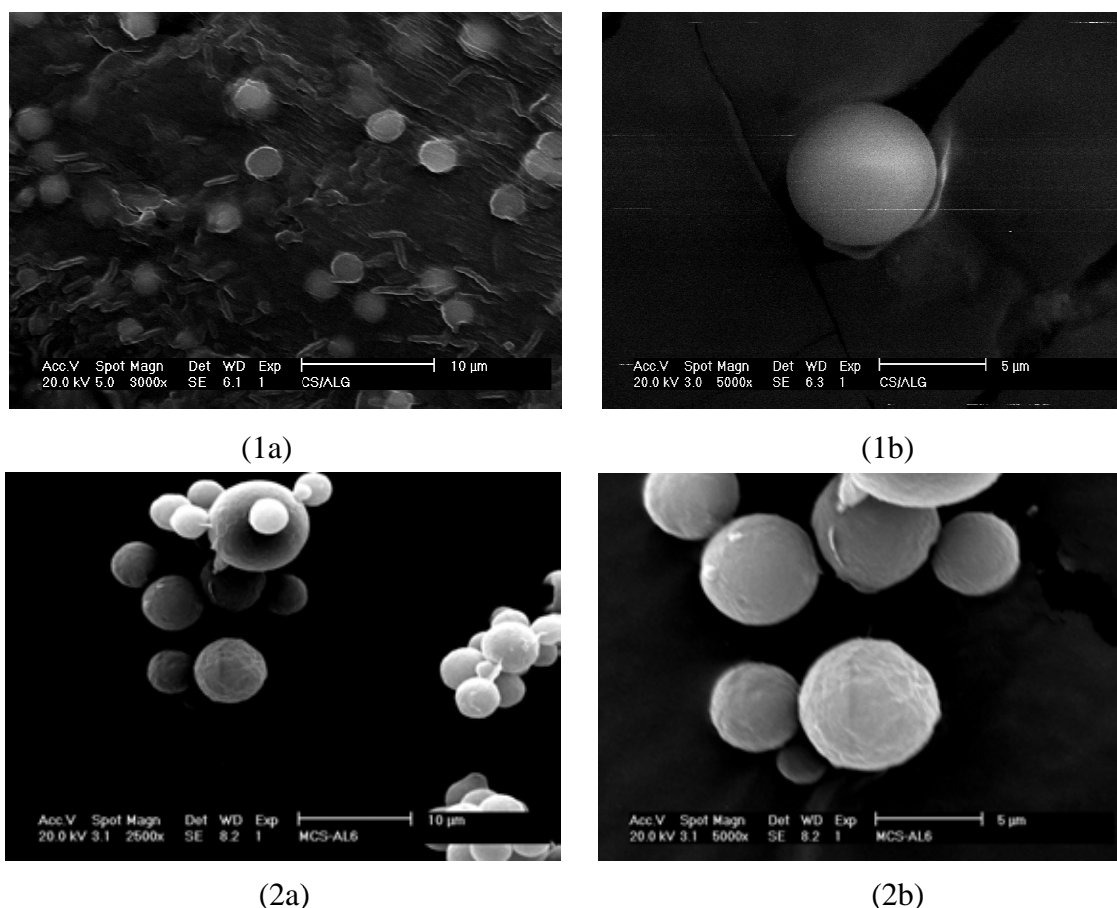
Figure 4.12 Scanning electron micrographs of CS/ALG (1a-b) and mCS/ALG (2a-b) without CPT

The SEM micrographs of CS/ALG and mCS/ALG microspheres were shown in Figure 4.12. The surface morphological appearance of mCS/ALG microspheres was compared with the CS/ALG microspheres. Without camptothecin, both of the CS/ALG and mCS/ALG microsphere were in a generic spherical shape. Smoothness on the surface could be clearly seen at high magnification and without visible pores.

The preparation of polyelectrolyte of mCS and ALG microsphers by electrospray was investigated. When a polyanionic or polycationic aqueous solution containing a polyelectrolyte with the opposite charge, a spherical interface consisting

of a polyelectrolyte complex was formed by electrostatic interaction to produce microspheres [5].

(1a)   (1b)

(2a)   (2b)
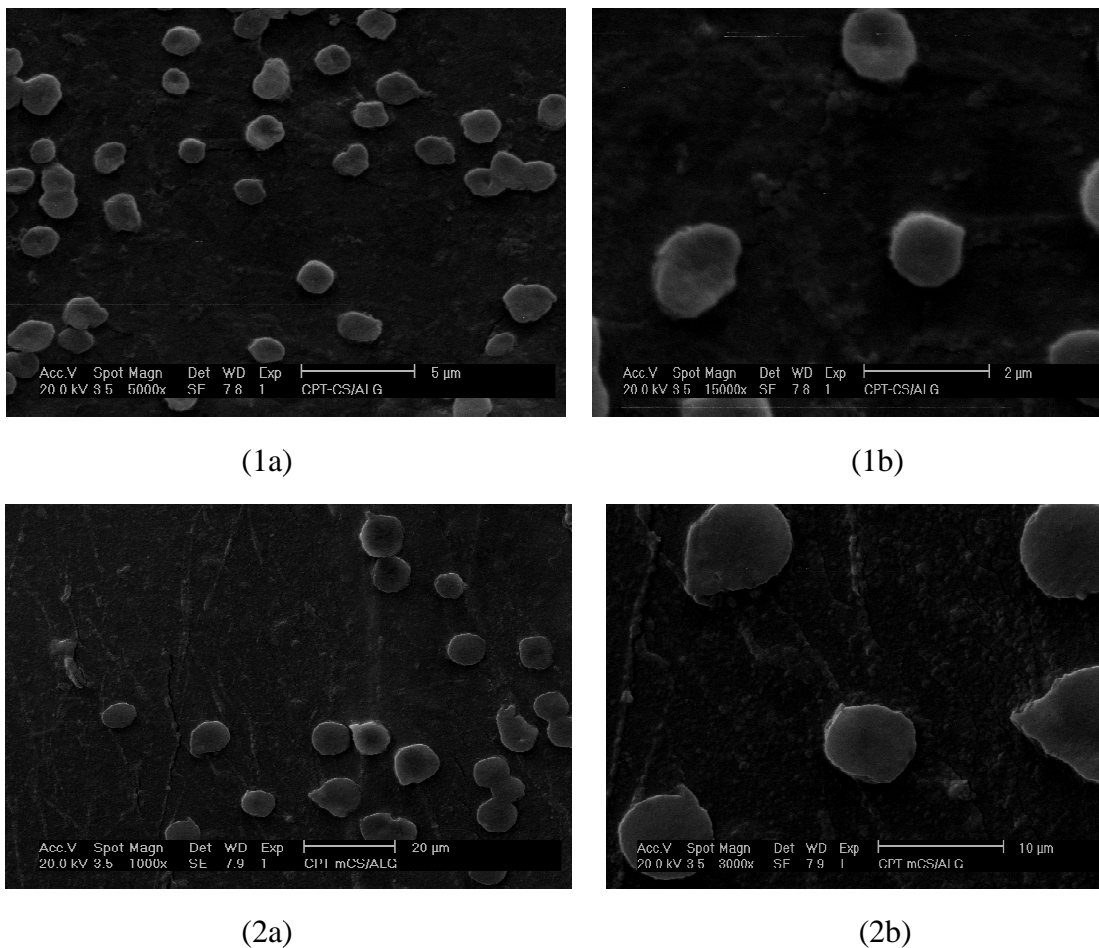
Figure 4.13 Scanning electron micrographs of CS/ALG (1a-b) and m-CS/ALG (2a-b) with 1%CPT

Figure 4.13 showed the surface morphological appearance of CPT loaded were CS/ALG and mCS/ALG were prepared by the electrospray ionization technique.

4.2.2 Particle size, size distribution

The size distribution of CS/ALG, mCS/ALG, 1%CPT-CS/ALG, and 1%CPT-mCS/ALG microspheres were presented in Table 4.3

The size distribution of CS/ALG and mCS/ALG without CPT particles size was approximately 2.33 and 2.98 µm, respectively with PDI (CS/ALG and mCS/ALG microsphers) approximately 0.82 and 0.87, respectively. PDI was used to measure for the width of the particle size distribution (from 0 = monodisperse to 1 = polydisperse [26]).

In case of the size distributions of CS/ALG and mCS/ALG with CPT microspheres showed that they were in the range approximately from 3.15-3.42 µm with PDI from about 0.69 to 0.88. In addition, when CPT was loaded onto polymer it results in increasing the mean size of spheres.

Table 4.3 Effect of composition on morphology of the microsphere

Abbreviations	Shape	Bead size ± SD (µm) by nanosizer	Zetapotential (mV)	Polydispersity (PDI)
CS/ALG	Spherical	2.33± 0.05	-6.06 ± 0.67	0.82 ± 0.10
mCS/ALG	Spherical	2.98 ± 0.36	-4.87 ± 1.31	0.87 ± 0.08
CPT-CS/ALG	Spherical	3.15[a] ± 0.37	-17.23 ± 1.36	0.69 ± 0.18*
CPT-mCS/ALG	Spherical	3.42[a] ± 0.09	-10.90 ± 0.90	0.88 ± 0.07

*The mean difference is insignificant ($P>0.01$) compare to CS/ALG microspheres

[a] The mean difference is significant ($P<0.01$) compare to CS/ALG microspheres

4.2.3 Zeta potential (Zp)

Zeta potential measurements will give information about the overall surface charge of the particles and how this is affected by changes in the environment (e.g. pH, presence of counter-ions, adsorption)[27]. When considering the zeta potential, that is surface charge, it can greatly influence particle stability in suspension through the electrostatic repulsion between particles.

Alginate is an anionic polysaccharide effected to the zeta potential of alginate was negative (~ -80 mV, pH 7)[28]. Due to chitosan and its derivatives carrier high positive charge, the preparation of CS/ALG and mCS/ALG polyelectrolyte complexes made the Zp increase [29]. As could be seen from these results shows the Zp of polyelectrolyte complexs were increased from ~80 mV, which is reported from the literature reviews of orginal ALG to -6.06 and -4.87 mV for CS/ALG and mCS/ALG, respectively. Moreover, from these results revealed that CS/ALG has the lower positive Zp than the mCS/ALG due to the positivity of the CS in zeta potential relates to the portion of the chitosan that has been protonated and dissolved in water. In the alkylated salt of mCS, the $-NH_2$ group was converted to a quaternary ammonium group and that desribes the higher positivity of the derivatives in comparison to the chitosan itselt [30].

Zeta potential values are also of interest for the characterization of the microspheres since CPT-loaded microspheress display Zp values -17.23 and -10.90 mV (CPT-CS/ALG, and CPT-mCS/ALG, respectively) as seen in Table 4.3. Zeta potential is function of the surface charge of colloidal dispersions. It is commonly used to predict and control dispersion stability. Zeta potential data suggest the potential physical stability of microsphers in aqueous dispersion state and confirm the presence of CPT on microspheres surface [31].
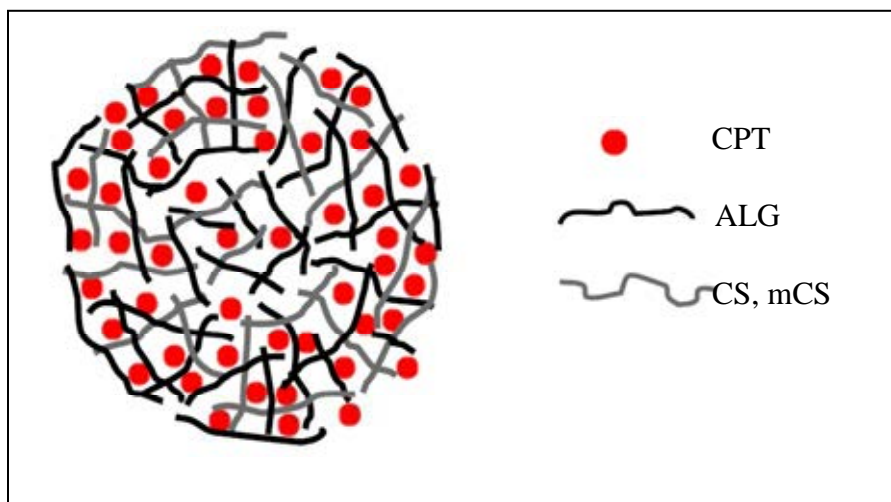
Figure 4.14 Schematic microstructure of CPT-loaded ALG/CS or ALG/mCS mirospheres

The microstructure of CPT-CS/ALS and CPT-mCS/ALS microspheres were speculated as Figure 4.14 to explained the encapsulated CPT of polymers. It could be understood by associating the polymer solidification process with the CPT loading process. ALG and CS derivatives gradually formed homogeneous network, which was just like many cage. CPT could easily enter the inside because of the loose structure outside microspheres. With the soldification process proceeded, the CPT was hindered because the structure of microspheres became compact due to the matrix formation between ALG and CS.

Mucoadhesiveness of microspheres

Mucoadhesiveness of microspheres was measured as a way to test their ability to bind to the mucosal surfae of the body (mucoadhesiveness). The results of *in vitro* mucoadhesive of the spheres with mucin in three different buffers (pH 1.2, 4.0, and 6.4) are shown in Table 4.4 by PAS method**.**

Table 4.4 Effect of composition on mucoadhesive property of the CS compared with CS/ALG microsphers

Abbreviations	Adsorbed of mucin at pH 1.2 (mg) ($\pm SD$, *n*=3)	Adsorbed of mucin at pH 4.0 (mg) ($\pm SD$, *n*=3)	Adsorbed of mucin at pH 4.0 (mg) ($\pm SD$, *n*=3)
CS	0.06 ± 0.01	0.31 ± 0.05	0.42 ± 0.03
mCS	0.38 ± 0.01	0.79 ± 0.03	0.75 ± 0.01
CS/ALG	0.16 ± 0.01	0.44 ± 0.03	0.51 ± 0.01
mCS/ALG	0.30 ± 0.01	0.61 ± 0.01	0.65 ± 0.02
CPT-CS/ALG	0.17 ± 0.03	0.53 ± 0.01	0.59 ± 0.03
CPT-mCS/ALG	0.31 ± 0.01	0.60 ± 0.01	0.66 ± 0.02

At the low pH (SGF, pH1.2), the microspheres prepared from CS/ALG with CPT absorbed mucin about 2.9-fold more than, whist the mCS/ALG and CPT-mCS/ALG exhibited excellent mucoadhesiveness,with 5.27- and 5.60-fold higher than that of the native chitosan. In contrast, the mucoadhesive of the CPT-CS/ALG microspheres showed ~1.67- and 1.38-, whist the CPT-mCS/ALG microspheres exhibited approximately 1.86- and 1.55- fold compared to the unmodified chitosan at pH 4.0 and 6.4, respectively. From these results indicated that polyelectrolyte complex between CS derivatives and ALG showed incresing in mucoadhesive when compared with the unmodified CS due to CS/ALG increasing in flexibility of its CS backbone structure and polar functional group. As a result of this, they are able to interact with the mucus chains and show good mucoadhesiveness. This is supported by the study of Wittaya-areekul *et at*. (2006) and Huang *et al.* (2000) demonstrating

that the adhesive capabilities of CS/ALG hydrogels can be improved by tethering of long flexible chains to a particle surface. The resulting hydrogels exhibit increased mucoadhesive properties due to enhanced anchoring of the flexible chains with the mucosa[1].

In these work, the mCS/ALG showed strongly increased in mucoadhesive ability than CS/ALG due to the addition of the thiol groups because of the electrostatic and hydrophobic effects. With respect to the electrostatic effect, this is due to the remaining NH_3^+ moieties of both the CS backbone and the HT side chain being able to interact with either the COO^- or SO_3^- groups on the mucin carbohydrate side chain in an acidic media. For the hydrophobic effect, the $-CH_2$ moieties of HT interact in part with the $-CH_3$ groups on the mucin side chains which, lead to a high mucoadhesive adsorption. Therefore, the effects of both electrostatic and hydrophobic effects have impact on the mucoadhesion of mCS/ALG microspheres.

However, the mCS/ALG microspheres showed reducing mucoadhesion level compared to mCS at all tested pH conditions, indicating that after the mCS formed polyelectrolyte complex with ALG, the carobxylate groups of ALG were interacted with protonated amino groups of chitosan throught electrostatic interaction, which is likely to be due to the fact that the influence of the positive charge of mCS/ALG was not enough to increase the mucoadhesion when compared with mCS.

4.2.3 Characterization of microspheres

4.2.3.1 Fourier transform infrared spectroscopy (FTIR)

FTIR spectroscopy was used to determine the chemical interaction of the samples as displayed in Figures 4.15 and 4.16

Figure 4.15 and 4.16 represents FTIR spectra of pure alginate, chitosan, pure CPT, CS/ALG microspheres, mCS/ALG microspheres, 1%CPT-CS/ALG microspheres, and1%CPT-mCS/ALG microspheres.

The FTIR spectrum of alginate (Fig. 4.15a, 4.16a) showed a distinct peak at 3422 cm^{-1} which was due to the O-H groups presented on the structure. The symmetric peak around 1618 cm^{-1} and the asymmetric peak around 1412 cm^{-1} was be due to COO^- stretching vibration. The peak at 1024 cm^{-1} was due to C-O-C stretching in the intra- and intermolecular between polymer's repeating units.

The FTIR spectrum of chitosan (Fig. 4.15b) also showed the peak at 3428 cm^{-1} corresponding to the O-H stretching. The small peak of amide bond at 1635 cm^{-1} and a small protonated amino peak at 1599 cm^{-1} resulting from partial *N*-deacetylation of chitin. The peak near 1370 cm^{-1} which was due to –CH_3 bending and the peak at 1153 cm^{-1} was attributed to C-O-C stretching.

The FTIR of polyelectrolyte complexes made from CS and ALG microspheres are shown in Figure 4.18c. The peaks at 1592 cm^{-1} and 1407 cm^{-1} are associated with symmetric COO^- stretching vibration, and asymmetric COO^- stretching vibration, respectively. The peak near 1407 cm^{-1} was due to the asymmetric COO^- stretching vibration of carboxyl group in alginate and the broad peaks from 1407-1413 cm^{-1}, are observed after complexation of alginate with the chitosan polymer[32]. Considering that, the observed changes in the absorption bands of CS/ALG microspheres may be explained by existance of interaction between CS and ALG ocurring during complexation process. (Fig. 4.17) [33].
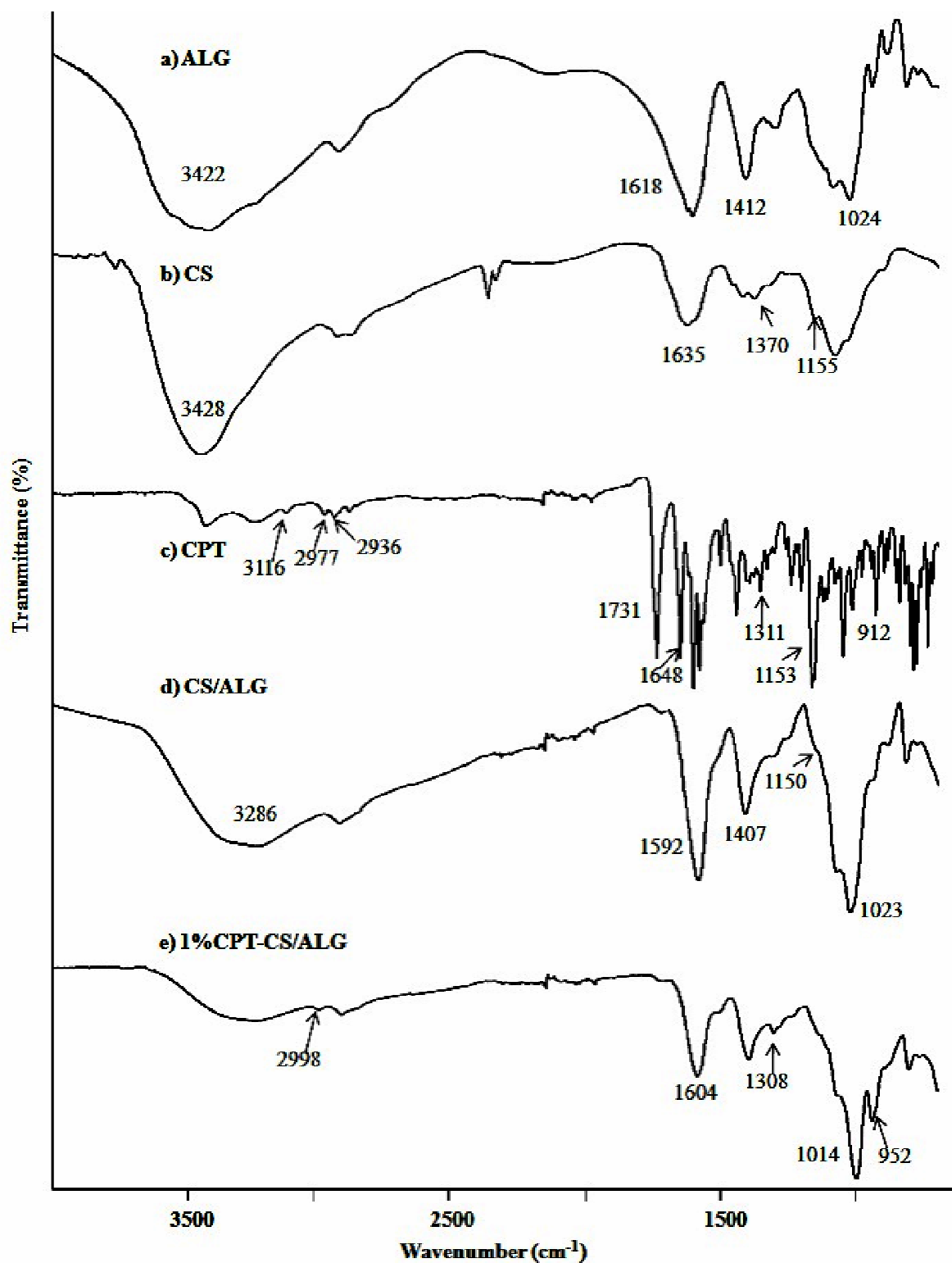
Figure 4.15 FTIR spectra of (a) ALG, (b) CS, (c) CPT, (d) CS/ALG, and (e) 1%CPT-CS/ALG
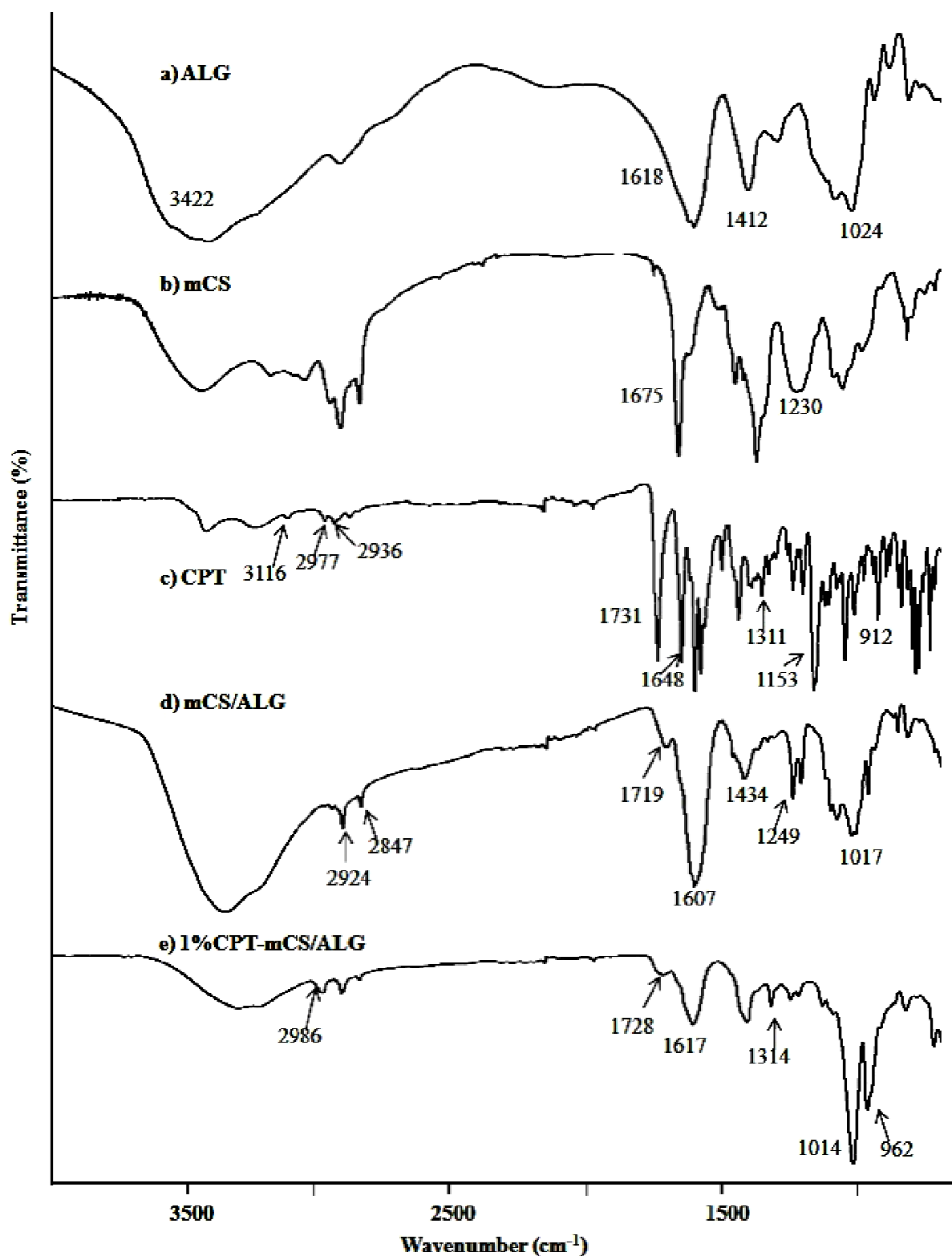
Figure 4.16 FTIR spectra of (a) ALG, (b) mCS, (c) CPT, (d) mCS/ALG, and (e) 1%CPT-mCS/ALG
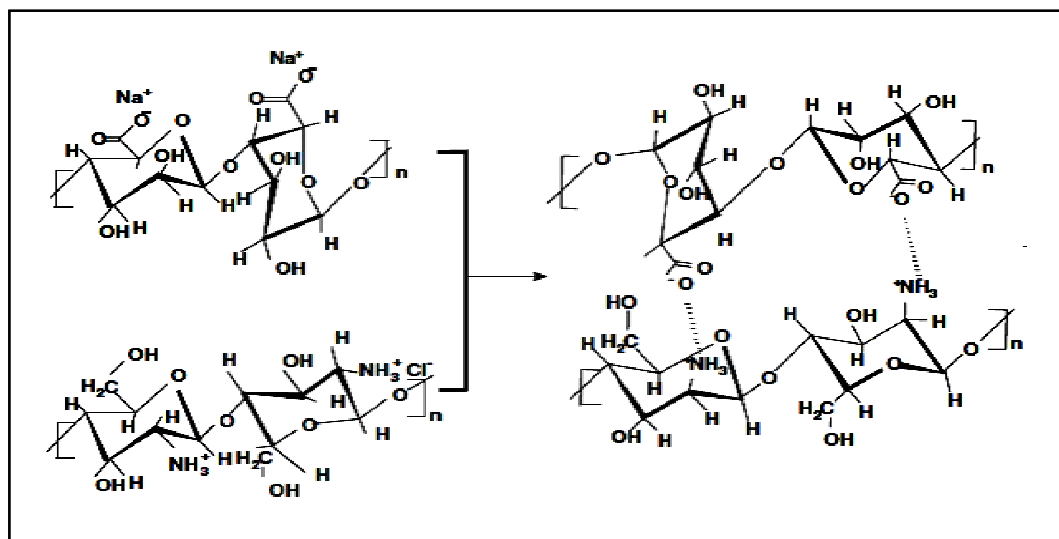
Figure 4.17 Structural representation of CS/ALG ion complex formation reaction between anion group (COO⁻) of sodium alginate and the protonated cation group (-NH₃C) of chitosan[34].

The FTIR spectrum of CPT (Fig. 4.15d, 4.16d) as can be seen, the main characteristic peaks of CPT are at around 1731 cm^{-1} and 1648 cm^{-1} were due to stretching vibration of C=O ketone and ester groups, respectively. The existence of one or more aromatic ring in a structure is normally readily determined from the C-H and C=C-C related vibrations. The C-H stretching occurs above 3000 cm^{-1} and is typically exhibited as a multiplicity of weak to moderate bands, compared with the aliphatic C-H stretch. The aromatic compounds show the presence of C-H stretching vibrations around 3100-3000 cm^{-1} range. In amino quinoline, the modes were observed at 3116, 2977, and 2936 cm^{-1} [29]. The position of the band 1598-1434 cm^{-1}, assigned to the skeletal vibrations of the phenyl ring[30]. The C-H in-plane bending vibrations are observed in the region 1350-950 cm^{-1} and are usually medium to weak. The C-H out-of plane bending modes are usually of weak intensity arises in the region 600-900 cm^{-1} [31].

The FTIR spectrum of 1%CPT-CS/ALG microspheres was shown in Fig. 4.16d, 1%CPT loaded CS/ALG, there were additional absorption peaks at 2998 corresponding to aminoquinoline peak of CPT. The peak at 1308 cm^{-1} and 952 cm^{-1} were due to C-H in-plane bending vibrations of CPT. These CPT characteristic peaks were broadened or shifted in the formulations suggesting definite interactions between CPT and CS/ALG [35] and because of effect of CaCl$_2$, confirming the successful loading of CPT on CS/ALG microparticles.

In order to define the interaction between the drug and the mCS/ALG in the microphers, samples of mCS, mCS-ALG, and CPT-mCS/ALG were investigated.

The mCS (Fig. 4.16b), which is QCS: HT sample (1:0.1 (w/w) ratio), the band at 1675 cm^{-1} is attributed to the stretching vibration of the C=O acetamide group of mCS. Compared with CS, the absorption band at 1230 cm^{-1} corresponds to an increased level of alkyl group
C-C bonds.

The FTIR spectra of polyion complex made from the mCS and ALG are shown in Fig. 4.16c. The spectral of mCS/ALG shows the new characteristic absorption bands at 1719 cm^{-1} and 1249 cm^{-1} were observed due to the asymmetric and symmetric stretching of –COO$^-$ groups respectively. The band appearing at 1607 cm^{-1} in the spectrum of polyion complex microspheres can be assigned to a symmetric –NH$_3$C and –N(CH$_3$)$_3$C deformation, and broad bands appearing at 2500 cm^{-1} confirm the presence of –NH$_3$C group in the polyion complex microspheres. The spectra confirmed that the carboxylate groups of sodium alginate were dissociated to COO$^-$ groups which complexed with protonated amino groups of modified chitosan throught electrostatic interaction. Morover, as the polyion complex formation proceeds, the O-H bonding would also be expected because of an increase in intermolecular interaction such as hydrogen bonding between sodium alginate and modified chitosan [34].

The FTIR spectra of 1%CPT-mCS/ALG are shown in Figure 4.16d. As can bee seen,the three characteristic peak at 2986 cm^{-1} and 1728 cm^{-1}corresponding to aminoquinoline peak and ketone peak of CPT, 1314 cm^{-1} and 962 cm^{-1} were due to C-

H in-plane bending vibrations of CPT appear in the FTIR of 1%CPT-mCS/ALG, indicating that CPT were loaded on microspheres.

4.2.3.2 Thermogravimetric analysis (TGA)

Thermagravimetric analysis (TGA) is a useful technology to characterize the thermal behavior of materials, which is correlated to their structure, hydrophilic properties and association states, and can further the presence of interaction between chitosan and alginate [36]. The TGA thermograms of the ALG, CS, mCS, CS/ALG, mCS/ALG, 1%CPT-CS/ALG, and 1%CPT-mCS/ALG nanoparticles were shown in Figure 4.18 and 4.19.

The TGA thermograms of ALG (Figure 4.18 a) showed a weight loss of water about 16.3 % (30 °C to 104 °C). Afterwards, the degradation of ALG occurred in the temperature range from 233 to 307 °C with 35.4 % weight loss.

The TG curve of the unmodified CS (Figure 4.18 b) showed two stages of weight loss, the first being water loss (13.5% of the total weight) at 26 °C to 160 °C, whilst the second stage was from ~208 ° to 288 °C, accounting for a loss of 34.6% of the total weight and was ascribed to the degradation of CS backbone.

The TGA thermograms of CS/ALG microspheres (Figure 4.18 c) showed a broad transition wih a relatively three different stages of weight loss. The first stage range between ~30 °C to 147.0 °C attributed to a dehydration process while the second one denotes the temperature of alginate degradation [37]. The last stage of weight loss at 147 °C-341.4 °C may due to thermal degradation of the CS complex.

Inclusion complexes of CPT with CS/ALG (Figure 4.18 d showed weight loss of complexes were shift to higher stage from 341.4 °C to 382.0°C due to decomposition of CPT.

Previous works detected three different regimed of mCS (Figure 4.19 b). The first released of free water and breakage of hydrogen bonds at < 100 – 160 °C, at 187 to 250 °C (23.3% total weight) is attributed to the thermal degradation of the HT, whilst the final stage at 250-440 °C(42.8% total weight) was attributed to the decomposition of the QCS matrix**.**

Additionally, the third stage of weight loss starts at 222.3 °C to 304.8 °C during which there was 54.9 % weight loss due to the degradation of CS. While TGA thermograms of mCS/ALG microspheres (Figure 4.19c) showed three stages of weight. The location of the first decomposition peak seems to be similar for CS/ALG microspheres, a two-step decomposition process ocurring at 193.1°C and 278.4°C for HT. The final rate of weight loss curve for ALG and mCS reveals two additional small and broad peaks at 274.8°C and 317.0°C. However, CS/ALG and mCS/ALG microspheres were shift in the position of the last decompositon step (304.8°C and 317.0°C, respectively) due to decomposition of modifiedchitosan in the polymer matrix. This result is in line with the behavior of polymer, as stated above. We suggest that the shift of the last decompostion temperature of mCS to higher value is a result of inter- and intramolecular disulfide interaction, which result in a higher polymer thermal stability. It is well established that intramolecular interactions increase the thermal stability of polymer, thus leading to higher decompostion tempertue [38].

Inclusion complexes of CPT with mCS/ALG (Figure 4.19 d) showed weight loss of complexes were shift to higher stage from 317.0°C to 379.9°C for CPT-CS/ALG and CSP-mCS/ALG, respectively) due to decomposition of CPT.
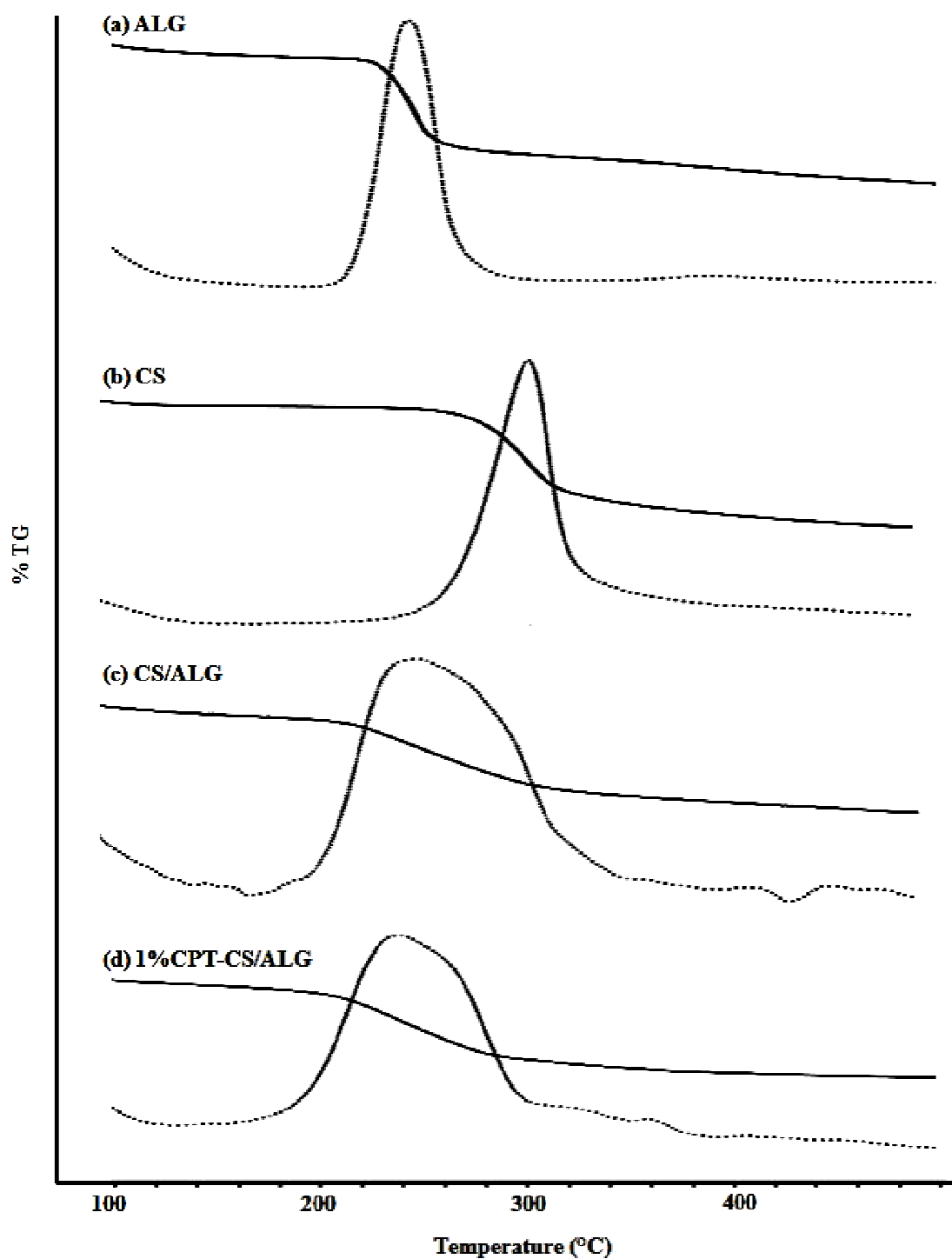
Figure 4.18 TGA thermogram of (a) ALG, (b) CS, (c) CS/ALG microspheres and
(d) 1% CPT-CS/ALG microsphers
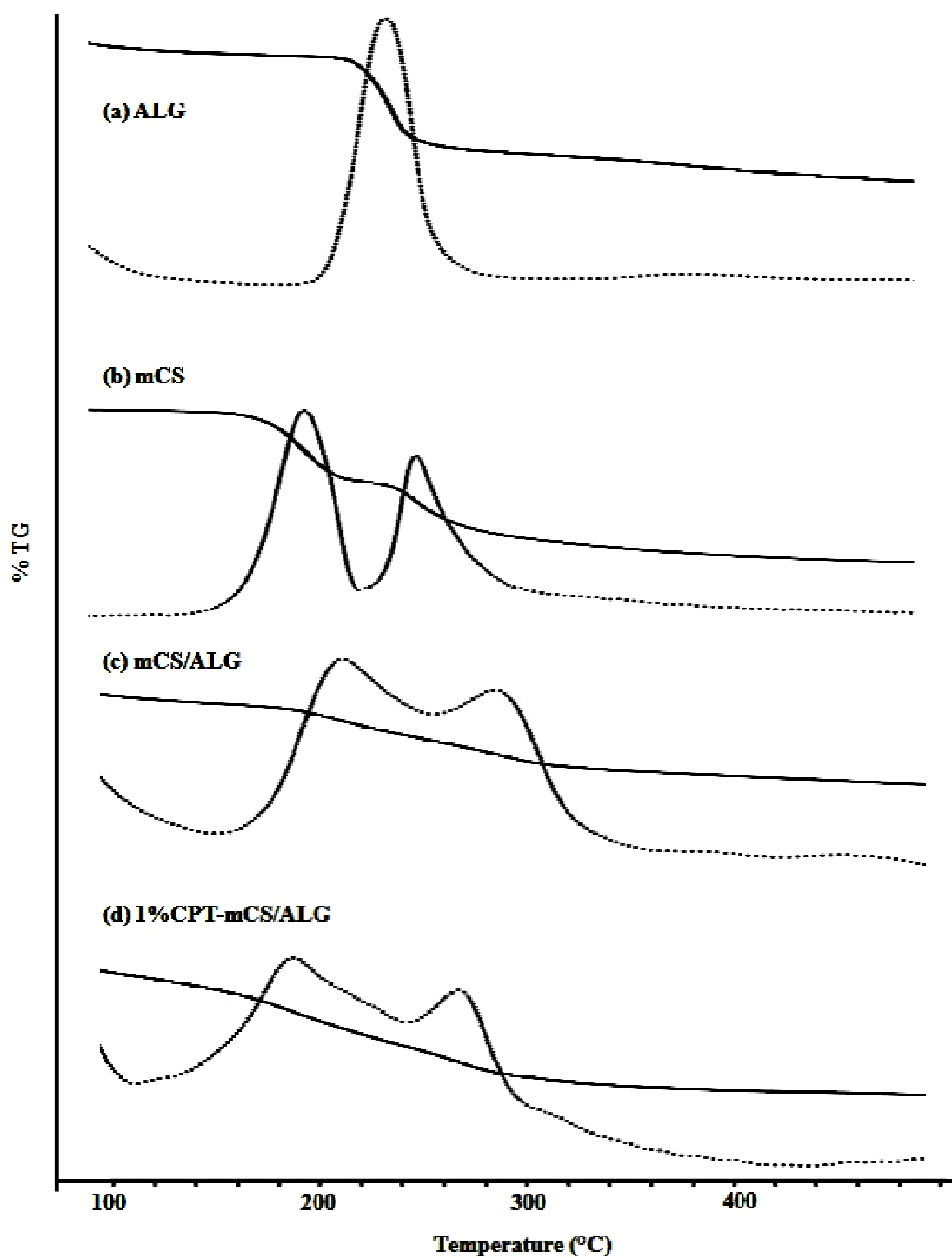
Figure 4.19 TGA thermogram of (a) ALG, (b) mCS, (c) mCS/ALG microspheres and (d) 1% CPT-mCS/ALG microsphers

4.2.4 Evaluation of drug encapsulation efficiency (%EE)

The percentages of encapsulation efficiency (%EE) of the CPT loaded CS/ALG and mCS/ALG microspheres were given in Table 4.5.

The encapsulation efficiency and loading capacity of drug within CPT loaded CS/ALG and mCS/ALG microspheres were analyzed using UV/Vis microplate reader spectroscopy at $\lambda_{max} = 370$ nm.

In this work, the amount of CPT, which is loading on encapsulation efficiency were investigated to achieve the high percentage of encapsulation efficiency. The encapsulation efficiency of microspheress 1.0% CPT loaded CS/ALG and mCS/ALG were 74.3% and 69.6% respectively. (Table 4.5)

This result explained that the electrospray technique can produce high percentage encapsulation at about 70% encapsulation.

Table 4.5 Encapsulation of CPT loaded polymer microspheres*

Formulations	% Encapsulation
• CS/ALG	-
• 1%CPT-CS/ALG	74.3 ± 2.11
• mCS/ALG	-
• 1%CPT-mCS/ALG	69.6 ± 0.71

* mean ± SD (*n*=3)

From these results, the CPT is statistically insignificant (*P*<0.01) encapsulation efficiency between CS/ALG and mCS/ALG microspheres.

4.2.5 *In vitro* CPT release profiles

        The release of CPT drug from CS/ALG and mCS/ALG microspheres were performed at a function of time intervals in buffers pH 1.2, 4.0, and 6.4 (SGF, vaginal fluids, and SIF, respectively) at 37°C (Figure 4.21-4.25).
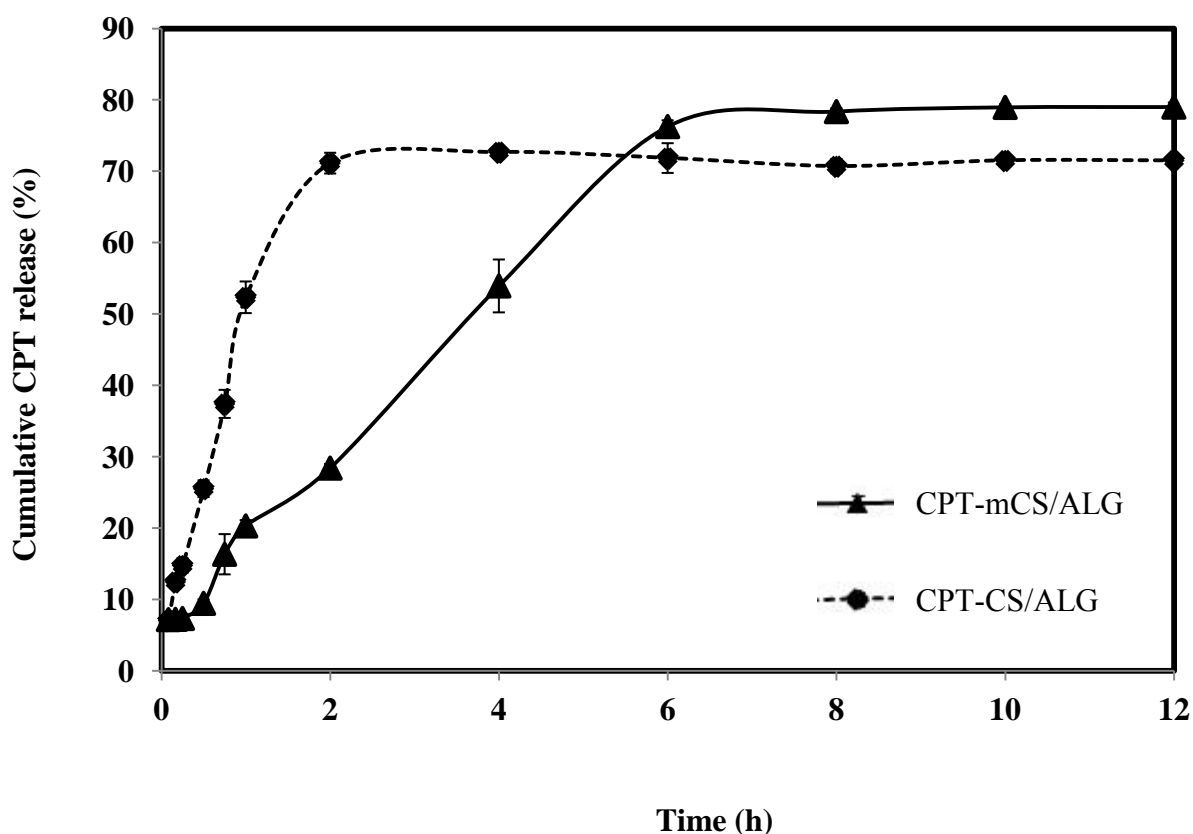
Figure 4.20 Release profiles of camptothecin (CPT) from CS/ALG and mCS/ALG in pH 1.2, 37°C (average± SD, *n*=3).

        As can be seen from Figure 4.21-4.23, the cumulative drug release percentage are approximately 70% and 78% for CS/ALG and mCS/ALG in pH 1.2 respectively and ~ 70% for both CS/ALG and mCS/ALG in pH 4.0 respectively. Moreover, the release behavior in pH 6.4 (Figure 4.24) was significantly lower than that in pH 1.2 and 4.0. Most of CPT released from the spheres in the first 12 h.

In order to mCS/ALG is cumulative release percentage approximately 50% in ~ 3.5, 9.0, and 7.5 h for pH 1.2, 4.0, and 6.4, respectively. But, the CS/ALG released faster up to ~ 50% in the first hour in pH 1.2 and approximately 6.0 and 5.5 h, in pH 4.0 and 6.4, respectively.
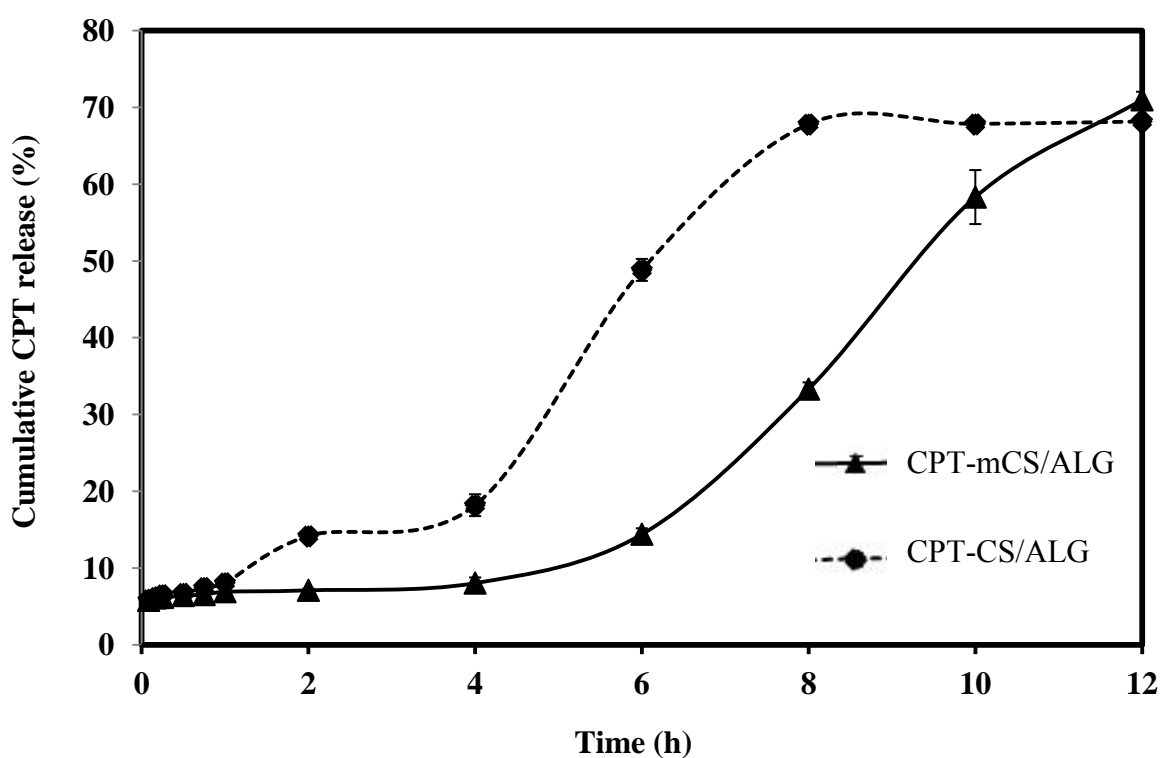
Figure 4.21 Release profiles of camptothecin (CPT) from CS/ALG and mCS/ALG at pH 4.0, 37°C (average± SD, n=3)
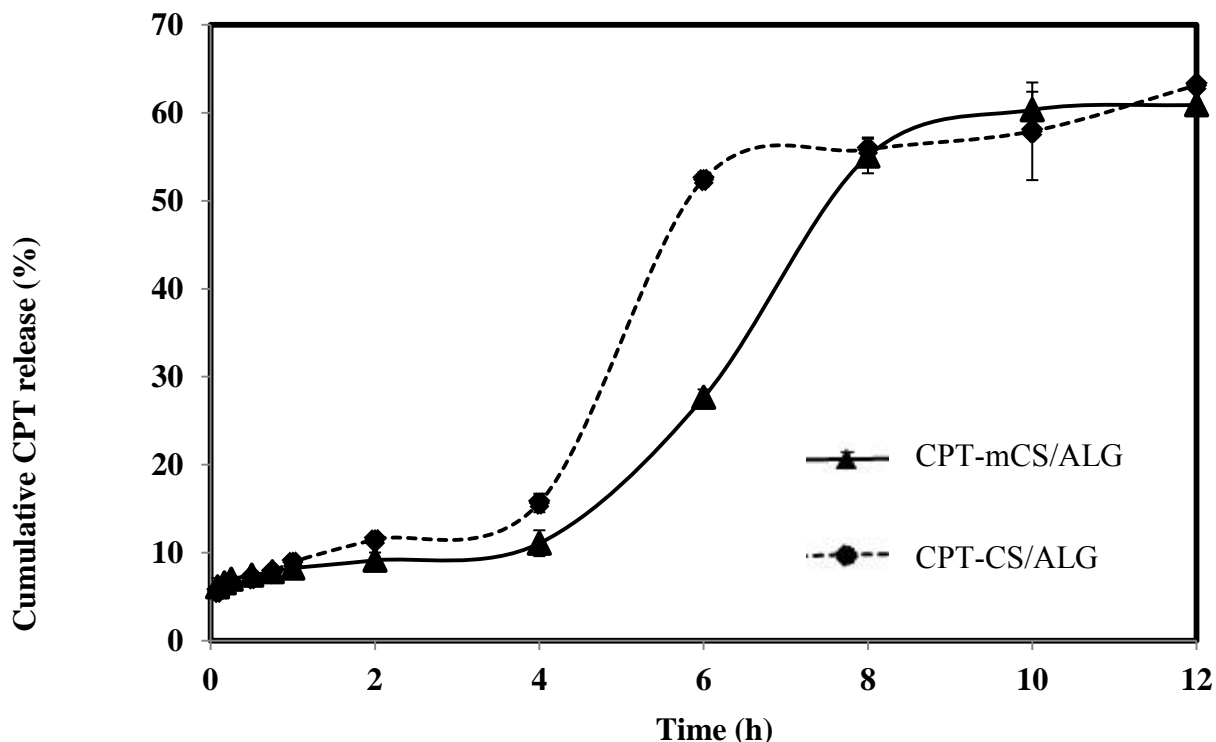
Figure 4.22 Release profiles of camptothecin (CPT) from CS/ALG and mCS/ALG at pH 6.4, 37°C (average± SD, n=3)

As a function of pH, figure 4.24-4.25 presents the releasing profile of CPT from CS/ALG and mCS/ALG in three different buffers (pH 1.2. 4.0, and 6.4). From these results shows the release rate of CPT from these microspheres in pH 1.2 was much higher than that in the environment of pH 4.0 and 6.4 for both CS/ALG and mCS/ALG micospherses.

Figure 4.24 shows that the release of CPT from spheres in pH 1.2 occurred very fast, the cumulative release percentage is up to 70% in the first hour. On the other hand, drug-loaded formulations released the drug slowly; it release only ~10% in the higher pH.

The effect of pH on the release rate of CPT from the mCS/ALG microspheres is showns in Figure 4.25. As can bee seen in figure 4.25, when pH of the medium is 1.2, the cumulative release of CPT from the spheres is ~20% within the first hour, and below 10% in both pH 4.0 and 6.4.

Overall, from these results indicated that CPT loaded mCS/ALG formulation released the drug slowly than CS/ALG.
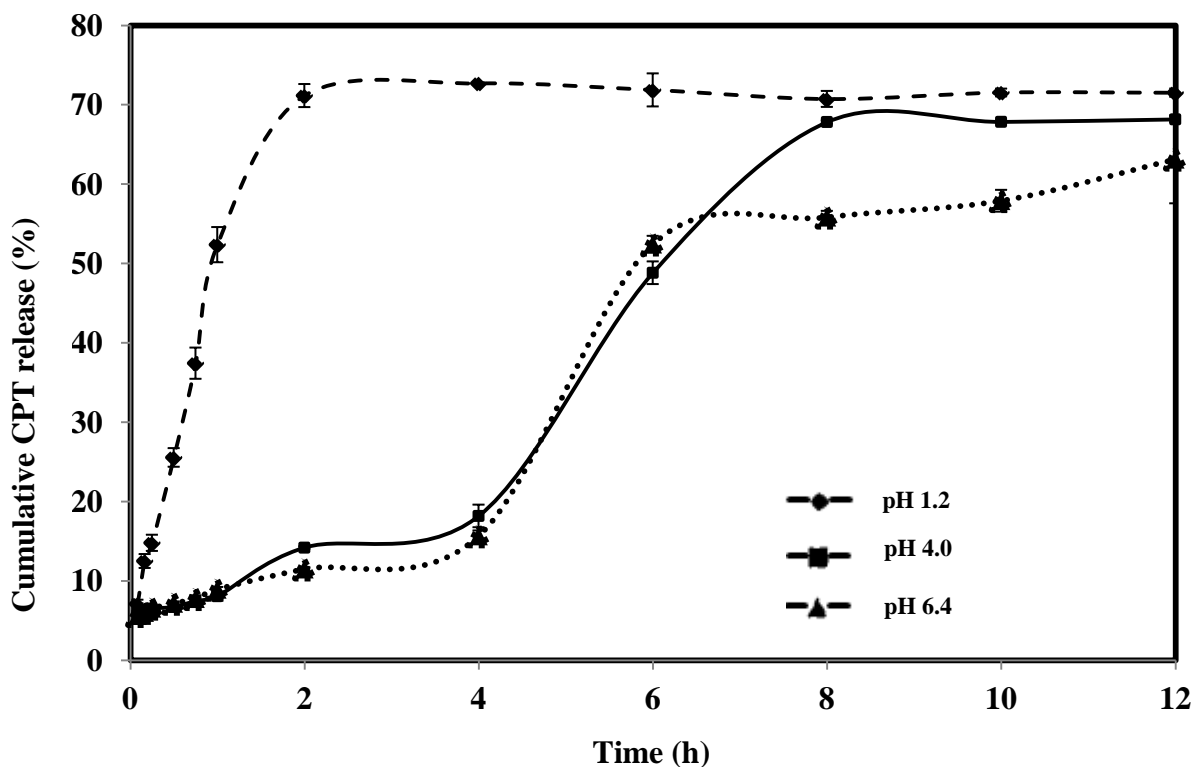
Figure 4.23 Release profiles of camptothecin (CPT) from CS/ALG in three different buffers, $37^{\circ}C$ (average± SD, $n=3$)

These difference of their drug release is reponsible for the swelling ratio of the microsphere with changing pH of the medium. The reason of these pH sensitive phenomenon was directly proportional to the swelling ratio of the polymer, that is the swelling ratio of CS and mCS before interact with ALG shows results in pH 1.2 > pH 4.0 > pH 6.4. This results indicated that the higher swelling ratios of the polymer create larger surface areas to diffuse the drug [1].

At pH 4.0 as can be seen from Figure 4.24 and 4.25, the effect of ALG on the release rate of CPT from polymer matrix was due the COO^- groups of ALG can convert to –COOH groups, and the hydrogen bonding can be formed among -OH, -

NHCO, -NH$_2$ group of CS/ALG in the acid solution, which is responsible for the small swelling ratio when pH <5 [2].

In order to mCS/ALG, another reason for the sustained release of CPT in which shows in Figure 4.25 within 4 h in all pH were that mCS/ALG microspherse seems to be the formation of disulfide bonds within the matrix microspheres. This cross-linking process might provide a tightened three-dimensional polymeric network leading to a more controlled drug release. Hence, the advantages of the controlled release system based on the mucoadhesive polymers can be improved by using their thiolated derivatives [3].
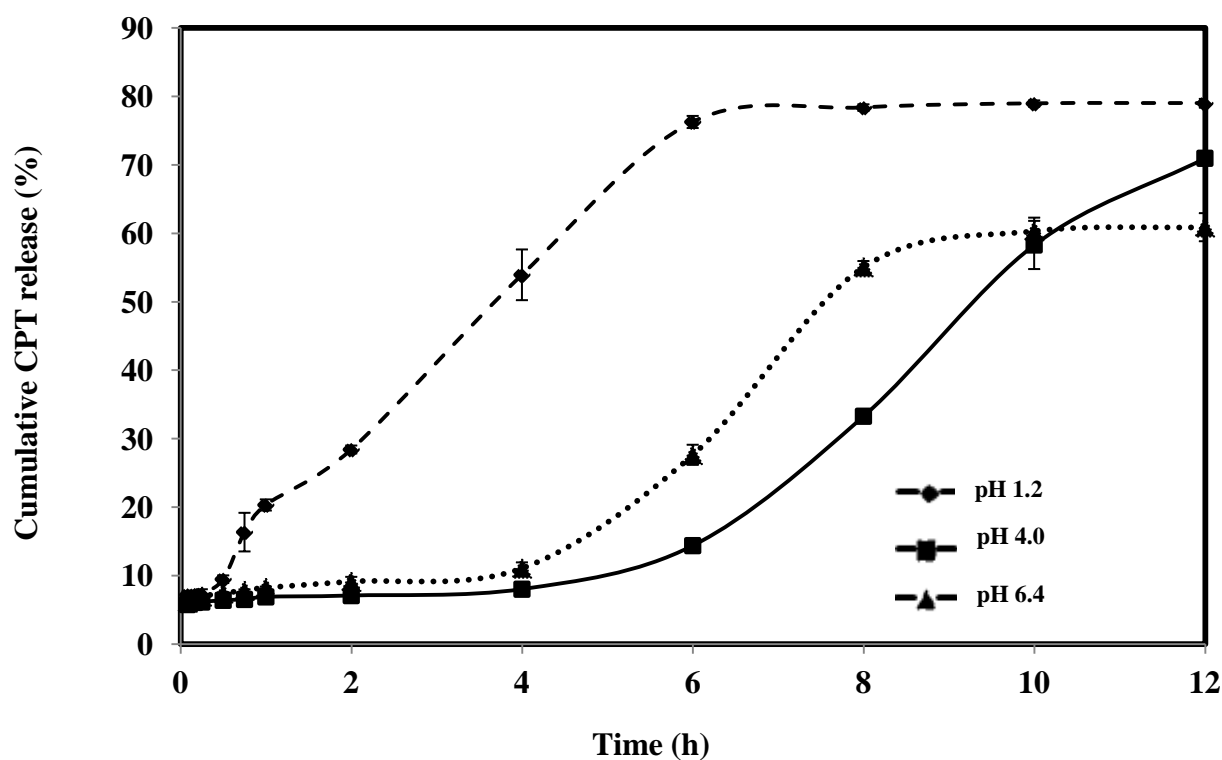
Figure 4.24 Release profiles of camptothecin (CPT) from mCS/ALG in three different buffers, 37°C (average± SD, *n*=3)

CHAPTER V

CONCLUSION

In this work, the thiolated chitosan and thiolated quaternized chitosan were successfully synthesized. HT was immobilized on CS and QCS by covalent bonding under mild conditions and thiolation resulted in strongly improved mucoadhesive properties and a good swelling behavior at a low pH. Because of these characteristics, the obtained thiolated CS derivatives (CS-HT and QCS-HT) appear to be promising novel polymers for the development of various drug delivery systems at mucus sites.

The results of electrospray ionization, which was used to prepare controlled release microspheres of Camptothecin (CPT), shows demonstrated that the electrospraying process is a facile technique for the production of CS/ALG and mCS/ALG microspheres. The morphology and size of these spheres can be manipulated by fixing the parameters as follows: working distance of 8 cm, needle gauge of 26 G, flow rate of 1.2 mL/h, stirring rate of 400 rpm and electrospraying voltage of 12 kV. The size distribution of 1%CPT-polymer (w/w) microspheres are narrow and produce approximately 70% drug entrapment efficiency. Thus, the electrospraying techinque could be a promising technique for the fabrication of microspheres-based drug delivery carrier. The CPT-polymer microspheres can be prolonged release of CPT. It was found that the release profiles of camptothecin were greatly improved upon using modifiedchitosan within 12 hours due to the mCS/ALG microspherse seems to be the formation of disulfide bonds within the matrix microspheres. This cross-linking process might provide a tightened tree-dimentional polymeric network leading to a more controlled drug release. Hence, the advantages of the controlled release system based on the mucoadhesive polymer can be improved by using their thiolated chitosan derivatives.

REFERNCES

[1]   Ludwig, A., *The use of mucoadhesive polymers in ocular drug delivery.* Advanced Drug Delivery Reviews, 57, 11(2005): 1595-1639.

[2]   Salamat-Miller, N., M. Chittchang, and T.P. Johnston, *The use of mucoadhesive polymers in buccal drug delivery.* Advanced Drug Delivery Reviews,57, 11 (2005): 1666-1691.

[3]   Ugwoke, M.I., et al., *Nasal mucoadhesive drug delivery: Background, applications, trends and future perspectives.* Advanced Drug Delivery Reviews, 57, 11 (2005): 1640-1665.

[4]   Madsen, F., K. Eberth, and J.D. Smart, *A rheological assessment of the nature of interactions between mucoadhesive polymers and a homogenised mucus gel.* Biomaterials, 19, 11-12 (1998): 1083-1092.

[5]   Andrews, G.P., T.P. Laverty, and D.S. Jones, *Mucoadhesive polymeric platforms for controlled drug delivery.* European Journal of Pharmaceutics and Biopharmaceutics, 71, 3 (2009): 505-518.

[6]   Grabovac, V., D. Guggi, and A. Bernkop-Schnurch, *Comparison of the mucoadhesive properties of various polymers.* Advanced Drug Delivery Reviews, **57**, 11 (2005): 1713-1723.

[7]   Agnihotri, S.A., N.N. Mallikarjuna, and T.M. Aminabhavi, *Recent advances on chitosan-based micro- and nanoparticles in drug delivery.* Journal of Controlled Release, 100, 1 (2004): 5-28.

[8]   Min, K.H., et al., *Hydrophobically modified glycol chitosan nanoparticles-encapsulated camptothecin enhance the drug stability and tumor targeting in cancer therapy.* Journal of Controlled Release, **1**27, 3 (2008): 208-218.

[9]   Son, Y.J., et al., *Biodistribution and anti-tumor efficacy of doxorubicin loaded glycol-chitosan nanoaggregates by EPR effect.* Journal of Controlled Release, 91, 1-2 (2003) : 135-145.

[10]   Sang Yoo, H., et al., *Self-assembled nanoparticles containing hydrophobically modified glycol chitosan for gene delivery.* Journal of Controlled Release, 103, 1 (2005): 235-243.

[11]   Kweon, D.-K., S.-B. Song, and Y.-Y. Park, *Preparation of water-soluble chitosan/heparin complex and its application as wound healing accelerator.* Biomaterials, 24, 9 (2003): 1595-1601.

[12]   Bhattarai, N., et al., *Electrospun chitosan-based nanofibers and their cellular compatibility.* Biomaterials, 26, 31 (2005): 6176-6184.

[13]   Bravo-Osuna, I., et al., *Mucoadhesion mechanism of chitosan and thiolated chitosan-poly(isobutyl cyanoacrylate) core-shell nanoparticles.* Biomaterials, 28, 13(2007): 2233-2243.

[14]   Muzzarelli, R.A.A. and F. Tanfani, *The N-permethylation of chitosan and the preparation of N-trimethyl chitosan iodide.* Carbohydrate Polymers, **5,** 4 (1985): 297-307.

[15]   Sandri, G., et al., *Nanoparticles based on N-trimethylchitosan: Evaluation of absorption properties using in vitro (Caco-2 cells) and ex vivo (excised rat jejunum) models.* European Journal of Pharmaceutics and Biopharmaceutics, 65, 1 (2007): 68-77.

[16] Jintapattanakit, A., et al., *Physicochemical properties and biocompatibility of N-trimethyl chitosan: Effect of quaternization and dimethylation.* European Journal of Pharmaceutics and Biopharmaceutics, 70, 2 (2008): 563-571.

[17] Roldo, M., et al., *Mucoadhesive thiolated chitosans as platforms for oral controlled drug delivery: synthesis and in vitro evaluation.* European Journal of Pharmaceutics and Biopharmaceutics, 57, 1 (2004): 115-121.

[18] Kast, C.E. and A. Bernkop-Schn   rch, *Thiolated polymers -- thiomers: development and in vitro evaluation of chitosan-thioglycolic acid conjugates.* Biomaterials, 22, 17 (2001): 2345-2352.

[19] Snyder, G.H., et al., *Use of local electrostatic environments of cysteines to enhance formation of a desired species in a reversible disulfide exchange reaction.* Biochimica et Biophysica Acta (BBA) - Protein Structure and Molecular Enzymology, 749, 3 (1983): 219-226.

[20] Kafedjiiski, K., et al., *Synthesis and in vitro evaluation of a novel thiolated chitosan.* Biomaterials, 26, 7 (2005): 819-826.

[21] Bernkop-Schnurch, A., *Thiomers: A new generation of mucoadhesive polymers.* Advanced Drug Delivery Reviews, 57, 11 (2005): 1569-1582.

[22] Hornof, M.D., C.E. Kast, and A. Bernkop-Schnurch, *In vitro evaluation of the viscoelastic properties of chitosan-thioglycolic acid conjugates.* European Journal of Pharmaceutics and Biopharmaceutics, 55, 2 (2003): 185-190.

[23]   Kast, C.E., et al., *Chitosan-thioglycolic acid conjugate: a new scaffold material for tissue engineering?* International Journal of Pharmaceutics, 256, 1-2 (2003): 183-189.

[24]   Schmitz, T., et al., *Synthesis and characterization of a chitosan-N-acetyl cysteine conjugate.* International Journal of Pharmaceutics, 347, 1-2 (2008): 79-85.

[25]   Bernkop-Schnurch, A., M. Hornof, and T. Zoidl, *Thiolated polymers-- thiomers: synthesis and in vitro evaluation of chitosan-2-iminothiolane conjugates.* International Journal of Pharmaceutics, 260, 2 (2003): 229-237.

[26]   Jakubowski, H., *The determination of homocysteine-thiolactone in biological samples.* Analytical Biochemistry, 308, 1 (2002): 112-119.

[27]   Gao, Y., L.B. Li, and G. Zhai, *Preparation and characterization of Pluronic/TPGS mixed micelles for solubilization of camptothecin.* Colloids and Surfaces B: Biointerfaces, 64, 2 (2008): 194-199.

[28]   Opanasopit, P., et al., *Incorporation of camptothecin into N-phthaloyl chitosan-g-mPEG self-assembly micellar system.* European Journal of Pharmaceutics and Biopharmaceutics, 64, 3 (2006): 269-276.

[29]   Cortesi, R., et al., *Formulation study for the antitumor drug camptothecin: liposomes, micellar solutions and a microemulsion.* International Journal of Pharmaceutics, 159, 1 (1997): 95-103.

[30]   Ertl, B., et al., *Poly(d,l-lactic-co-glycolic acid) microspheres for sustained delivery and stabilization of camptothecin.* Journal of Controlled Release, 61, 3 (1999): 305-317.

[31]   Norbedo, S., et al., *Synthesis of 6-amino-6-deoxyhyaluronan as an intermediate for conjugation with carboxylate-containing compounds: application to hyaluronan camptothecin conjugates.* Carbohydrate Research, 344, 1 (2009): 98-104.

[32]   Dong, L., et al., *Synthesis and release behavior of composites of camptothecin and layered double hydroxide.* Journal of Solid State Chemistry. 183, 8: 1811-1816.

[33]   Watanabe, M., et al., *Preparation of camptothecin-loaded polymeric micelles and evaluation of their incorporation and circulation stability.* International Journal of Pharmaceutics, 2006. 308, (1-2): 183-189.

[34]   Kawano, K., et al., *Enhanced antitumor effect of camptothecin loaded in long-circulating polymeric micelles.* Journal of Controlled Release, 112, 3 (2006): 329-332.

[35]   Xu, Y., et al., *Preparation of dual crosslinked alginateï€"chitosan blend gel beads and in vitro controlled release in oral site-specific drug delivery system.* International Journal of Pharmaceutics, 336, 2 (2007): 329-337.

[36]   Hoffman, A.S., *Hydrogels for biomedical applications.* Advanced Drug Delivery Reviews, 54, 1 (2002): 3-12.

[37]   Kindermann, C., et al., *Tailor-made release triggering from hot-melt extruded complexes of basic polyelectrolyte and poorly water-soluble drugs.* European Journal of Pharmaceutics and Biopharmaceutics, (0).

[38]   Bigucci, F., et al., *Chitosan/pectin polyelectrolyte complexes: Selection of*
        suitable preparative conditions for colon-specific delivery of
        vancomycin. European
        Journal of Pharmaceutical Sciences, 35, 5 (2008): 435-441.

[39]   Jimenez-Kairuz, A.F., D.A. Allemandi, and R.H. Manzo, *The improvement of*
        aqueous chemical stability of a model basic drug by ion pairing with
        acid groups of polyelectrolytes. International Journal of Pharmaceutics,
        269, 1 (2004): 149-156.

[40]   Wilhelm, O., L. Mรกdler, and S.E. Pratsinis, *Electrospray evaporation and*
        deposition. Journal of Aerosol Science, 34, 7 (2003): 815-836.

[41]   Oh, H., K. Kim, and S. Kim, *Characterization of deposition patterns produced*
        by twin-nozzle electrospray. Journal of Aerosol Science, 39, 9 (2008):
        801-813.

[42]   Veuillez, F., et al., *Factors and strategies for improving buccal absorption of*
        peptides. European Journal of Pharmaceutics and Biopharmaceutics,
        51, 2 (2001): 93-109.

[43]   Madsen, F., K. Eberth, and J.D. Smart, *A rheological examination of the*
        mucoadhesive/mucus interaction: the effect of mucoadhesive type and
        concentration. Journal of Controlled Release, 50, 1-3 (1998): 167-178.

[44]   Capra, R.l.H., et al., *Rheological, dielectric and diffusion analysis of*
         mucin/carbopol matrices used in amperometric biosensors. Sensors
        and Actuators B: Chemical, 124, 2 (2007): 466-476.

[45]   Smart, J.D., *The basics and underlying mechanisms of mucoadhesion.*
        Advanced Drug Delivery Reviews, 57, 11 (2005): 1556-1568.

[46]   Peppas, N.A. and J.J. Sahlin, *Hydrogels as mucoadhesive and bioadhesive materials: a review.* Biomaterials, 17, 16 (1996): 1553-1561.

[47]   Senyigit, Z.A., et al., *A comprehensive in vitro and in vivo evaluation of thiolated matrix tablets as a gastroretentive delivery system.* Drug Delivery. 18, 6: 405-414.

[48]   Thongborisute, J. and H. Takeuchi, *Evaluation of mucoadhesiveness of polymers by BIACORE method and mucin-particle method.* International Journal of Pharmaceutics, 354, 1-2 (2008): 204-209.

[49]   Leong, K.W. and R. Langer, *Polymeric controlled drug delivery.* Advanced Drug Delivery Reviews, 1, 3 (1988): 199-233.

[50]   Bajpai, A.K., et al., *Responsive polymers in controlled drug delivery.* Progress in Polymer Science, 33, 11 (2008): 1088-1118.

[51]   Ulbrich, K. and V.r. ฺubr, *Polymeric anticancer drugs with pH-controlled activation.* Advanced Drug Delivery Reviews, 56, 7 (2004): 1023-1050.

[52]   Jaworek, A. and A.T. Sobczyk, *Electrospraying route to nanotechnology: An overview.* Journal of Electrostatics, 66, 3-4 (2008): p. 197-219.

[53]   Yao, J., et al., *Characterization of electrospraying process for polymeric particle fabrication.* Journal of Aerosol Science, 39, 11 (2008): 987-1002.

[54]   Kruis, F.E., H. Fissan, and A. Peled, *Synthesis of nanoparticles in the gas phase for electronic, optical and magnetic applications--a review.* Journal of Aerosol Science, 29, 5-6 (1998): 511-535.

[55]   Jaworek, A., *Micro- and nanoparticle production by electrospraying.* Powder Technology, 176, 1 (2007): 18-35.

[56]   Yin, L., et al., *Drug permeability and mucoadhesion properties of thiolated trimethyl chitosan nanoparticles in oral insulin delivery.* Biomaterials, 30, 29(2009): 5691-5700.

[57]   Snyman, D., et al., *The relationship between the absolute molecular weight and the degree of quaternisation of N-trimethyl chitosan chloride.* Carbohydrate Polymers, 50, 2 (2002): 145-150.

[58]   Sieval, A.B., et al., *Preparation and NMR characterization of highly substitutedN-trimethyl chitosan chloride.* Carbohydrate Polymers, 36, 2-3 (1998): 157-165.

[59]   Kilcoyne, M., et al., *Periodic acid-Schiff's reagent assay for carbohydrates in a microtiter plate format.* Analytical Biochemistry. 416, 1: 18-26.

[60]   Muzzarelli, R.A.A., *Chitosan-based dietary foods.* Carbohydrate Polymers, 29, 4 (1996): 309-316.

[61]   Matsuda, A., et al., *Immobilization of laminin peptide in molecularly aligned chitosan by covalent bonding.* Biomaterials, 26, 15 (2005): 2273-2279.

[62]   Bernkop-Schnurch, A., C.E. Kast, and D. Guggi, *Permeation enhancing polymers in oral delivery of hydrophilic macromolecules: thiomer/GSH systems.* Journal of Controlled Release, 93, 2 (2003): 95-103.

[63]   Dong, Y., et al., *Influence of degree of molar etherification on critical liquid crystal behavior of hydroxypropyl chitosan.* European Polymer Journal, 2001. 37, 8: 1713-1720.

[64]   Sun, L., et al., *Preparation, characterization and antimicrobial activity of quaternized carboxymethyl chitosan and application as pulp-cap.* Polymer, 2006. 47, 6: 1796-1804.

[65]   Dung, P.l., et al., *Water soluble derivatives obtained by controlled chemical modifications of chitosan.* Carbohydrate Polymers, 24, 3 (1994): 209-214.

[66]   Prabaharan, M. and S. Gong, *Novel thiolated carboxymethyl chitosan-g-[beta]-cyclodextrin as mucoadhesive hydrophobic drug delivery carriers.* Carbohydrate Polymers, 2008. 73, 1: 117-125.

[67]   Spinelli, V.A., M.C.M. Laranjeira, and V.T. Fvere, *Preparation and characterization of quaternary chitosan salt: adsorption equilibrium of chromium(VI) ion.* Reactive and Functional Polymers, 61, 3 (2004): 347-352.

[68]   Zhang, C., et al., *Synthesis and characterization of water-soluble O-succinyl-chitosan.* European Polymer Journal, 39, 8 (2003): 1629-1634.

[69]   Rossi, S., et al., *Characterization of chitosan hydrochloride-mucin rheological interaction: influence of polymer concentration and polymer:mucin weight ratio.* European Journal of Pharmaceutical Sciences, 12, 4 (2001): 479-485.

[70]   Johnson, P. and K.D. Rainsford, *The physical properties of mucus: Preliminary observations on the sedimentation behaviour of porcine gastric mucus.* Biochimica et Biophysica Acta (BBA) - General Subjects, 286, 1 (1972): 72-78.

[71]   He, P., S.S. Davis, and L. Illum, *In vitro evaluation of the mucoadhesive properties of chitosan microspheres.* International Journal of Pharmaceutics, 1998. 166, 1: 75-88.

[72]   Palmberger, T.F., J. Hombach, and A. Bernkop-Schnurch, *Thiolated chitosan: Development and in vitro evaluation of an oral delivery system for acyclovir.* International Journal of Pharmaceutics, 348, 1-2 (2008): 54-60.

[73]   Leitner, V.M., G.F. Walker, and A. Bernkop-Schnurch, *Thiolated polymers: evidence for the formation of disulphide bonds with mucus glycoproteins.* European Journal of Pharmaceutics and Biopharmaceutics, 56, 2 (2003): 207-214.

[74]   Lai, S.K., et al., *Micro- and macrorheology of mucus.* Advanced Drug Delivery Reviews, 61, 2 (2009): 86-100.

[75]   Yu, Q., et al., *Preparation and properties of chitosan derivative/poly(vinyl alcohol) blend film crosslinked with glutaraldehyde.* Carbohydrate Polymers. 84, 1 : 465-470.

[76]   Wu, Z.M., et al., *Disulfide-crosslinked chitosan hydrogel for cell viability and controlled protein release.* European Journal of Pharmaceutical Sciences, 37, 3-4 (2009): 198-206.

[77]   Paula, H.C.B., F.J.S. Gomes, and R.C.M. de Paula, *Swelling studies of chitosan/cashew nut gum physical gels.* Carbohydrate Polymers, 48, 3 (2002): 313-318.

[78]   Khalid, M.N., et al., *Water state characterization, swelling behavior, thermal and mechanical properties of chitosan based networks.* European Journal of Pharmaceutical Sciences, 15, 5 (2002): 425-432.

[79]   Lee, S.J., S.S. Kim, and Y.M. Lee, *Interpenetrating polymer network hydrogels based on poly(ethylene glycol) macromer and chitosan.* Carbohydrate Polymers, 41, 2 (2000): 197-205.

[80]   Thrimawithana, T.R., et al., *In-vitro and In-vivo evaluation of carrageenan/methylcellulose polymeric systems for transscleral delivery of macromolecules.* European Journal of Pharmaceutical Sciences, (0).

[81]   Wittaya-areekul, S., J. Kruenate, and C. Prahsarn, *Preparation and in vitro evaluation of mucoadhesive properties of alginate/chitosan microparticles containing prednisolone.* International Journal of Pharmaceutics, 312, 1-2 (2006): 113-118.

[82]   Fukui, Y., et al., *Preparation of monodispersed polyelectrolyte microcapsules with high encapsulation efficiency by an electrospray technique.* Colloids and Surfaces A: Physicochemical and Engineering Aspects. 370, 1-3: 28-34.

[83]   Mschwitzer, J. and R.H. Müller, *Spray coated pellets as carrier system for mucoadhesive drug nanocrystals.* European Journal of Pharmaceutics and Biopharmaceutics, 62, 3 (2006): 282-287.

[84]   Zadaka, D., A. Radian, and Y.G. Mishael, *Applying zeta potential measurements to characterize the adsorption on montmorillonite of organic cations as monomers, micelles, or polymers.* Journal of Colloid and Interface Science. 352, 1: p. 171-177.

[85]   Klemmer, K.J., et al., *Complex coacervation of pea protein isolate and alginate polysaccharides.* Food Chemistry. In Press, Corrected Proof.

[86] Guo, J., et al., *Chitosan-coated liposomes: characterization and interaction with leuprolide.* International Journal of Pharmaceutics, 260, 2 (2003): 167-173.

[87] Sadeghi, A.M.M., et al., *Preparation, characterization and antibacterial activities of chitosan, N-trimethyl chitosan (TMC) and N-diethylmethyl chitosan (DEMC) nanoparticles loaded with insulin using both the ionotropic gelation and polyelectrolyte complexation methods.* International Journal of Pharmaceutics, 355, 1-2 (2008): 299-306.

[88] Irpanli, Y., et al., *Comparative evaluation of polymeric and amphiphilic cyclodextrin nanoparticles for effective camptothecin delivery.* European Journal of Pharmaceutics and Biopharmaceutics, 73, 1 (2009): 82-89.

[89] Silva, M.d.S., et al., *Paraquat-loaded alginate/chitosan nanoparticles: Preparation, characterization and soil sorption studies.* Journal of Hazardous Materials. 190, 1-3: 366-374.

[90] Zhang, Y., et al., *Preparation and evaluation of alginate-chitosan microspheres for oral delivery of insulin.* European Journal of Pharmaceutics and Biopharmaceutics. 77,1: 11-19.

[91] Smitha, B., S. Sridhar, and A.A. Khan, *Chitosan-sodium alginate polyion complexes as fuel cell membranes.* European Polymer Journal, 418, (2005): 1859-1866.

[92] Subramanian, N., et al., *Experimental and theoretical investigation of the molecular and electronic structure of anticancer drug camptothecin.* Spectrochimica Acta Part A: Molecular and Biomolecular Spectroscopy. 78, 3: 1058-1067.

[93]   Tangirala, R.S., et al., *Synthesis and biological assays of E-ring analogs of camptothecin and homocamptothecin.* Bioorganic & Medicinal Chemistry, 14, 18 (2006): 6202-6212.

[94]   Swaminathan, S., et al., *Cyclodextrin-based nanosponges encapsulating camptothecin: Physicochemical characterization, stability and cytotoxicity.* European Journal of Pharmaceutics and Biopharmaceutics. 74, 2: 193-201.

[95]   Li, X., et al., *Characterization and biodegradation of chitosan-alginate polyelectrolyte complexes.* Polymer Degradation and Stability, 2009. 94, 1: 1-6.

[96]   Mladenovska, K., et al., *5-ASA loaded chitosan-Ca-alginate microparticles: Preparation and physicochemical characterization.* International Journal of Pharmaceutics, 345, 1-2 (2007): 59-69.

[97]   Davidovich-Pinhas, M. and H. Bianco-Peled, *Physical and structural characteristics of acrylated poly(ethylene glycol)-alginate conjugates.* Acta Biomaterialia. 7, 7: 2817-2825.

[98]   Huang, X. and C.S. Brazel, *On the importance and mechanisms of burst release in matrix-controlled drug delivery systems.* Journal of Controlled Release, 2001, 2-3: 121-136.

APPENDICES

APPENDIX A

Standard curve of *L*-cysteine Hydrochloride

The concentration versus peak absorbance of *L*-cysteine. are presented in Table 1A. The plot of calibration curve of L-cysteine hydrochloride is illustrated in Figure 1A.

Table 1A Absorbance of various concentrations of *L*-cysteine Hydrochloride by UV spectrometer

Concentration (µmol/g)	Abs.
8.42	0.053
16.80	0.110
25.30	0.172
42.10	0.287
84.20	0.572
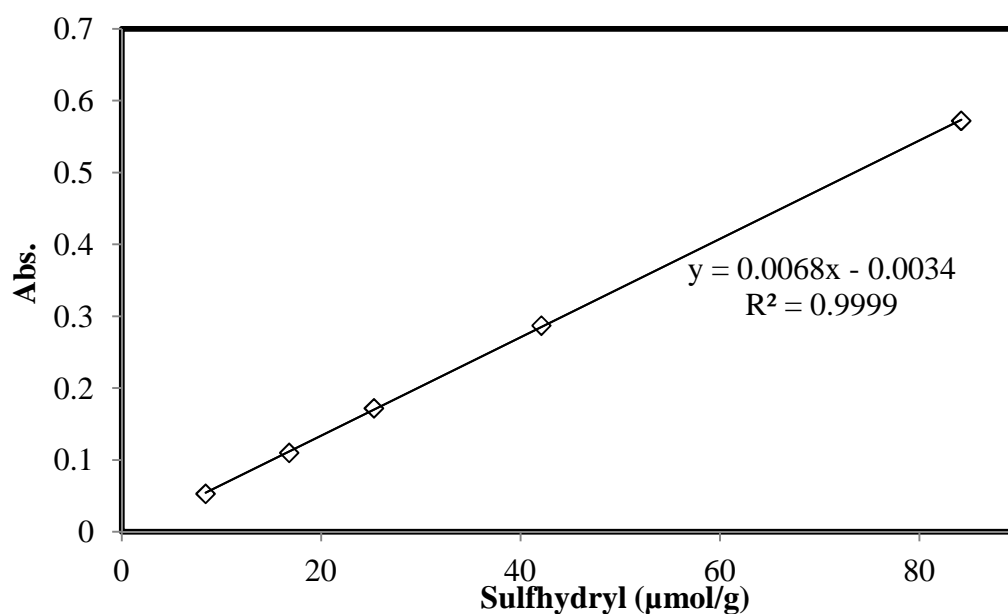
Figure 1A Standard cureve of *L*-cysteine Hydrochloride by UV spectrometer

Table 2A Absorbance thiol groups at various ratio of CS-HT by UV spectrometer

Batch	CS-HT ratio	Abs.	Abs.	Abs.	thiol (µM)	SD
CS-HT	1.0:0.05	0.210	0.299	0.201	35.12	0.05
CS-HT	1.0:0.10	0.407	0.422	0.473	64.12	0.03
CS-HT	1.0:0.50	0.397	0.305	0.311	49.99	0.05
CS-HT	1.0:1.00	0.317	0.394	0.314	50.57	0.04
QCS-HT	1.0:0.10	0.198	0.254	0.204	32.48	0.03

Table 3A Absorbance disulfide groups at various ratio of CS-HT by UV spectrometer

Batch	CS-HT ratio	Abs.	Abs.	Abs.	disulfide (µM)	SD
CS-HT	1.0:0.05	0.652	0.777	0.532	61.32	0.12
CS-HT	1.0:0.10	0.655	0.691	0.707	40.15	0.03
CS-HT	1.0:0.50	0.565	0.732	0.648	45.67	0.08
CS-HT	1.0:1.00	1.588	1.828	1.838	220.05	0.14
QCS-HT	1.0:0.10	0.453	0.429	0.565	38.74	0.07

APPENDIX B

Calibration curve of mucin (type II)

The concentration versus peak absorbance mucin glycoprotein (type II) determined by UV as the same condition described in Chapter III is presented in Table 1B. The plot of calibration curve of mucin is illustrated in Figure 1B.

Table 1B Absorbance of various concentrations of mucin (type II) at pH 1.2, 4.0, and 6.4 UV spectrophotomer

	HCl (pH 1.2)	Acetate buffer (pH 4.0)	PBS (PH 6.4)
Concentration (mg/ 2mL)	Absorbance	Absorbance	Absorbance
0.25	0.121	0.399	0.560
0.50	0.186	0.858	0.917
0.75	0.402	1.112	1.553
1.00	0.518	1.489	1.953
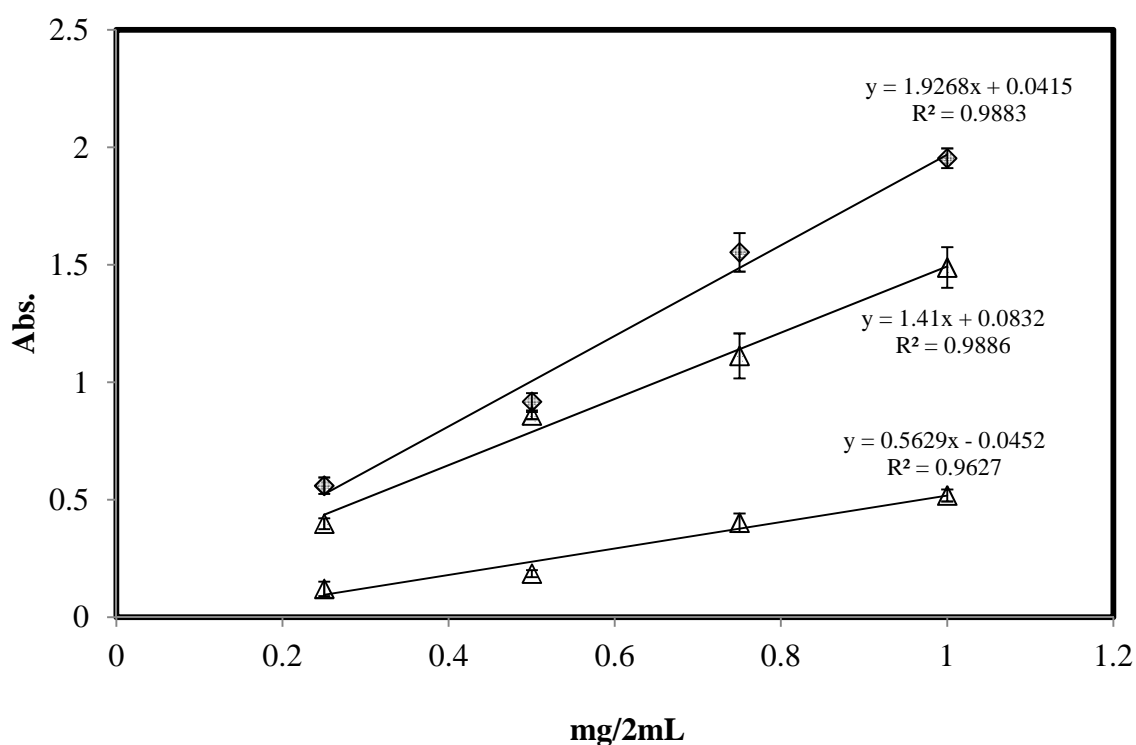
Figure 1B Standard curve of mucin at pH 1.2, 4.0, and 6.4

Table 2B Absorbance of free and adsorpbed mucin at various ratios of CS-HT in pH 1.2 by UV spectrophotomer

Batch	CS-HT ratio	Abs.	Abs.	Abs.	Free mucin (mg)	Absorbed mucin (mg)	SD
CS	-	0.491	0.482	0.485	0.94	0.06	0.01
CS-HT	1.0:0.05	0.393	0.384	0.411	0.79	0.22	0.02
CS-HT	1.0:0.10	0.415	0.387	0.383	0.78	0.22	0.02
CS-HT	1.0:0.50	0.395	0.397	0.341	0.75	0.25	0.03
CS-HT	1.0:1.00	0.368	0.379	0.368	0.75	0.26	0.01
QCS-HT	1.0:0.10	0.298	0.308	0.309	0.62	0.38	0.01

Table 3B Absorbance of free and adsorpbed mucin at various ratios of CS-HT in pH 4.0 by UV spectrophotomer

Batch	CS-HT ratio	Abs.	Abs.	Abs.	Free mucin (mg)	Absorbed mucin (mg)	SD
CS	-	1.065	1.078	0.992	0.68	0.31	0.05
CS-HT	1.0:0.05	0.735	0.701	0.724	0.45	0.55	0.02
CS-HT	1.0:0.10	0.683	0.668	0.633	0.41	0.60	0.03
CS-HT	1.0:0.50	0.777	0.714	0.722	0.46	0.54	0.03
CS-HT	1.0:1.00	0.788	0.774	0.755	0.49	0.51	0.02
QCS-HT	1.0:0.10	0.365	0.359	0.418	0.21	0.79	0.03

Table 4B Absorbance of free and adsorpbed mucin at various ratios of CS-HT in pH 6.4 by UV spectrophotomer

Batch	CS-HT ratio	Abs.	Abs.	Abs.	Free mucin (mg)	Absorbed mucin (mg)	SD
CS	-	1.183	1.125	1.147	0.57	0.42	0.03
CS-HT	1.0:0.05	0.730	0.718	0.728	0.35	0.65	0.01
CS-HT	1.0:0.10	0.583	0.577	0.559	0.27	0.72	0.01
CS-HT	1.0:0.50	0.689	0.672	0.655	0.32	0.67	0.02
CS-HT	1.0:1.00	0.758	0.747	0.816	0.37	0.62	0.04
QCS-HT	1.0:0.10	0.514	0.519	0.531	0.24	0.75	0.01

APPENDIX C

Calibration curve of CPT

Table 1C Absorbance of camptothecin drug in 10% (v/v) DMSO determined in 370 nm

Concentration (ppm)	Absorbance (avg.)
10	0.249
20	0.494
30	0.718
40	0.943
50	1.164

$y = 0.0228x + 0.0301$
$R^2 = 0.9996$
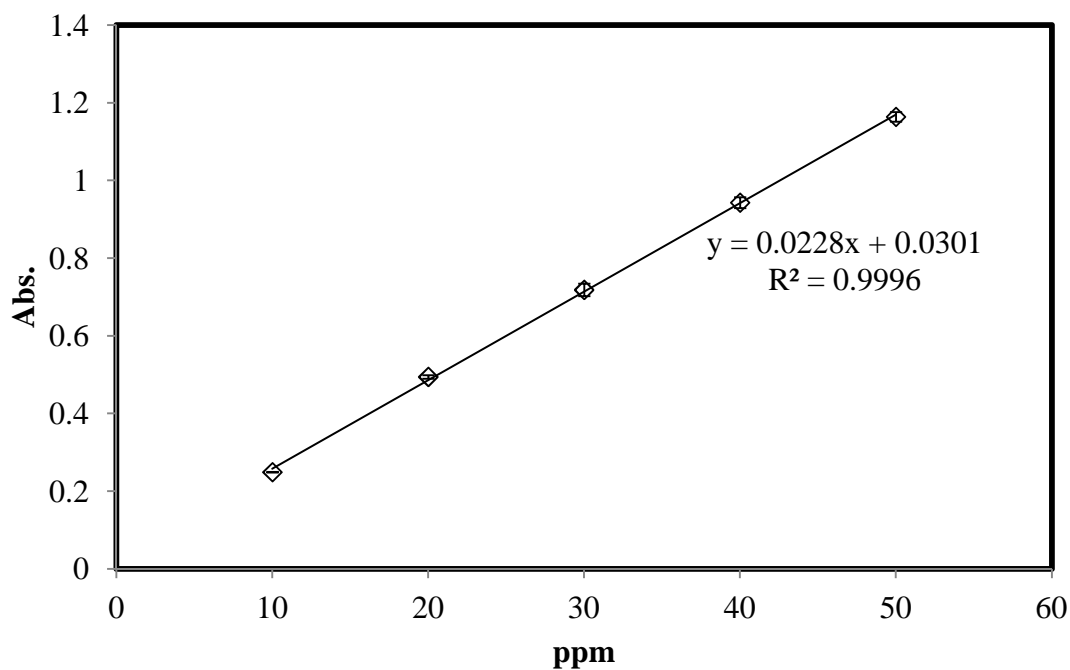
Figure 1C Calibration curve of camptothecin in 10% (v/v) DMSO determined in 370 nm.

Table 2C Absorbance of camptothecin drug in pH 1.2 determined in 370 nm

Concentration (ppm)	Abs.	Abs.	Abs.	AVG	SD
10	0.228	0.216	0.229	0.224	0.01
20	0.485	0.499	0.494	0.492	0.01
30	0.725	0.745	0.777	0.749	0.03
40	0.952	0.993	0.915	0.953	0.04
50	1.164	1.168	1.161	1.164	0.01

$y = 0.0234x + 0.0145$
$R^2 = 0.9961$
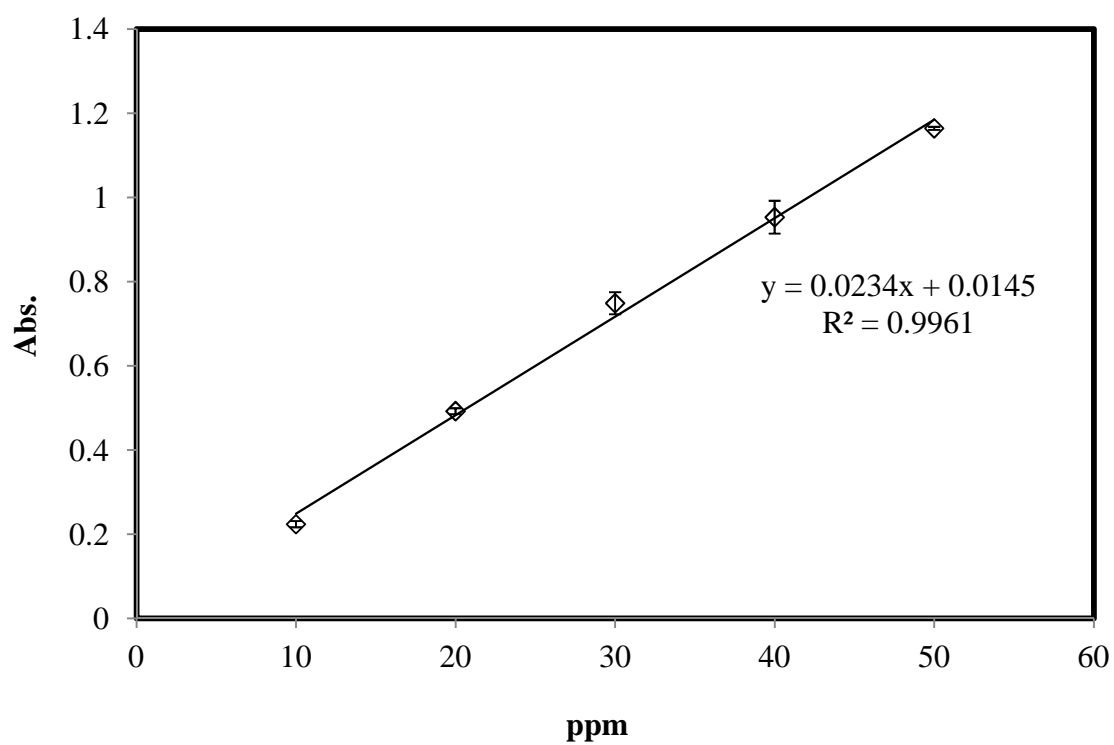
Figure 2C Calibration curve of camptothecin in pH 1.2 determined in 370 nm.

Table 3C Absorbance of camptothecin drug in pH 4.0 determined in 370 nm

Concentration (ppm)	Abs.	Abs.	Abs.	AVG	SD
10	0.251	0.251	0.246	0.25	0.01
20	0.473	0.491	0.485	0.48	0.01
30	0.711	0.735	0.752	0.73	0.02
40	0.935	0.941	0.952	0.94	0.01
50	1.161	1.162	1.165	1.16	0.01

$y = 0.0229x + 0.0282$
$R^2 = 0.9991$
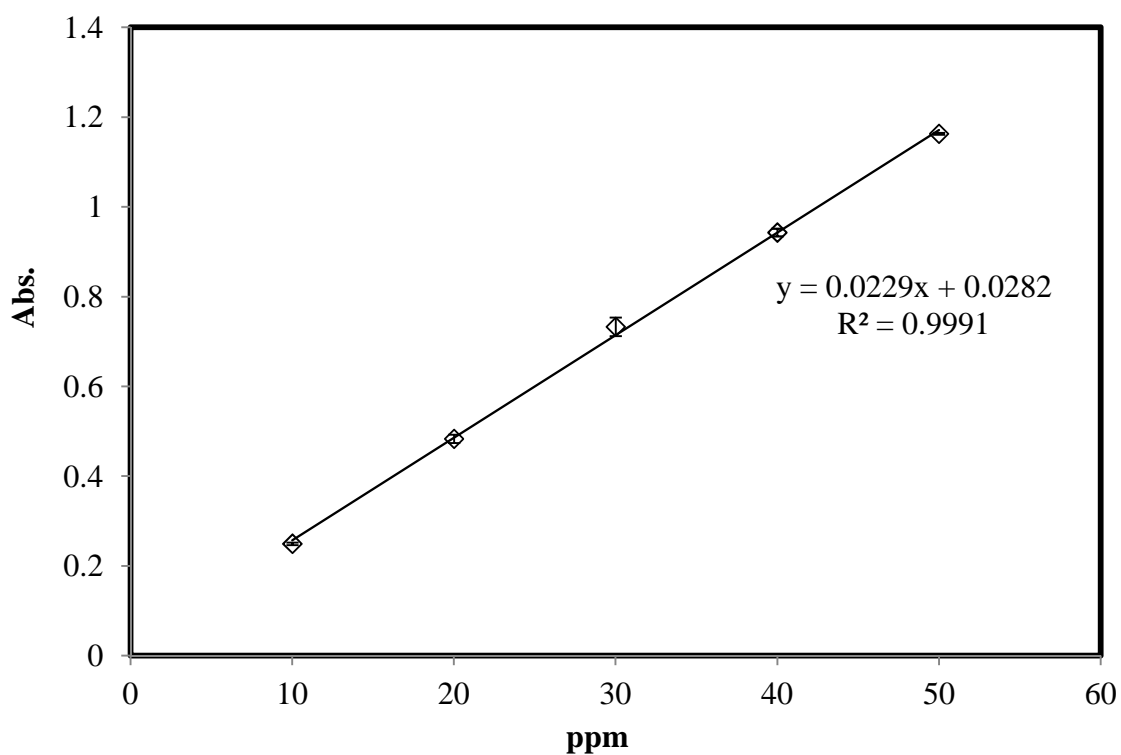
Figure 3C Calibration curve of camptothecin in pH 4.0 determined in 370 nm.

Table 4C Absorbance of camptothecin drug in pH 6.4 determined in 370 nm

Concentration (ppm)	Abs.	Abs.	Abs.	Mean	SD
10	0.234	0.221	0.243	0.233	0.01
20	0.428	0.461	0.454	0.448	0.02
30	0.708	0.694	0.696	0.699	0.01
40	0.949	0.968	0.955	0.957	0.01
50	1.055	1.054	1.102	1.070	0.03

$y = 0.0219x + 0.026$
$R^2 = 0.987$
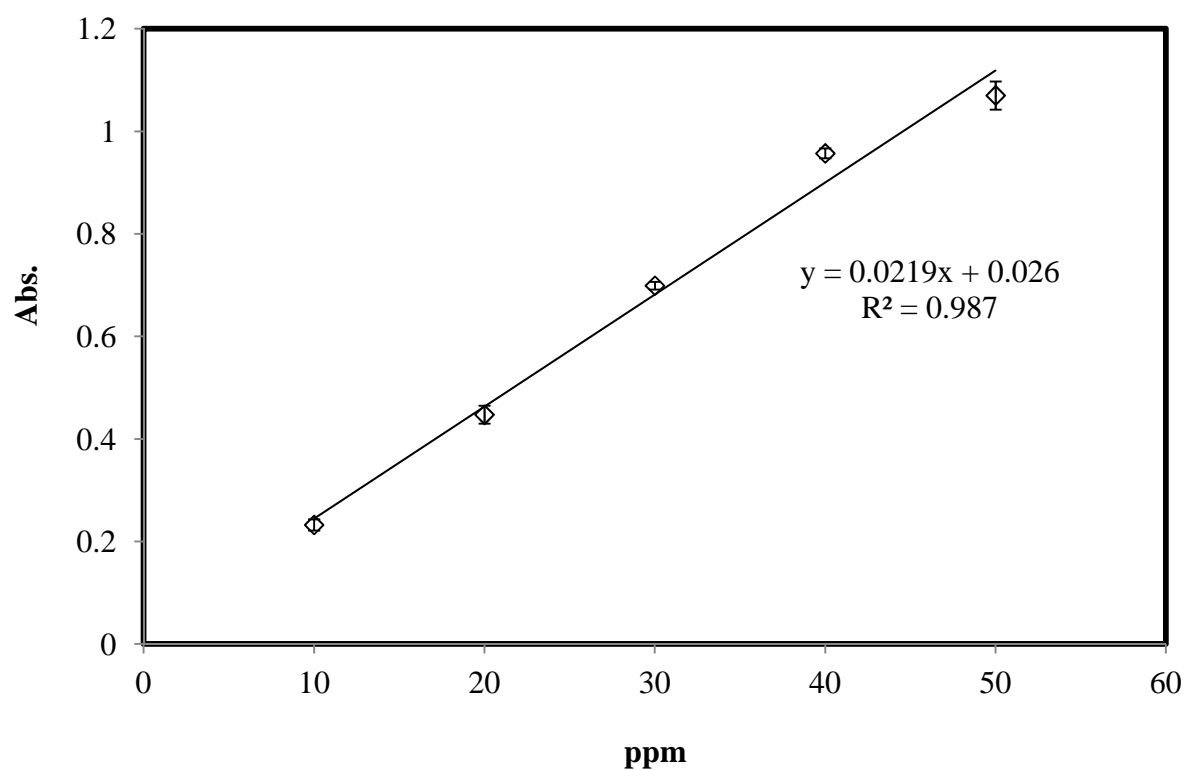
Figure 4C Calibration curve of camptothecin in pH 6.4 determined in 370 nm.

Appendix D

Cumulative Drug Release

Table 1C Cumulative CPT release from CS/ALG microspheres in pH 1.2

Time (min)	Amount of CPT release				
	1	2	3	Mean	SD
0	0	0	0	0	0
5	4.636	5.534188	5.576923	5.249288	0.53
10	9.209402	10.14957	8.397436	9.252137	0.87685
15	10.23504	12.11538	10.49145	10.94729	1.019688
30	18.65385	20.19231	17.88462	18.91026	1.175019
45	28.56838	29.0812	25.44872	27.69943	1.965967
60	40.32051	39.72222	36.21795	38.75356	2.216187
120	52.62821	51.21795	54.12393	52.6567	1.453201
240	53.69658	53.91026	53.78205	53.7963	0.107547
360	54.16667	54.59402	50.7906	53.18376	2.083525
480	51.30342	52.41453	53.31197	52.3433	1.006166
600	52.92735	52.45726	53.44017	52.9416	0.491608
720	52.84188	52.45726	53.48291	52.92735	0.518135

Table 2C Cumulative CPT release from mCS/ALG microspheres in pH 1.2

Time (min)	Amount of CPT release				
	1	2	3	Mean	SD
0	0	0	0	0	0
5	4.764957	4.722222	5.662393	5.049858	0.530902
10	4.764957	4.722222	5.747863	5.078348	0.580211
15	4.807692	4.764957	5.918803	5.163818	0.654186
30	7.286325	6.260684	6.388889	6.645299	0.558833
45	9.252137	10.49145	14.63675	11.46011	2.819973
60	13.31197	14.55128	14.85043	14.23789	0.815706
120	20.10684	19.25214	20.36325	19.90741	0.581783
240	35.32051	35.96154	42.02991	37.77066	3.702526
360	54.33761	53.26923	52.58547	53.39744	0.883076
480	54.46581	54.72222	55.40598	54.86467	0.486003
600	54.50855	55.14957	55.40598	55.27778	0.46225
720	54.9359	54.9359	56.04701	55.30627	0.6415

Table 3C Cumulative CPT release from CS/ALG microspheres in pH 4.0

Time (min)	Amount of CPT release				
	1	2	3	Mean	SD
0	0	0	0	0	0
5	4.183406	4.445415	4.398253	4.342358	0.139662
10	4.663755	4.620087	4.445415	4.576419	0.115535
15	4.663755	4.838428	4.969432	4.823872	0.153357
30	4.707424	5.0131	5.187773	4.969432	0.243134
45	5.49345	5.668122	5.406114	5.522562	0.133408
60	5.930131	6.235808	5.755459	5.973799	0.243134
120	10.38428	10.73362	10.38428	10.50073	0.164683
240	12.61135	12.65502	15.10044	13.4556	1.424634
360	36.84716	34.48908	37.0655	36.13392	1.428644
480	49.9476	50.34061	50.29694	50.19505	0.21541
600	50.03493	50.29694	50.29694	50.20961	0.151271
720	50.03493	50.64629	50.64629	50.4425	0.352965

Table 4 C Cumulative CPT release from mCS/ALG microspheres in pH 4.0

Time (min)	Amount of CPT release				
	1	2	3	Mean	SD
0	0	0	0	0	0
5	4.052402	4.008734	4.008734	4.02329	0.025212
10	4.270742	4.227074	4.270742	4.256186	0.025212
15	4.31441	4.401747	4.445415	4.387191	0.066704
30	4.489083	4.445415	4.576419	4.503639	0.066704
45	4.576419	4.663755	4.31441	4.518195	0.181805
60	4.838428	4.707424	4.576419	4.707424	0.131004
120	4.969432	4.882096	5.275109	5.042213	0.206367
240	6.497817	5.100437	5.40393	5.667394	0.735002
360	11.38865	9.68559	9.816594	10.29694	0.773801
480	24.62009	22.9607	23.31004	23.63028	0.874817
600	46.9345	40.9083	40.77729	42.87336	3.517656
720	51.43231	49.59825	49.59825	50.20961	1.058896

Table 5 C Cumulative CPT release from CS/ALG microspheres in pH 6.4

Time (min)	Amount of CPT release				
	1	2	3	Mean	SD
0	0	0	0	0	0
5	3.47032	4.748858	4.246575	4.155251	0.644143
10	4.063927	4.794521	4.474886	4.444444	0.366247
15	4.977169	4.703196	4.840183	4.840183	0.136986
30	5.022831	5.342466	5.525114	5.296804	0.254236
45	5.388128	5.616438	6.210046	5.738204	0.424273
60	6.347032	6.52968	6.940639	6.605784	0.304033
120	8.219178	8.584475	8.675799	8.493151	0.241621
240	12.37443	11.05023	11.3242	11.58295	0.698993
360	37.71689	39.81735	38.85845	38.79756	1.051551
480	40.41096	41.55251	41.96347	41.30898	0.804396
600	42.42009	41.73516	44.38356	42.84627	1.374674
720	42.78539	44.29224	53.05936	46.71233	5.548086

Table 6C Cumulative CPT release from mCS/ALG microspheres in pH 6.4

Time (min)	Amount of CPT release				
	1	2	3	Mean	SD
0	0	0	0	0	0
5	3.424658	4.474886	4.949772	4.283105	0.780435
10	3.652968	4.520548	5.634703	4.60274	0.993421
15	4.611872	5.159817	4.90411	4.891933	0.274175
30	5.251142	5.342466	5.041096	5.211568	0.154533
45	5.342466	5.43379	5.680365	5.48554	0.174793
60	5.616438	5.753425	5.954338	5.774734	0.169955
120	5.753425	6.30137	7.141553	6.398782	0.699172
240	6.894977	7.716895	8.648402	7.753425	0.877283
360	18.85845	18.21918	21.02283	19.36682	1.469336
480	39.54338	37.80822	38.32877	38.56012	0.890415
600	40.04566	42.87671	43.80822	42.24353	1.959566
720	40.41096	43.05936	44.44749	42.63927	2.050793

VITAE

Name	:	Mr. Kotchakorn Juntapram
Date of birth	:	Feb 24, 1986
Nationality	:	Thai
Address	:	56/1 Moo 9, Phromkiri District, Nakhon Sri Thammarat, 80320

University Education : Bacherlor's Degree from Department of Chemistry, Faculty of Science, Thammasat university, 2005-2008

Master's Degree from Program of Petrochemistry and Polymer Science, Faculty of Science, Chulalongkorn university, 2008-2001

Conference attendance: Poster presentation "Synthesis and properties of mucoadhesive chitosan-homocysteine thiolactone for drug delivery system" at the 7th International Conference Advanced Materials in Asia-Pacific, Ishikawa High-Tech Exchange center, Ishikawa, Japan

Publications: **K. Juntapram**, N. Praphairaksit, K. Siraleartmukul, and N. Muangsin, Synthesis and evaluation of chitosan-homocysteine thiolactone as a mucoadhesive polymer., *Manuscript is revised for publication in carbohydrate polymer.*